Exploration of PV module topologies for energy yield optimization when non-uniform conditions are dominant

Maria-Iro Baka

School of ECE
National Technical University of Athens

This dissertation is submitted for the degree of
Doctor of Philosophy

Microprocessors and Digital Systems
Lab

November 2017

National Technical University of Athens
School of Electrical and Computer Engineering
Division of Computer Science
Microprocessors and Digital Systems Lab

Exploration of PV Module Topologies for Energy Yield Optimization when Non-Uniform Conditions are Dominant

PhD Thesis

of

Maria-Iro Baka

Supervisory Committee: DIMITRIOS SOUDRIS
KIAMAL PEKMESTZI
FRANCKY CATTHOOR

Approved by the 7-member committee on the 30th of November 2017

Dimitrios Soudris Assoc. Prof. NTUA (Supervisor)	Kiamal Pekmestzi Professor NTUA	Francky Catthoor Professor KUL
Stavros Papathanasiou Professor NTUA	Dimitrios Tsoukalas Professor NTUA	Dr. Ezster Voroshazi

Kostas Siozios
Assoc. Prof. AUTH

Athens, November 2017

Dedicated to my family . . .
and especially my mother . . .

Acknowledgements

It has been a long journey...

Obtaining a PhD degree is far from just research and technical work. It is a dive to unfamiliar waters, where you get to explore new ideas, overcome obstacles and in the end discover your true self. This is not a journey you can complete on your own so I would like to thank the people who supported me all these years.

First of all I want to express my gratitude to my supervisors and mainly Prof. Francky Catthoor and Prof. Dimitrios Soudris who always stood beside me through all the difficult phases of my PhD "experience". Their guidance was essential and they always kept me motivated despite the difficulties that were arising.

I was lucky enough to conduct research both in NTUA and in IMEC. I would like to thank both teams for their support. From Athens, a special thanks goes to Dr. Antonis Papanikolaou who was there for my first steps. Our collaboration might have been short-lived, but the foundation was built... I would also like to thank Dimitris Anagnostos, who as a member of the same project, always stood by me and provided solutions when I got tunnel vision!

The periods I spent in Leuven were very fruitful for my research thanks to the wonderful and capable people who were surrounding me. I would like to thank all of them and especially the PVMT team, Eszter, Tom, Jonathan, Arvid, Philippe and Imre. I really enjoyed the balance of the team and their motivation and love for work really inspired me. Although members of the team, I would like to thank these two people separately, Hans and Patrizio. So, Hans thanks for providing me with a great model and helping me gain a proper perspective of life! To Patrizio (aka my George): thank you for making the end of the journey beautiful you and most of all thank you for being you...

Of course nothing is possible without friends surrounding you. I consider myself extremely fortunate to have amazing people in my life which I get to call my friends. I would like to thank all my colleagues in microlab and especially my office mates, Dimitris and Giorgos. Harry cannot be considered just an office mate, as I simply cannot imagine my life without him... (you will never get rid of me...). At this time I believe that words are poor and I could never be able to express the love I feel for all my friends who were there for me and a list simply won't do. Just know I love you all and I need you...

Last but sure not least, I would like to thank my family for simply being there. My mother Antiopy for her patience, my father George (G.) for his support and my brother Yannis for his ability to bring balance. Love you more than you know...

To the next journey...
Maro

Abstract

Photovoltaic systems, which convert solar energy to electrical energy, are an attractive solution for future clean energy provision on site. However, the performance of commercial PV installations degrades non-linearly with the presence of non-uniform operating conditions. The reliability and future operation of the PV modules can be compromised by potential creation of hot spots, especially in locations where non-uniform conditions and partial shading are frequent. The performance of the PV array degrades non-linearly when operating under non-uniform conditions. Partial shading can occur in different levels of the PV array, between PV modules or within the module itself. The focus of this thesis is for partial shading which occurs on the module level.

Conventional modules do not allow all cells to operate on their Maximum Power Point (MPP) when partial shading conditions are present. The design of custom topologies, based on the specific run-time operating conditions of the module, thus allowing the majority of the cells to operate at their MPP, showed promising results in terms of recovered power. This led to the investigation of module topologies which would enable multiple run-time configurations depending on the current operating conditions of the PV module (partial shading, irradiation, ambient temperature, wind velocity). The granularity level of the module was explored by taking into consideration the increased manufacturing cost due to additional elements and the increased resistivity in the active path of the current. A cell-string architecture is proposed where the cell-string string is defined as the minimum power producing element and cannot be divided at run-time. Dynamic elements (switches), local converters and a supporting network are added to allow extraction of more power during conditions of partial shading.

A methodology is proposed to select how cell-strings are formed in the PV module and the characteristics of the required supporting electrical network to enable reconfiguration. Two main templates are examined; a row/column template and a snake-like template. In order to evaluate the performance of different module configurations, a detailed and accurate simulation environment is required. A highly accurate physics-based bottom-up model is used, where all additional elements are included. This allows the comparison of different module templates in terms of energy-yield. Simulations have been performed under relevant

and realistic operating conditions. Both static and dynamic shading scenarios have been considered and the performance of different module topologies has been evaluated and benchmarked to current industrial solutions. Such a benchmark allows to determine the energy-yield gain that can be expected by the different proposed templates. This together with other cost aspects, e.g. initial fabrication cost and complexity of control scheme, allows to determine the most promising configurations. Also, long-term financial analysis is performed for the two most promising reconfigurable templates. Finally a method to speed-up the simulation process is introduced.

Περίληψη

Τα Φωτοβολταϊκά συστήματα, τα οποία μετατρέπουν την ηλιακή ενέργεια σε ηλεκτρική, είναι μια υποσχόμενη λύση για παραγωγή καθαρής ενέργειας. Η επίδοση όμως των παραδοσιακών Φωτοβολταϊκών συστημάτων φθίνει μη γραμμικά όταν λειτουργούν υπό μη-ομογενείς συνθήκες. Η αξιοπιστία και η σωστή μελλοντική λειτουργία των Φ/Β μονάδων κινδυνεύουνε από πιθανή δημιουργία hot-spot. Αυτό συμβαίνει ειδικότερα σε εγκαταστάσεις όπου μη ομοιόμορφες συνθήκες και μερική σκίαση των Φ/Β μονάδων είναι συχνή. Η επίδοση των Φ/Β μονάδων φθίνει μη-γραμμικά σε λειτουργία μη-ομοιόμορφων συνθηκών. Μερική σκίαση και μη ομογενείς συνθήκες μπορούν να παρουσιαστούν σε διάφορα επίπεδα του φωτοβολταϊκού συστήματος, μεταξύ PV module ή μέσα στο ίδιο το PV module. Η δουλειά αυτή εστιάζει στο επίπεδο των Φ/Β πανέλων.

Τα πιθανά οφέλη σε ανακτώμενη ενέργεια εξετάζονται όταν η πλειονότητα των κυψελών λειτουργεί στο μέγιστο σημείο ισχύος με σχεδιασμό τοπολογιών προσαρμοσμένες στις εκάστοτες εξωτερικές συνθήκες. Αυτό οδηγεί στη μελέτη δυναμικών τοπολογιών που προσαρμόζουν τις συνδέσεις μεταξύ των κυψελών ανάλογα με τις συνθήκες λειτουργίας. Ο βαθμός λεπτομέρειας (granularity level) μιας Φ/Β μονάδας για να αυξηθεί η ενέργεια σε συνθήκες σκίασης, εξετάζεται με βασικά κριτήρια κόστους το αυξημένο κόστος παραγωγής λόγω προστιθέμενων στοιχείων και την αυξημένη αντίσταση στην ενεργή ροή του ρεύματος. Μια αρχιτεκτονική στο επίπεδο του cell-string προτείνεται, όπου ένα cell-string ορίζεται ως η ελάχιστη μονάδα παραγωγής ισχύος, αποτελείται από σειριακά συνδεδεμένες κυψέλες και δεν διαιρείται στο χρόνο λειτουργίας. Δυναμικά στοιχεία (διακόπτες), τοπικοί μετασχηματιστές και ένα ηλεκτρικό δίκτυο υποστήριξης προστίθενται για να επιτραπεί η εξαγωγή περισσότερης ενέργειας σε συνθήκες μερικής σκίασης.

Προτείνεται μια μεθοδολογία επιλογής cell-strings όπως και του δικτύου υποστήριξης που επιτρέπει την δυναμική αλλαγή της τοπολογίας. Δύο βασικά πρότυπα Φ/Β μονάδων εξετάζονται. Στο πρώτο τα cell-string σχηματίζονται από τις σειρές/στήλες ενός Φ/Β πανέλου ενώ στο δεύτερο αλλάζουν και οι συνδέσεις εντός της βασικής μήτρας των κυψελών. Προκειμένου να αξιολογηθεί η επίδοση διάφορων τοπολογιών, χρειάζεται ένα αναλυτικό και ακριβές μοντέλο. Χρησιμοποιήθηκε ένα μοντέλο το οποίο στηρίζεται στη φυσική και όπου όλα τα προστιθέμενα στοιχεία συμπεριλαμβάνονται. Αυτό επιτρέπει την σύγκριση μεταξύ τοπολογιών σε όρους ενέργειας. Προσομοιώσεις στατικών και δυναμικών σεναρίων λειτουργίας πραγματοποιήθηκαν και οι επιδόσεις διαφορετικών τοπολογιών που επιτρέπει την σύγκριση με τοπολογίες που είναι διαθέσιμες στη βιομηχανία. Οι πιο υποσχόμενες τοπολογίες μπορούν να προσδιοριστούν με βάση την ενεργειακή επίδοση καθώς και άλλα κριτήρια κόστους, όπως το κόστος παραγωγής. Επίσης, πραγματοποιείται μια ανάλυση για τις δύο πιο υποσχόμενες τοπολογίες για μακροπρόθεσμα οικονομικά κέρδη. Τέλος προτείνεται μια μέθοδος η οποία επιτρέπει την επιτάχυνση του περιβάλλοντος της προσομοίωσης, ενώ διατηρείται υψηλό επίπεδο ακρίβειας.

Table of contents

List of figures

List of tables

Chapter 1

Introduction

1.1 Context and Motivation

Solar energy is one of the cleanest forms of energy as no emission of greenhouse gases or other air pollutants is present. Sunlight is converted to electricity by using photovoltaics (PV) devices. The basic component of a PV system is the solar cell which is a device that absorbs light and converts it directly to electricity through the photovoltaic effect. In commercial installations, multiple PV cells are interconnected and are integrated into a single, long-lasting, stable unit: a PV module. The modules are connected in series to form module-level strings, which are in turn connected in parallel forming the PV array. The array is connected to a central converter/inverter, equipped with a Maximum Power Point Tracker (MPPT) to maximize the generated power [1].

A Maximum Power Point tracker is needed as the generation of power of a PV system depends on the external operating conditions. The main parameters that affect the operation of a PV cell, thus the entire PV system, are incident irradiation and internal temperature. The incident irradiation of a PV system depends on the solar irradiation (position of the sun, angle of the PV modules) and potential shading sources on the PV array. The internal temperature of the cells is affected by the external/ambient temperature, the wind/air flow and the operating point of the cells. The incident irradiation mainly affects the short-circuit current of a cell, while changes of the internal temperature mainly shift the open-circuit voltage. This necessitates a tracking/control mechanism to constantly track the optimum operating point. Three factors render the received irradiation the most important parameter of the PV systems operation: the larger range of possible values of irradiation, the proportional dependence of the short-circuit current and the series connection of the PV cells.

Optimally, the entire PV system operates under uniform conditions. In recent years however, the constant growth of the PV market has led to installations of PV systems in non-

ideal locations where uniform operating conditions are not usually the norm. Installations in urban areas (rooftops, Building Attached Photovoltaics (BAPV)) have increased, while there is an emerging market for Building-Integrated Photovoltaics (BIPV) and solar vehicles. These systems operate often under non-uniform conditions, however the energy demand is high even in non-ideal conditions.

The most common cause of non-uniformity in PV systems is partial shading of the PV array. Partial shading of the PV system can either occur due to static objects (trees, chimneys, bird droppings etc) or due to moving objects, where clouds and soiling through dust/sand are the most common. Also others can be present, like pedestrians or birds. In BAPV systems, casting shadows by nearby obstacles are hard to prevent due to limited space and the system power requirements. Incident shade, though, can be caused by dynamic objects such as clouds, where the direction, shape and density profile of the shadow cannot be known beforehand with high accuracy.

When the PV system is illuminated in a non-uniform manner, significant power losses are observed. The power loss is not necessarily linear to the casted shade, as also the operation of fully illuminated cells is affected. Furthermore, local hot-spots threaten the proper operation of the system and can cause permanent destruction of PV modules.

Industrial PV installations deal with non-uniform conditions by including bypass and blocking diodes in the PV array and in cases, by distributing control to the module level. Under inhomogenous conditions, bypass diodes protect the PV cells, however the power produced by the PV system is reduced due to the presence of diodes, as either part of the current is bypassed or the overall current is reduced, as shown in the following Sections. Distribution of control to the module level enables a more independent operation of the PV modules, but non-uniform operating conditions within the module still result to a reduction of the overall energy yield.

1.2 Objectives of the research activities

The main objective of this work is to improve the performance of PV systems in locations/installations where non-uniform conditions are dominant. The focus is on the exploration of module topologies/configurations where the basic criterion is the optimization of the energy-yield.

The examined module topologies are dynamic and require additional elements to support reconfiguration depending on the run-time operating conditions of the PV array.

The additional elements, which are needed to enable multiple run-time instantiations of the module, alter the active current path under different operating conditions. The price to

pay for this additional flexibility is that extra resistive losses are introduced in the PV module even when operating under uniform conditions. Multiple design-time instantiations of PV modules need to be evaluated for different operating conditions in order to understand under which conditions reconfigurable modules can be beneficial and which are the most promising templates for such reconfigurable topologies.

In order to explore and evaluate the potential benefits of different module topologies, a simulation environment is needed where the losses induced by all additional elements are incorporated.

1.3 What can be improved further in the current approaches?

Several studies focus on the optimization of the performance of PV installations under conditions of partial shading. We will now show the differences of works focusing on partial shading with a systematic classification of the method applied to deal with non-uniformity. A first split of the studies focusing on improving the PV system's efficiency under non-uniform conditions is based on the main approach applied. The three categories are improvement of system components, alteration of the interconnection of the PV array and introduction of extra elements in the PV array.

Improving system components, such as solar cell's efficiency and the losses in wire interconnections improve the overall efficiency of the PV system under any type of operating conditions. The studies which fall into this category and target operation under non-uniform conditions are the ones which focus on the optimization and refinement of the Global Maximum Power Point Tracking (GMPPT) algorithm [2]. In most PV systems, bypass diodes are present in the configuration to protect PV cells from hot spot heating. This leads to multiple peaks in the P-V (Power-Voltage) curve of the system and the PV system can be stuck on local maxima. Also, the characteristics of bypass elements affect the characteristics of the systems P-V curve. Several works focus on the improvement of MPP tracking techniques (aiming for better speed and accuracy) [3], while others work on the optimization of the bypass elements [4].

The second category involves studies which alter the interconnection of the PV components, without adding any additional elements in the PV array. Under uniform conditions, simple series connections of the cells in the module and series connection of the modules themselves yield the optimal results because the PV arrays current cannot exceed the one produced by a single cell, thus resistive losses are minimized. However, under non-uniform conditions, altering the configuration of the PV array with a combination of series and parallel connections can improve the overall performance. In [5] the effects of clouds is evaluated

for different interconnection schemes of the modules. In the modules themselves, either the connections of the cells themselves can be altered or the configuration of diodes can be changed to minimize the power losses under partial shading [6].

In both categories above, the presence of bypass elements signifies that under non-uniform conditions either part of the array operates on a sub-optimal point or another part is bypassed.

To remedy this, in the last category, as stated, additional elements are included in the PV array. This can be further divided in static configurations and dynamic configurations of the PV system. In static configurations, no dynamic elements are present (mainly switches). Addition of elements in static configurations of the PV system include distribution of the MPP tracking, such as Power Optimizers [7] and Micro-Inverters in different levels of the PV array [8] and the increase of the number of bypass diodes applied to allow a finer granularity level of non-uniformity mitigation [9]. The presence of bypass elements implies that instantaneous power can be potentially bypassed or reduced. On the other hand, static distribution of the MPP tracking leads to unnecessary active elements under uniform conditions which increase power and resistive losses. For instance, any power optimizer must continuously process the whole power produced by a PV module, independently of the presence of non-uniformity within the module itself. This leads to additional losses (power optimizers efficiency is lower than 100%) even when the power optimizer is not needed at all.

Dynamic configurations of the PV array involve the addition of dynamic elements which allow reconfiguration of the array at run-time. This type of approach requires also a control mechanism to determine the optimal configuration according to the operating conditions [10].

For our focus and objective, this last class of work is the most promising, as reconfiguration of the PV system allows the PV array to adapt to the dynamic operating conditions. Most of the studies focus on reconfiguration of the PV array, in the module level, by enabling multiple interconnections between the modules. This means that non-uniform conditions within the module is not addressed. The latter represents the focus of this study where the goal is to allow multiple run-time instantiations of the module itself. Studies where the granularity level is in the module level or higher can be seen as complementary to this work. On the other hand, studies dealing with sub/intra-module level reconfiguration either allow limited flexibility and do not optimize the performance of the module for most shading patterns or introduce too much resistive losses. These are more analytically discussed in Chapter 2.

1.4 Contributions

Given the state-of-the-art and the gaps, as identified in Section 1.3, in this work we want to explore dynamic configurable topologies at the intra-module level. This is up to the point where the module connects to the rest of the PV array. A design approach and modeling/exploration methodology are presented in order to decide on the granularity level of the architecture and the reconfiguration options. The concept of a cell-string is introduced which is the minimum power generating element of the module and cannot be divided at run-time. The selection of cell-strings, size and geometry, defines the granularity level of the PV module and determines the flexibility of the topology. Dynamic elements (switches), local converters and a supporting network are added to allow extraction of more power during conditions of partial shading.

The proposed approach is applied to create parameterized templates of rectangular PV modules. Design instantiations of the module (where the parameters have specific values) depend on the electrical characteristics of the solar cells and on the location of the installation, in other words on the expected operating conditions.

Two basic module templates are examined. The first comprises of cell-strings which are the rows/columns of the module. The limitation of this approach is the limited flexibility of the module to shades which move in a direction perpendicular to the cell-strings. A vertical split of the columns is then made to allow flexibility of the module in more shading patterns. This leads to a larger number of cell-strings and thus a bigger supporting network. These topologies have been evaluated for several static shading patterns.

In the second type examined, the module is divided again in cell-strings in a way that a small number of cell-strings allow a similar flexibility of the module as when the vertical split is applied. These configurations are called "snake topologies". The potential run-time instantiations of these templates are limited to two main configurations; one for uniform conditions and one for significant non-uniformity.

In order to evaluate the performance of module configurations, modeling methodology supported by a detailed and accurate simulation environment is required. A physics-based bottom-up model is used, where all additional elements are included. This allows the comparison of different module templates in terms of energy-yield. A cost function is then analyzed to evaluate the gain-cost balance of different topologies. By taking several cost aspects into consideration (initial cost, energy-yield...) the most promising configurations are determined.

1.5 Outline

Chapter 2 provides an overview of the proposed state-of-the-art solutions which deal with inhomogeneous operating conditions of the PV array. The main methods for partial shading mitigation are discussed and the limitations of each approach are analyzed.

Chapter 3 introduces the basic concepts of the proposed reconfiguration scheme of PV modules. The components required to allow reconfiguration are presented and their potential interconnections are examined.

Chapter 4 focuses on the application of the concepts of reconfigurable modules in rectangular modules, where cells are organized in an N by M matrix. A template where the columns/rows of the module are selected as cell-strings is examined and the size of the supporting electrical network for reconfiguration is discussed. A vertical split of cell-strings is suggested to increase flexibility. The consequences of this division of the cell-strings on the supporting electrical network are discussed. Finally simulation results for representative static shading patterns are presented.

Chapter 5 presents a the snake-like templates of modules. The interconnections of cell-strings and the supporting network are examined and simulation results are shown for uniform conditions and representative static shading patterns.

Chapter 6 goes more into detail in snake toplogies and their design instantiations and a more analytical cost assessment is performed. The simulation model is discussed and the performance of the proposed modules under dynamic shading conditions are presented.

Chapter 7 describes the proposed methodology to speed up the simulation environment.

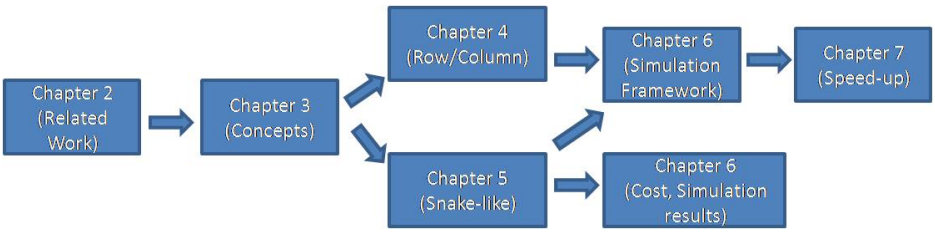

Fig. 1.1 Chapter Flow

Chapter 2

Related Work

As stated in Section 1.1, partial shading and non-uniform conditions heavily degrade the performance of the PV array. The optimization of the PV system is the focus of several studies. These studies are classified intro three main categories, based on the approach of dealing with the problem of partial shading; (i) Improvement of system components, (ii) Alterations of interconnections of system components and (iii) Introduction of elements in the PV array.

2.1 Improvement of system components

In [11] a review of Maximum Power Tracking techniques is performed. Not all methods examined in this work target arrays where partial shading is present. Simple approaches such as curve-fitting techniques, fractional short-circuit current or open-circuit voltage can be used when the system operates under uniform conditions. However when the PV array operates under non-uniform conditions and multiple peaks are present in the P-V (Power-Voltage) curve, these techniques cannot ensure the operation of the system at the Global Maximum Power (GMPP) Point. It has to be noted here that multiple peaks can occur only when bypass diodes are present within the elements of the PV array which are controlled by the converter/inverter. When no bypass elements are present, simple tracking algorithms can efficiently track the optimal operation point. The Perturbation & Observation and Hill Climbing methods are also referred in this review, which with some modification, such as voltage sweeps and variable steps, can be used to track the GMPP when multiple peaks are present in the P-V curve. Some more advanced bio-inspired techniques are suggested as more appropriate to deal with multiple peaks found in the P-V characteristics. The algorithms and techniques are reviewed based on their cost, their complexity and the required monitoring among others.

In [2] the Authors review several Maximum Power Point tracking algorithms and some of their variations. Algorithms based on the Perturbation and Observation (P&O) technique, the Incremental Conductance method and Intelligent MPPT techniques are examined. They also examine techniques which are designed for partial shading conditions, meaning that the algorithms are designed to locate the GMPP between potentially multiple maxima. Some bio-techniques are also described and deemed more suitable of locating the global MPP among multiple local peaks.

In [12] the Authors focus on methods to mitigate partial shading effects in PV systems. One class of the methods examined includes modified techniques to properly detect the global MPP. The techniques described are the Power Curve Slope, Load-Line Maximum Power Point Tracking, Dividing Rectangles Technique, Power Increment Technique, Instantaneous Operating Power Optimization, Fibonacci search, Artificial Neural Networks and the Particle Swarm Optimization. These techniques are evaluated based on their tracking speed, tracking accuracy, implementation complexity and their convergence ability.

All the methods in this GMPPT category, aim at extracting the maximum power of a static PV configuration under dynamic operating conditions and partial shading. However, when the PV system is subject to partial shading which causes multiple maxima to occur in the P-V curve, the goal of an optimized MPPT algorithm is to successfully locate and operate at the global maximum. This means that depending on the situation a substantial part of the available power which could ideally be harvested in the array is not exploited. That is so because parts of the array are either bypassed or forced to operate far from their optimal point. This will be further analyzed in Section 3.1. For the complex dynamic shading scenarios which are our focus, these losses will occur too frequently to lead to a good overall gain/cost trade-off.

2.2 Alteration of interconnections of system components

2.2.1 Interconnections of PV modules/cells

In [13] the Authors compare the performance of several configurations of the PV array under non-uniform conditions. The configurations examined are Series, Parallel, Series-Parallel (SP), Total-Cross Tied (TCT), Bridge-Link(BL) and Honey-Comb (HC). These layouts of the PV array are shown in Figure 2.1. These configurations are examined with two different bypass configurations, one for each module (36 cells in series) or two for each module. Several shading patterns are examined for different sizes of a PV array. In general, the Authors conclude that in most cases the TCT outperforms the other configurations and

classify the TCT best suited for a symmetrical array size, while the HC configuration is better for asymmetrical array sizes. It has to be noted here, that all configurations present multiple peaks when two diodes are present in the module and the comparison is made on the GMPP of each configuration. This requires an advanced MPP tracker where operation on the global maximum can be ensured. Furthermore, depending on the shading pattern, different configurations operate better. A limitation of this works is that he model used neglects the effects of connecting wires. This is shown by the same performance of all configurations under uniform conditions, where different current levels and length of wires lead to different resistive losses. In [14] a similar study is performed, where two different simulation models are used to compare SP array configuration with TCT, but the study is limited to one shading pattern.

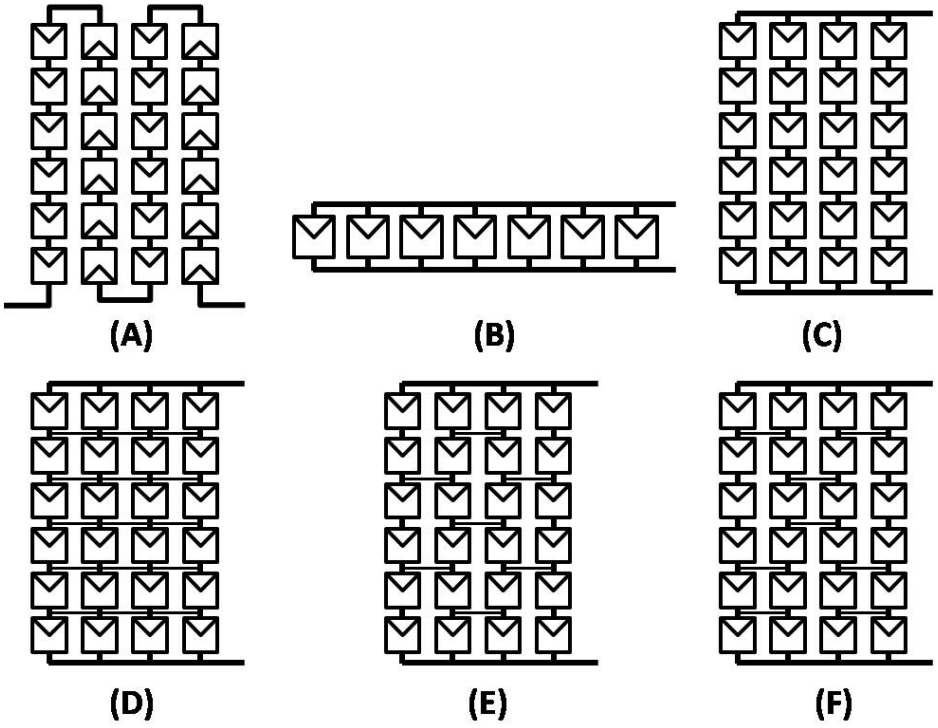

Fig. 2.1 Different interconnection types, (A) Series (B) Parallel (C) Series-Parallel (D) Total-Cross-Tied (E) Bridge-Linked (F) Honey-Comb

In [15] the Authors compare different configurations of the module under different classes of shading patterns and based on the result define rules to come up with optimal configurations shading patterns. As shading is dynamic, the optimal configuration is not universal which further motivates reconfigurable PV arrays. In[5] the Authors compare the performances of SP, TCT, BL and HC configurations under dynamic shading conditions. It is shown through simulation that the TCT increases significantly the power output, but it is

noted that the larger number of interconnections in TCT schemes leads to an increase of the cable losses. In [16] the Authors verify the superior performance of the TCT interconnection scheme of the PV array under conditions of partial shading with experimental results. With the cost of introducing more connections between the PV modules of the array, it is shown that shaded PV modules have less influence on the entire array compared to a simple SP connection scheme. This is validated experimentally in a PV plant which was subjected to static partial shading.

Alteration of the interconnections of the module aims to lessen the presence of multiple peaks in the P-V curve of the array under conditions of partial shading. This is achieved by decreasing the effects of current mismatch by allowing alternative paths between the modules. Under some shading patterns, mismatch effects are reduced and the P-V curve is smoothed, allowing MPPT to successfully track at the optimal point, but for the majority of shading patterns there is little to no gain. The PV array is still subject to present multiple peaks on the P-V curve leading once again parts of the array to be bypassed or produce a very limited amount of energy.

2.2.2 Bypass configurations

Within the module, different bypass configurations have been considered as well. Modules with overlapping diodes and non-overlapping are compared in [6]. Overlapping diodes provide more current paths when the module is partially shaded, but may lead to power consumption on bypassed cells by creating negative voltages across them, while power consumption in modules with no overlapping diodes is limited to the power which is used by the bypass diodes themselves, if no cells are in reverse bias. The Authors note that partial shading losses are dependent on the configuration of the bypass diodes in the array.

In [17] and [18] the Authors investigate the effect of partial shading with two different bypass configurations. It is shown that the most important factor is not the number of bypass diodes used but instead the configuration and the shape of the bypass section matters more. This can be taken into account when designing a PV plant by installing the PV panels with an orientation that is best suited for the expected shade. In [9] a different layout of the bypass sections is proposed which is able to handle better shades moving in different directions.

In [19] two new module layouts with bypass diodes and halved cells are simulated under different shading patterns and compared to a standard industrial PV module. The first module layout consists of six matrices connected in series,where each matrix comprises of two parallel strings of 12 series-connected halved cells. The second one is a series connection of 72 matrices where each matrix is a parallel connection of two halved cells. All layouts, including the industrial one, are equipped with three bypass diodes equally distributed in the

module. They show through simulation results that by increasing the degree of parallelism in the module can improve the performance under partial shading conditions.

It is shown that the reduction of the granularity level of the bypass diodes improves the performance of the PV array, compared to industrial PV modules. Ideally, with a huge cost overhead, bypass diodes could be placed across each cell. When the incident shade blocks all irradiation, thus reducing the power generation ability of shaded cells to zero, bypass diodes provide one of the best solutions. However, in the majority of shading scenarios shaded cells are capable of producing energy. The utilization of bypass elements, apart of the fact that they consume power, aim to bypass shaded cells when the incident shade limits the current of the overall PV array and the energy produced by shaded cells cannot be harvested.

So for the complex dynamic shading patters which are our main focus in this thesis, also this category fails to provide a good gain/cost trade-off.

2.3 Introduction of elements in the PV array

2.3.1 Localization of MPP tracking

In recent years power conversion at the string level (series connected modules) and power optimizers/microinverters at the module level are widely available in industry. Power processing elements and independent control of smaller PV elements is useful to harvest more power from a partially shaded PV plant.

In [20] the benefits of distributed architectures are illustrated for locations where the PV plant is subject to heavily partially shading conditions. However, when the power control is distributed in the PV array, several potential problems may occur and partial shading can still affect the performance of the PV array. In [21] the Authors compare the performance of an array with a central inverter and an array with string level inverters. They note that when distributing control and decreasing the system modularity, the interaction between generator and inverter needs to be taken into account to avoid power losses. In [22] a static analysis of the performance of a distributed system is made. It is noted that when utilizing local converters, depending on the interconnection of converters, mismatch may lead to failure under certain operating conditions. Differences in irradiation (large current mismatches) can lead to current mismatches at the converters. They note that design of converters for PV application should take into account, apart from the efficiency, the expected operating range and the voltage at the input of the central inverter. These issues are addressed in [23] where the Authors investigate power optimization with cascaded dc/dc converters in the module level. They propose an additional control strategy to prevent overload of the dc-bus and to

ensure robustness under rapidly changing irradiation conditions. In [24] the Authors propose an intelligent module equipped with a local dc/dc converter. They investigate and simulate several algorithms and converter topologies for individual control of the module and show that distributed control schemes are more efficient in BIPV systems. In [25] a field evaluation of distributed systems in comparison with a centralized system is done. It is shown that under uniform or light mismatch conditions, a centralized system produces more energy than a distributed system. Under heavily non-uniform conditions the distributed system performs better. In locations where shade is expected, distributed systems can increase the annual energy yield, despite the lower performance in homogeneous conditions. In [26] a performance analysis of different types of configurations of the array, central inverter, module level buck dc/dc converter, module level buck/boost converter and per string dc/dc converter, is made and the potential benefits of distributed control are shown. It is noted that the potential benefits heavily depend of the location of the PV setup and the expected shading patterns of the PV array.

In [27] the Authors develop a detailed model to investigate the effect of localizing the power control units in different levels of the PV array. They consider placement of power optimizers in the string, module, substring (bypass section) and cell level to mitigate partial shading losses. Under the shading scenarios considered, power optimizers in the module level show promising gain, while conversion at the cell level is beneficial when irregular patterns are present. They also compare local power conversion with (theoretical) cell-level bypass diodes. The power generation of topologies with fine-grain bypass diodes or local converters is affected by the size of the shaded fraction and the incident shade density. When the potential energy of the shaded part of the array is significant, power optimizers show more potential. A similar study is done in [28] where the Authors develop a model to simulate the effects of distributed control at the module level and a the cell level. They show opportunities of recovering power in different levels of the array.

A finer granularity level of distribution of power processing elements in performed in [29] . The module is divided into pixels, where each pixel consists of a number of series connected solar cell. Each pixel has a dedicated local dc/dc converter which is responsible to track the MPP of the pixel. Local inverters are also present in the module, where an inverter is connected to five local dc/dc converters. The local converters are cascaded. Thus mismatch due to different current levels can create problems in the interconnection of the converters. Different sizes of pixels are considered, but as the focus of the converters utilized targets low-power IC industry, pixels consisting up to 5 cells are suggested. A scaled-down prototype of two pixels with three cells is tested. The granularity level of this work aims for the independent operation of all pixels. Shading patterns which create significant irradiation

differences between pixels, and thus lead to a mismatch current, will create problems in the interconnection of the converters. Moreover, this will disable the use of all pixels at their corresponding MPP. Moreover, the hardware added in each module is significant and given the power losses under uniform operating conditions, the overall gain of the system is not ensured.

Design of application specific converters for distributed PV arrays are the focus of the work in [30] and [31] . Improving dc/dc converters and module electronics is the focus of research in power electronics. It is however complementary to the focus of this thesis.

Distribution of the power processing units is critical in improving the performance of the PV system in partial shading conditions. However, the presence of bypass diodes in the configuration of the controlled elements still creates multiple peaks in the power curve necessitating the use of complex MPPT techniques. Furthermore, depending on the irradiation conditions, mismatch effects can be moved to the converter stage. The converters must be designed to handle different voltages and their interconnection must ensure that the mismatch of the modules in current and voltage can be handled. When the power processing elements are finer-grained (in the submodule level) the static configuration means that potentially significantly more power is processed than needed. Also losses are clearly present under uniform conditions. Hence, this category is again not sufficiently well suited for reaching the overall gain/cost trade-off in systems with dynamic shading conditions which are our main focus.

In [32] distribution of control is studied by utilizing differential local converters. In principle, these converters process only the excess current under mismatch conditions. Ideally, under uniform conditions the power is only processed at the central converter/inverter unit. In [7] the Authors propose a finer-level of of distributed control in the submodule leve with differential converters. Local dc/dc converters, submodule-integrated converters (subMICs) replace the bypass diodes of a conventional module allowing the power of each bypass section, in this work called a submodule, to be processed separately when needed. As the submodules do not contain any bypass diodes, the voltage that reaches the local converters is similar independently of the shading pattern of the PV array. This allows a parallel connection of the local converters and ensure a steady voltage input at the inverter stage. Although these converters process less power under uniform conditions, parasitic losses cannot be avoided. The cost of each converter does not allow to connect one across every few cells, which means that fine-grained shading patterns induce losses within the module. Furthermore combining the components of Differential Power Processing converters (DPP) with switches is not straight forward and thus reconfigurable topologies can be quite complex to be applied with these elements.

2.3.2 Dynamic elements in the PV array

In [10] the Authors review proposed solutions to deal with inhomogeneity in the PV array. The focus of the review is dynamical reconfiguration of the PV array to optimize performance when mismatch occurs and for meeting load requests, while also examining works which deal with non-uniformity by distributing of the power processing elements. They divide reconfigurable PV systems in three main categories (plus hybrids), based on the available options for reconfiguration, independently of the level where reconfiguration occurs. The three approaches are reconfigurable strings, reconfigurable series-parallel and reconfigurable cross-tied. They then proceed to compare algorithms which control the run-time instantiation of the reconfigurable PV plant. They categorize the control schemes in six basic solutions: Programmed Reconfiguration Algorithms, Exhaustive Evaluation Reconfiguration Algorithms,Sorting Reconfiguration Algorithms, Distributed Reconfiguration Algorithms, Classical Optimization Algorithms and Computational Intelligence Algorithms. A comparison and evaluation of existing architectures and control mechanisms is performed and the advantages and disadvantages of each solution are discussed. The most relevant studies and approaches will be discussed in more detail.

In reconfigurable topologies, dynamic elements are added in the configuration of the array to allow run-time alteration of the connections of the PV elements. One important concept of these dynamic solutions and approaches is the granularity level of the architecture, which is linked to the maximum part of the PV array that has fixed connections, thus no dynamic controllable components. Bypass diodes can be included in elements which are otherwise permanently interconnected and provide alternative current paths in the case of shading within the granularity of the system. The problems and power losses which occur due to bypassing have been discussed in Sections 2.1 and 2.2.2 and will not be further analyzed here as the goal of reconfigurable approaches is to avoid mismatches and bypassing. It is considered here that shading patterns within the granularity of the array cannot be effectively handled. One other aspect of reconfigurable topologies, which is related but not identical to the granularity of the system, is the flexibility of the architecture. The flexibility of the system depends on the number of distinct configurations that are possible for the PV array and the potential independent operation of the PV elements by enabling temporally local power processing. The degree of flexibility provides some insight on the number of different shading scenarios and operating conditions that can be effectively handled by reconfiguration of the array. As dynamic elements are added in the PV array to allow reconfiguration, the current does not flow through the minimal active path. The extra elements consume power either by increasing the resistivity of the active path (switches,extra wires) or by introducing losses due to non-ideal efficiency (power processing elements). These losses have to be taken

into account, as they decrease the performance of the PV system under uniform conditions and consume part of the recovered power when the system is operating in non-homogeneous conditions.

To enable multiple connections of the PV system, additional elements are added in the PV array. These elements, such as switches and local power processing elements increase the initial fabrication cost of the PV system. Reconfigurable PV arrays are characterized by their multiple run-time connections of the PV elements. To determine the best possible configuration at run-time, information about the current operating conditions are needed as input of a control process/scheme which in turn configures the system in the best possible manner. The complexity of this scheme increases the initial manufacturing cost of the PV system. which has to be compensated by the recovered energy. Furthermore, the reconfiguration process potentially results in different series-parallel combinations of PV elements to connect to power processing elements. The ranges of current and voltage which reach the stage of the converter can be quite wide, necessitating the design of a converter which can handle efficiently a wide ranges of operating voltage.

In [33] the Authors propose a reconfiguration procedure to optimize the performance of a PV field which main structure is a parallel connection of two strings of series connected panels. The goal is to ensure that under non uniform conditions, each of the two strings comprises of a modules with similar current. The number of the modules in each string should be sufficient to ensure that the voltage requirements of the inverter are met. Depending on the external conditions, a module can either be completely disconnected from the PV field, or be connected to string 1 or 2. In order to determine the state of each module, the IV curve of each panel is needed. The algorithm allocates certain modules in each string and based on the number of non-sorted modules a heuristic or an exhaustive search determines the state of the rest of the array. The two strings must share a similar voltage. With the presence of bypass diodes, this is not ensured by the same number of modules in each strings. In this approach, partially shaded modules are potentially left out of the configuration and in order to equalize fully illuminated modules can be left out as well. With the addition of a few elements, this topology yields better results compared to a static PV array. However, under certain shading conditions, shaded modules will not contribute to the power generation. As only two PV strings are formed in this topology, when more than two irradiation levels are present, it is not easy to divide the modules into strings. Connecting modules in series which do not have the same current level does lead to mismatch losses, while dropping a module out of the PV array excludes it from any potential power generation. Moreover, partial shading within modules themselves is not addressed. (1)

The number in the parenthesis here is used to refer to this work in Table 2.2, where the advantages and disadvantages of each work are summarized.

A PV array which partially allows reconfiguration is presented in [34]. Their PV configuration is based on the observation that TCT (Total-Cross Tied) interconnection reduces the partial shading losses. In this interconnection, the PV array is organized by having n PV modules in parallel connection (in rows) and m number of such groups connected in series.(Figure 2.1). In order to maximize the production of the PV array, the goal is to minimize the Irradiance level mismatch index, which provides information about the differences of normalized total irradiance in the rows. The PV array they propose may consist of a fixed part and a reconfigurable part or can be totally reconfigurable which allows larger flexibilty. The number of switches required depends on the size of the reconfigurable part and the fixed part. For a layout which has M rows and N reconfigurable modules, a total of M x N switches are required. It is noted here, that the number of rows is constraint by the required voltage of the PV array. To find the optimum configuration, a branch and bound algorithm is needed, where some information of each module's irradiance level is needed as an input. This approach is beneficial when each module is uniform, however non-uniformity within the module itself remains a significant issue and bypass diodes are utilized. So this leads to a too negative cost/gain trade-off. (2)

A similar approach is used in [35] as well. The Authors propose a dynamic photovoltaic array which uses irradiation equalization reconfiguration strategy to optimize the performance under partial shading conditions. Their proposed PV architecture is purely dynamic, in the sense that there is no fixed part and reconfigurable part, but all the modules can effectively change position in a run-time configuration. The main difference with the approach proposed in [34] is the possibility to change the dimensions of the TCT array, meaning that a N by M TCT matrix can become a $N/2$ by $M*2$ TCT layout. This leads to a variable voltage at the inverter/converter and thus the MPPT's characteristics should allow a larger input voltage range. This PV array outperforms conventional PV plants during partial shaded conditions, but the fluctuating voltage in the central power processing unit puts constraints on its design. Once again, finer-grained shading patterns are not addressed. (3)

The Authors of [36] apply dynamic electrical array reconfiguration (EAR) strategy on the photovoltaic generator of a grid-connected PV system based on a plant-oriented configuration to improve its energy production when the operating conditions of the solar panels are different. The proposed worked is similar to the ones proposed in [34] and [35] as the main purpose of reconfiguration is to equalize the current produced by each row of the TCT interconnection of modules. Again information of the irradiation levels of each module is required by the control unit. Once again, the overall performance of the system is

improved for partial shaded PV arrays, but the granularity level of the reconfigurable array does not improve the performance of a partially shaded module. Since bypass diodes are still present in these PV arrays design, multiple peaks can still be present at the central inverter stage, necessitating a complex MPPT algorithm. (4)

A reconfigurable PV architecture with a module level granularity is proposed in [37] and [38]. The basic configuration for this PV system is the central-inverter topology, where the modules are connected in series to form strings, and the strings are connected in parallel and connected to the central inverter. This configuration performs well under uniform conditions, but significant losses occur when the PV array is partially shaded. Under partial shading conditions, the Authors propose a configuration where some complete strings are formed and the remaining modules form a partial string. The partial string is connected to the central converter through a dc/dc converter which ensures that the required voltage is reached. To enable this, a Flexible Switch Array is introduced which allows different connections of the modules. Two buses are available; one to connect the full strings directly to the inverter and one to connect the partial string to the converter. The types of switches introduced are S_{sr} which are used for series connections of modules, S_{by} which are used to bypass a shaded module, and S_{pu}, S_{pd}, S_{nu} and S_{nd} which potentially connect a module to the positive and negative terminals of the two buses. The total number of switches depends on the number of modules (N) in the system and requires four for each module ($4N$) plus two switches for each busline. So this amounts to a large amount of switches for practical module topologies. In order to find the optimal configuration, thus the position of each switch, a controller is utilized which requires measured current and voltage of each module. The shaded modules are bypassed through the bypass switch, while the rest (active modules) either form only full strings or full strings and a partial string. This depends on the number of active modules. This can be beneficial compared to a fixed array, however non-uniformity within the module itself is not addressed. Furthermore a shaded module is bypassed and cannot contribute to power generation, even if the amount of shade allows a considerable amount of power to be harvested. (5) (6)

The Authors in [39] also consider a PV array with reconfigurable switches. The modules used in this work are slightly different from industrial modules, as they are comprised of 10 series strings with 20 parallel cells in each string. Modules with and without bypass diodes are examined. When bypass diodes are used, they are placed in parallel to each string of the module.The PV array presented is a 3x4 TCT layout and 28 switches are required for the proposed approach. In the general case of an array of NxM modules, the number of required switches is (2*N*M+M). In order to select the optimal configuration for specific external conditions, voltage and current information for each module are required. Based

on that information, potential values for the current and the entire array are selected. If a module, due to shading, cannot meet the requirements for the power generation, it is dropped out of the run-time configuration. Compared to a fixed configuration, the Authors prove that this reconfigurable approach can improve the overall performance of the PV system under non-uniform conditions of the PV array. However, the switches mainly function as bypass elements for shaded modules which could potentially contribute to the generated power. Moreover, when modules equipped with bypass diodes are used, the power curve of the array may have multiple peaks. This requires an advanced MPP tracker to ensure operation on the optimal point or the control algorithm of the switches should predict the appropriate operating point. (7)

A dynamic configuration of the PV array with a module level granularity is proposed in [40]. The main structure of the PV array is a SP connection of the modules. Modules are connected in series to form strings and these strings are then connected in parallel to form the array. The main concept is to optimize the connections of the modules depending on the external conditions. In order to avoid mismatch, each module of the string must share a similar current. The parameters of the modules are estimated by measuring the IV curves of the strings.This method works as the modules in this work are considered to have only one diode/module. In a reconfigurable array where all the modules are flexible, the potential configurations of an array (with limitations on the input voltage of the inverter) in a SP connection are less than with a TCT connection, rendering finding the optimal configuration in a SP connections simpler. However, the Authors claim that with modifications, the monitoring procedure and proposed algorithm can work with TCT arrays. Once again the architecture granularity and the need of similar currents through the modules of the string translate in potential power losses under partial shading conditions. (8)

In [41] a dynamic topology of a module is proposed, which consists of a fixed part and a solar adaptive bank. The fixed part is formed by a M by N structure of cells connected in a TCT interconnection, while the adaptive bank has M solar cells. The same principles can be scaled up to PV modules instead of PV cells. Under uniform irradiation, the adaptive bank is utilized by forming one additional column to the fixed matrix. By including M^2 switches, the cells of the adaptive bank can connected to any row of the fixed array. The goal is to ensure that all rows have similar current. They propose two algorithms to reconfigure the PV structure. A bubble-sort method which requires voltage monitors on the rows of the fixed array and the cells of the adaptive bank and a model-based method which estimates the currents of the rows of the fixed structure and the adaptive bank. Depending on the shading conditions, the cells in the adaptive bank may not be sufficient to equalize the different currents of the fixed array. Furthermore, if this approach is applied in solar cells, it requires a

significant number of monitors, while if modules are used presence of bypass diodes may still result in power losses due to bypassing withing the module itself. (9)

In [42] a similar approach as in [41] is used, but with a finer granularity. A fuzzy control algorithm is used to determine the optimal configuration depending on the irradiation conditions. A solar panel is divided into a fixed and reconfigurable part. However, the finer granularity in this approach requires monitoring devices in lower level to estimate the shading conditions of each row of the TCT interconnection to feed the control algorithm. (10)

In [43] and [44] the Authors propose a reconfigurable PV module architecture to mitigate the effects of partial shading. The granularity level of the architecture is on the cell/macro-cell level. Cells are organized in a rectangular layout and each cell, with the exception of the last cell of the module (output) is equipped with three switches. Two of the switches enable the potential connection of neighboring cells in parallel, while one switch potentially connects neighboring cells in series. Based on the observation that the Vmpp is less susceptible to external conditions under partial shading conditions, the cells of the module are divided into groups of parallel connected cells. These groups are then connected in series, leading to the requirement of each group having a similar overall current. They claim that this principle can also be applied in multiple PV modules connected in series, without adding any extra conversion elements, where all groups of the PV modules involved have to share a similar current. The optimal configuration is chosen by a processor programmed with an appropriate control algorithm. Required input information for the controller are the irradiation levels of each cell. The algorithm tracks the optimal configuration by taking into account variable conversion losses, thus once the desired input of the converter is decided, the best division of each module for the specific irradiation conditions can be found based on principles of dynamic programming. The cell used in this work has a power of 1.2W in STC, with a short-circuit current lower than 0.6A and a open-circuit voltage of 3.3V. These characteristics, which are far from the ones of industrial cells, allow resistive losses to be negligible. This means that the benefits of this approach requires cells with low current. (11) (12)

A dynamic configuration in the module level of the PV array is also discussed in [45]. A reconfigurable PV array with two states is proposed. Once again, the observation is that a parallel connection of PV units is most resilient to partial shading conditions. The initial PV array comprises of an SP array of n parallel connected strings with m series connected modules per string and this is state 1 in this work (m by n). By utilizing some switches and bypass diodes (n swtiches and n*2 diodes), the system can by reconfigured to form a new array with a dimension of ($m/2$ by $2n$). Having less modules connected in series and increasing the parallel connections renders the system more resilient in partial shading. Some strain is put to the central converter/inverter as the voltage at the input of the power unit can

vary significantly. The simplicity of this architecture of having two possible states, allows selection of the best configuration by comparing the two respective GMPP. However, as bypass diodes are still present within the module, partial shading in the module can result into power losses and locating the optimal operation point of each configuration requires an advanced MPP tracker. (13)

In [46] a dynamic PV architecture is proposed where the granularity is on a substring level. Each substring consists of a number of series connected cells. The substring discussed in this work consists of 24 solar cells with no bypass within the substring, but the size of the substring can be easily changed. They propose an array connection by creating power channels of series connected substrings. Each power channel contains substrings with a similar instantaneous power level and has a dedicated dc/dc converter. In order to allow different configurations of the array, switches are introduced. The number of switches needed depends on the number of substrings in the array and the number of power channels (dc/dc converters). As each substring is potentially connected to any channel, the number of switches required are $3 * N_s * N_c$, where N_s and N_c the number of substrings and channels respectively. The number of available channels determines the number of clustering (different irradiation groups) which can be succesfully handled by the dynamic PV array. The position of the switches is determined by a control algorithm which requires measurement of IV curves from all the substrings in order find the optimal configuration for the run-time operating conditions. As the substrings are divided into groups based on their current generation, each channel may contain a different number of substrings. The local converters must be able to handle the potentially wide range of voltage input. The Authors prove through simulation that this approach can yield better results for different irradiation conditions compared to static arrays and dynamic arrays which are based on the concept of irradiance equalization in TCT topologies. Although the granularity level is finer than that of a module, non-uniformity within the substring can still be an issue. By decreasing the size of each substring however the number o switches required for a same sized array can be significantly high. (14)

In [47] a different reconfiguration approach is discussed. The basic architecture of a parallel connection of strings (cells connected in series) is maintained, while each cell is equipped with extra elements allowing it to temporarily be bypassed from the array. The time-domain array-reconfuguration (TDAR) allows each cell to be active for a certain period of time, depending on it's relative operating conditions to the string it is connected, and in bypass mode for the reminder of the cycle. Each string is defined by the most powerful cell, which ensures the minimum required voltage for the power processing unit and determines the current of the string. By tracking the power of each cell and with a bypass capacitor, each cell contributes its maximum power to the string. The bypassing - or inactive cells in certain

moments causes voltage fluctuation of the string which are handled by a boost converter to regulate the voltage. This approach requires extra components per cell and leads to a trade-off on the power processing unit which should be able to handle voltage fluctuations. (15)

In [48] a reconfiguration array where a cell level architecture of a PV module is presented. Each cell of a 4 by 4 structure can be connected to any of the cells of the array with the help of a switching network. Each cell is equipped with a bypass diode. A microcontroller is utilized to arrange the configuration of the array based on information on the current levels of each cell which are obtained based on information of the bypass diodes. The case considered in this work is one where a cell is either illuminated or completely shaded. Thus all shaded cells are removed in the array. The reconfiguration aims to eliminate multiple peaks on the PV curve and enable a simple algorithm to track the MPP of the cells. To enable such a structure, multiple hardware is required and when more irradiation levels are present, the reconfiguration strategy is unclear. Moreover, the PV array described can result to parallel strings of cells where each string having a different number of cells, thus leading to potential voltage mismatches. (16)

The advantages and disadvantages of each study are summarized in the following Table. Notations are High (H), Medium (M) and Low (L). The first four characteristics refer to energy generation, where the best value is High (H). The next four involve the extra cost elements of each approach, thus the optimal value is Low (L).

	(1)	(2)	(3)	(4)	(5)(6)	(7)	(8)	(9)	(10)	(11)(12)	(13)	(14)	(15)	(16)	PROPOSED
Granularity	L	L	L	L	L	L	L	M/L	M/L	H	L	M	H	H	M
Energy in uniform conditions	H	H	H	H	H	H	H	M	M	L	H	M	M	M	H/M
Flexibility	L	L	L	L	L	L	L	M	M	H	L	M	L	H	M
Lack of activity of local power process unit	H	H	H	H	M	H	H	H	H	H	H	L	M	H	M
Control Algorithm	M	M	M	M	M	M	M	H	M	H	L	H	L	H	L
Switches Overhead	?	L	L	L	L	L	L	H	H	H	L	H	L	H	M
Converters Overhead	L	L	L	L	M	L	L	L	L	L	L	M	H	L	M
Range of power processing unit	M	M	H	H	M	M	M	M	L	M	M	H	M	L	L/M

Fig. 2.2 Advantges and Disadvantages of each approach

Patents

(1) In [49] the Inventors introduce a dynamic PV array which comprises of two run-time instantiations. The granularity level is on the level of a number of cells. Each row of the

panel is divided in two strings of permanently series connected cells and they specifically design for four rows of cells. Depending on the operating conditions, the array either operates by each row forming a string of series connected cells or by connecting in parallel the two parts of a row and having short strings with half the number of cells. The switching occurs mainly depending on the operating conditions and the load demand and is targeted for space applications. The proposed configuration has a relative simple switching circuit and control and thus a low fabrication cost overhead. However, the two types of configuration allows gain for specific shading patterns, but no gain for many others. As a result it is even possible that the overhead incurred by the additional circuits dominates the achieved gain. Even an overhead of 1% under uniform irradation conditions will typically neutralize the non-uniform gains unless the latter occur sufficiently often.

(2) An architecture for configuring the cell interconnections is introduced in [50]. The Inventors propose a fully regular/uniform very fine-grain grid-like interconnection network placed between the cells of a panel, allowing to interconnect cells in any sequence and any configuration (series or parallel). The configuration of the network can be performed at manufacturing time, or at in-the-filed operation if switches and a controller exist. This is a very broad patent which includes a lot of possible configurations. However, the Authors do not provide information on the optimization of the configuration depending on the operating conditions, but focus on the reconfiguration itself, the transistors, the mechanical switches, wires that are cut or overloaded like fuses. So this cannot be compared directly to our proposals due to missing information.

(3) (4) In [51] the Inventors propose a dynamic architecture at the module level, where the interconnection of the modules in series or in parallel is decided at run-time.Multiple inverters can be utilized. As the reconfiguration takes place in the module level, non-uniform conditions within the module cannot be handled and are not addressed. A similar approach for module level reconfiguration is used by the Inventors in [52]. These patents have a simple switching circuit and a relative low fabrication cost. They provide some gain for specific coarse-grain shading patterns, but the static configuration at the module level does not allow gain in fine-grained shading patterns. As a result it is likely that the non-zero overhead incurred by the additional circuits dominates the achieved gain. It will depend on the types of non-uniformity the panel is exposed to.

(5) In [53] reconfiguration of cells takes place altering the number of interconnections of series and parallel cells to ensure a required voltage output for a load. They turn parallel connected strings into series connected strings to boost the voltage when a minimal voltage threshold is not met any longer. Again the additional circuitry is simple with a low fabrication cost overhead. Reconfiguration occurs only when a voltage threshold is not met and this work

is not intended at all to deal with imbalances within the PV array due to non-homogeneous operating conditions.

(6) In [54] a structure is proposed, where local power elements are placed for a number of cells. Each local inverter/converter tracks the individual operating point of the dedicated cells and reconfiguration occurs after the local power units to control the flow to the load. Multiple local dc/dc converters are needed, but a relatively small network of switches and wires. The static cell string configuration so will only give gain for specific shading patterns, and not for many others. The microconverters need to have a high efficiency to allow the losses to be lower than the gains. And as a result the fabrication cost overhead will be quite high and strongly negatively affect the overall gain/cost trade-off.

(7) In [55] reconfiguration is possible between all of the cells because at the very lowest levels switches are present. These switches are considered to be part of a "printed circuit board" and they appear to exclude the case where these switches would be tighter integrated on the solar module substrate. The goal of the reconfiguration is to allow the array to meet the power requirements of the load. When a voltage threshold is not met yet, more cells are accumulating the voltage up till that threshold. No local conversion is present and the cell array can be susceptible to mismatches. This allows a high flexibility for the module,but requires a high fabrication cost as each cell is equipped with switches. The absence of any local power processing elements means that certain imbalances cannot be mitigated. The limitation of the PCB implementation makes this also not suited enough for today's fabrication technologies.

The advantages and disadvantages of the above patents are summarized in the following Table.

The proposed approach aims to recover power under multiple operating shading conditions. The goal is to increase the flexibility of the module, while limiting the losses under uniform conditions. Reconfiguration allows the development of such a method which is discussed in the following chapters.

	(1)	(2)	(3)(4)	(5)	(6)	(7)	PROPOSED
Granularity	M	H	L	M	L	H	M
Energy in uniform conditions	H	L	H	H	M	L	H/M
Flexibility	L	H	L	L	M	H	M
Lack of activity of local power process unit	H	H	M	H	L	H	M
Control Algorithm	L	?	M	L	M	M	L
Switches Overhead	M	H	L	L	L	H	M
Converters Overhead	L	L	L	L	H	L	M
Range of power processing unit	M	M	H	M	M	M	L/M

Fig. 2.3 Advantges and Disadvantages of each approach (patents)

Chapter 3

Concepts of Reconfigurable Topologies

The main goal of reconfigurable topologies is to increase the energy-yield production of the PV array by allowing the module to adapt to the external and internal operating conditions. The reconfiguration approach that is applied here aims to allow the majority of cells to operate close to their optimal point by avoiding mismatch effects. This is achieved by refining the granularity level from PV module to groups of cells (cell-string) and enabling independent operation of groups of cells depending on the operating conditions of the module itself. Each group of cells is connected separately to a local converter, which tracks the optimal operation point of the group. This is enabled by including in the module's topology a supporting electrical network at design time. This supporting network consists of potentially extra wires, switches, local converters, bypass diodes, controllers and allows multiple instantiations of the PV module at run time.

This chapter includes a motivational example for applying this reconfiguration approach in PV modules and then cost aspects which are taken into account. Next, the basic concepts of the reconfiguration approach that is applied are introduced, namely exploration of the granularity level of the module, the supporting electrical network and their interconnections. Finally, the run-time instantiations of such reconfigurable modules are discussed.

3.1 Motivation for Reconfigurable Topologies

The goal of the following example is to illustrate the benefits of reconfigurable topologies compared with conventional series-connected modules under non-uniform operating conditions.

A partially shaded industrial module is illustrated in Figure 3.1. The I-V and P-V curves of the module for two different shading densities are shown in Figures 3.2 and 3.3. The position of the bypass diodes and the shape of the casted shadow create two local maxima

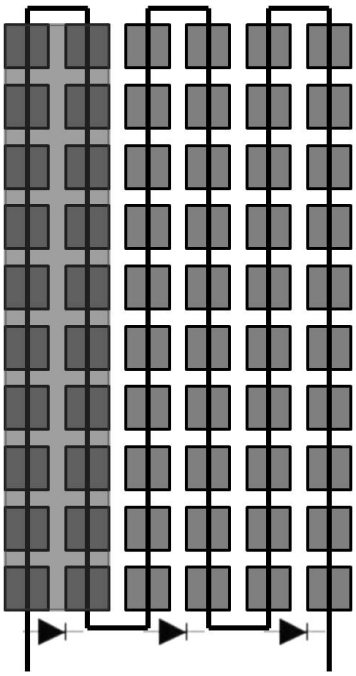

Fig. 3.1 Partially shaded conventional PV module

on the PV curve. The instantaneous curves corresponding to the industrial template of a PV module can be divided in two regions, where in each region the active current path differs. In the first region (low voltages), the bypass diode across the shaded cells conducts the excess current of the fully illuminated cells. In the second region (high voltages), the overall current is limited to the current produced by the poorer cells and no diode is active. Depending on the density of the casted shadow, thus on the current produced by the shaded cells, the position of the global MPP differs and can be located either in region I or region II. In both cases there is a power loss that can potentially be recovered.

The ideal power produced by a PV module is the output of a custom designed topology for the specific operating conditions and shading pattern. Adding the individual maximum power points of all cells is an unrealistic estimation of the ideal power. A custom topology should extract the maximum available power of the module, including resistive and conversion losses. Custom topologies do not have bypass elements or dynamic elements (switches). Given an N by M layout of cells and a known operating scenario, a custom topology is designed to extract the maximum power with the minimum losses. Hence that will be our practical ideal reference point for comparison. Obviously, these custom topologies are in practice not really usable because the operating points will vary over time. So very quickly this will also give rise to additional shading losses.

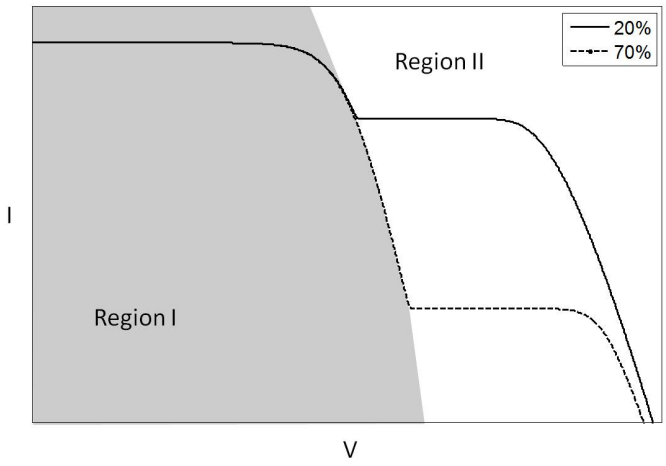

Fig. 3.2 I-V curves of conventional PV module under different densities of partial shading

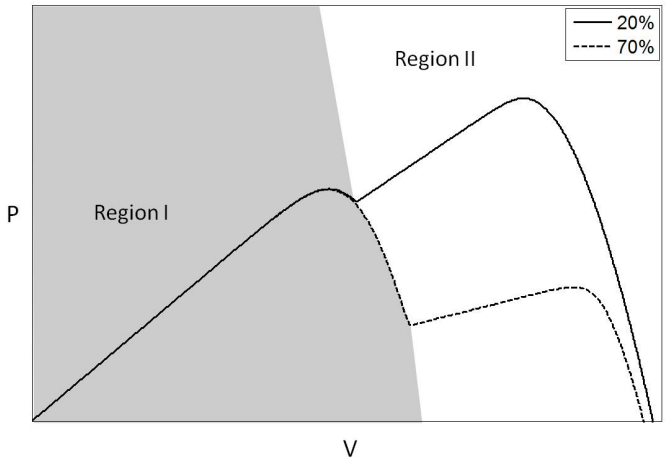

Fig. 3.3 P-V curves of conventional PV module under different densities of partial shading

When the MPP of the conventional module lies in region I, the power recovered by the custom topology originates from the shaded cells which would otherwise be bypassed. In the case where the MPP lies in the second region, power is recovered from the fully illuminated cells where the current is no longer reduced, due to the connection of shaded and unshaded cells with individual converters.

Reconfigurable topologies aim at enabling as much as possible independent operation of groups of cells with different operating conditions. The goal is to enable at run-time, a module configuration which can harvest energy as close as possible to the energy produced by a custom designed topology for the specific operating conditions, while still taking into account the increased manufacturing cost of extra components.

3.2 Gain-cost balance of reconfigurable PV modules

The goal of the proposed approach is to increase the overall energy-yield of a PV by enabling control in the submodule level. It is evident that additional elements required for the fabrication of reconfigurable modules increase the manufacturing cost. Furthermore, the added elements in the active current path induce power losses which should be taken into account. The main cost aspects for designing reconfigurable module are discussed now in more detail.

The gain of reconfigurable modules stems from energy recovered during non uniform operating conditions. When cells of the module have different I-V characteristics, altering their interconnection can increase the overall performance of the module and whenever non-uniform conditions are present, a reconfigurable module can recover energy which otherwise would be lost. Degradation of cells through time can also lead to non-uniformity and under such degradation conditions, the use of reconfigurable topologies can be very beneficial. The expected level of non-uniformity within the module plays an important role to the overall gain which can be obtained by applying reconfiguration. This energy accumulates throughout the lifetime of the module.

Reconfigurable modules require inclusion of additional elements in the module.These elements introduce resistive losses when they are active. The goal of reconfiguration is to come as close to a custom designed topology for the specific operating conditions by utilizing dynamic and knob-controlled elements. Given that extra devices are present, the active current path deviates from the minimal required, and part of the energy is consumed in additional resistive losses. What should also be taken into account is degradation of the extra components through time, leading to additional inefficiencies. Furthermore, these elements

occupy area which is excluded from producing any energy. All these energy losses are again accumulated throughout the lifetime of the module.

Finally, the investment cost has to be taken into account. This mainly involves the initial cost of the module; cost of additional elements, manufacturing, fabrication cost and maintenance cost.

The recovered energy and the energy losses can be expressed in financial terms by applying Feed-in tariffs (reference) and also by considering the savings due to self-consumption. This allows the formulation of (1), where $G(t)$ and $C(t)$ are the gain and cost which accumulate over time respectively, T is operation time and IC is the investment cost.

$$T * (G(t) - C(t)) - IC > 0 \tag{3.1}$$

A positive value of the left part of 3.1 translates to a gain which compensates for all the cost. The dominant cost aspect is the time dependent cost which is present whenever the module is in operation. Thus, the electrical losses are the most significant cost factor over a long-term usage in an environment where non-uniform conditions are reasonably common but where uniform conditions still occur for the majority of the time. Our goal is to maximize the time-dependent (gain-cost) term through improving the time-dependent gain, while simultaneously reducing the time-dependent cost. And as an overall design constraint, we should maintain a reasonable investment cost because manufacturers do not want their sales prices to be much above the one of standard modules. These cost aspects are partly dependent on one another. To increase the power harvested under partial shading conditions requires flexibility and a finer granularity level which in consequence increases the time-dependent cost as more resistive elements are present and the investment cost as the module becomes more complex.

3.3 Cell-string selection guidelines

First of all, the term cell-string should be defined. For the purpose of this work, a cell-string is the minimum power generating unit/element of the PV module/array and consists of cells connected permanently in series. The purpose of dividing the module to cell-strings is to have a knob-controlled series/parallel connection that allows the grouping of cell-strings which function under similar conditions. This enables reduction of mismatch effects that cause a decreased energy-yield and improves the module life time (component reliability impact). Each group of cell-strings is connected to a local dc/dc converter where the duty cycle, and

thus the voltage, is set to the near-optimal value for the specific group of cell-strings for the specific operating conditions.

In a conventional topology of the module, a bypass section can be interpreted as a form of a cell-string. Depending on the run-time conditions and the chosen operating point, the bypass diode corresponding to a specific bypass section is either active (bypassing the current and excluding the cells from power generation) or is inactive and the cells contribute to the overall power. Shaded cells within the bypass section cannot be distinguished and separated and the conditions of the poorest cell determines the state of the entire bypass section. When dividing the module into cell-strings, the series connection will cause the poorest cell of the cell-string to impose its limited current generating ability on the others.

Factors of selecting cell-strings:

- Size of cell-string: As a cell-string is formed by connecting cells in a series connection, it has to be noted, that non-uniform conditions within the cell-string cannot be addressed. If part of the cell-string is shaded, the entire cell-string will have a poor performance. A trade-off exists between generated power and architecture complexity. Ignoring power dissipation by additional elements, a fine-grain cell-level fully configurable architecture is optimal for power generation, but requires a complex supporting network of wires and switches to achieve a reasonable flexibility. On the opposite side, a conventional module with permanent series connection of cells has minimum manufacturing cost, but that option performs poorly under partial shading. An appropriate size has to be determined which balances the overhead cost and the flexibility of the module. The goal is to find a size of the cell-string that resides on the Pareto optimal trade-off curve, which will typically result in an intermediate value. Note that in practice the Pareto curve will be geo-location and plant specific. We expect however that the balanced cell-string size will be suitable for many plants in a region with similar meteorological and environmental conditions.

- Geometry: The geometry of the cell-string should not be confused with its size, although there is a correlation. As with bypass sections, the shape of the cell-string plays an important role under partial shading conditions. It is evident that cells belonging to the same cell-string should be in close proximity to ensure that there are minimum resistive losses within the cell-string. Additional wires to interconnect cells further apart leads to constant power losses due to the extra wiring required. Another aspect of determining the shape of the cell-string is to increase the possibility that an incident shade does not affect all cell-strings within the module.

- All cell-strings should optimally have the same size: As cell-strings are potentially grouped at run-time in parallel, the cell-strings must have the same number of series connected cells. It is possible to have two types of cell-strings in a module, but that would prohibit their parallel connection and the flexibility of the module will be reduced. It would also add to the manufacturing cost. So in this thesis, we will not further study this non-uniform size direction.

3.4 Supporting electrical network

The division of the module to cell-strings determines the granularity of the PV system. In order to extract power from the module, the cell-strings must be interconnected and connected to local power processing units. This is enabled by a supporting electrical network consisting of switches, extra wires and local dc/dc converters. As multiple run-time instantiations of the module are required to optimize the performance for different operating scenarios, multiple potential connections are enabled through the supporting network. The supporting electrical network can be divided into the interconnections between the cell-strings, the interconnection between the local converters and the connections of the cell-strings to the converters.

3.4.1 Inter-connections of Cell-strings

Once the module is divided into cell-strings, the cell-strings can potentially be interconnected in series, to increase the output voltage, or in parallel, for current increment. The cell-strings connection is configurable and it is decided at run-time which ones to group, mainly depending on how strongly they share similar electrical characteristics. Within a group, the current or the voltage of the cell-strings at their MPP should be similar. When the cell-strings within a group share the same voltage and current, this allows a choice between the type of connection of cell-strings and an important trade-off is involved here.

Series Connection

Series connections of two cell-strings requires one switch between the positive terminal of one cell-string and the negative terminal of the other cell-string. In order to avoid mismatch effects in a series connection, the cell-strings must share a similar current. In the series connection, the current of the connection is equal to the current produced by a single cell. As the current remains low, the losses in the resistive elements of the active path is low as well which is the main advantage of this type of connection. The voltage however is accumulated and surrounding switches which are inactive must withstand higher voltages

necessitating the use of larger and more expensive switches. Moreover the voltage of a group becomes unpredictable due to the voltage accumulation between cell-string and constraints like a larger input voltage range handling are forced to the local converters, making them less reliable, less efficient and more expensive. Another disadvantage of the series connection is the large dependency of the current on the operating conditions, thus the requirement of two cell-strings to share the same current for series connection may become harder.

Parallel Connection

Parallel connections of two cell-strings require two connections. One switch connects the negative terminals of two cell-strings while another switch connects the positive terminals of the same two cell-strings. The current accumulates, thus the resistive losses of succeeding wires and switches increase. The voltage of the group remains low and is equal to the voltage of a single cell-string (thus that voltage depends on the number of cells within the cell-string) while the current is the sum of the current produced by all the individual cell-strings of the group. The main advantage of connecting cell-strings (consisting of the same number of cells) in parallel, is that the voltage does not shift so much under different operating conditions. This renders mismatch effects on potential parallel connections unlikely. Parallel-connection leads to higher input current for the local converter, thus creates a wider input current range. The consequence is usually higher converter cost or lower efficiency at high current.

The supporting electrical network in principle should allow the potential interconnections of the cell-strings either in series or in parallel. When all interconnection are rendered possible, the size of the network is extensive. To provide some insight, in a module with N cell-strings, the number of potential series connections is N*(N-1) and the number of potential parallel connections are N*(N-1)/2. The number of potential group divisions of the module follows the Bell number sequence.

If all possible series and parallel connections are taken into account, the overhead caused by all the extra wires will lead to a decrease of the overall efficiency. The connections which are possible should be limited by removing long wires and connections which are less needed. The former anyway impose too much overhead compared to their expected gain. And the latter can be replaced by others that provide nearly the same overall gain at a lower cost/loss. Moreover, when they are not needed in order to enable an improvement of the energy yield or life time, then the switches and other added components should as much as possible be "hidden" from the dominant active paths in the topology. In the conventional approach, these added components do contribute continuously to the dominant active paths and hence cause a near-permanent overhead in power and reliability losses. We want to avoid that by the choice of our knob-controlled topology.

Note that as already motivated in Subsection 3.2 and formula 3.1, cost and gain should be seen here in a 3-dimensional objective space of time-dependent gain, time-dependent cost, and initial investment cost. Depending on the selection of cell-string and placement and number of local converters, decisions on pruning of more connections is made and will be analyzed in further chapters.

The interconnections of the cell-strings lead to the division of the module into groups of cell-strings. Since the current and the voltage of each group can differ, to extract the power, local converters are required. The maximum number of local dc/dc converters is in principle the number of cell-strings in the module. The number of local converters determines the number of different operating conditions that can be handled by our proposed type of reconfigurable modules. It is however unlikely and hence not efficient to have every single cell-string connected to a converter. This would lead to a local distribution of control rather than a reconfigurable module topology. The number of available local converters should be able to handle the majority of realistic shading patterns, but the use of more converters than necessary can lead to a decrease of the performance by increasing the active current path. Although the number of available converters is a parameter in reconfigurable topologies, the proposed range of this parameter is between 2 and maximally half the number of cell-strings.

Interconnection of converters

Each active local converter tracks the MPP of its corresponding group at run-time. The current and the voltage of each group can differ, but the outputs of the local converters have to be interconnected so each PV module has a single input and output point. The duty cycles of the converters are a suitable knob to enable different connections of the outputs. The two basic options, when connecting two components are voltage increment and current accumulation.

Voltage Increment When the converters are connected in series, as depicted in Figure 3.4, the output voltages of the converters are added up. The total voltage of the configuration is the addition of all the voltages at the outputs of the converters, while the same current should flow through the output of all converters. Since the current at the output stage of all converters has to be equal, the duty cycles of the converters should allow regulation to ensure it. The conversion range of the converters of course limits the maximum irradiation difference of the groups of cell-strings. In the case where the current difference exceeds the maximum limit, all available power cannot be recovered any longer and this quickly adds to a high practical energy yield loss. It is clear from this that the duty cycle of the converters

which are active in each configuration cannot be chosen independently, so guidelines can be derived from the above reasoning.

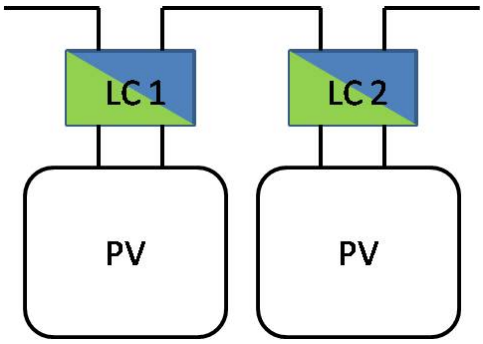

Fig. 3.4 Series connections of the converters

The purpose of having multiple converters is to be able to dynamically, at run time, decide the number of groups of cell-strings that need to be formed, and connect each group to a converter to track the optimal operation point. Not all local converters are necessarily active in a run-time instance of the module. A network of wires and switches is required to allow the "bypass" of unnecessary converters. Figure3.5 depicts the proposed minimal network of switches required to allow a dynamic number of series-connected converters to be active at run-time. This can be extended to any number of local dc/dc converters.

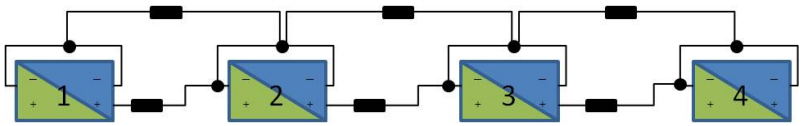

Fig. 3.5 Dynamically configurable series connections of the converters

Current Accumulation In the parallel connection of the converters, the outputs of the converters are connected in parallel (Figure 3.6). The current at the output stage of the converters are added, while the voltage should be the same at the output of all converters. The duty cycle of all converters should be regulated to ensure that the voltage at the output stage is the same. As in the series case, the duty cycle of the active converters cannot be decided independently. All groups must be able to reach the common voltage of the module's output. In this case the conversion range of converters limits the maximum voltage difference of the groups. High voltage differences unavoidably lead to power losses and to reduced life time.

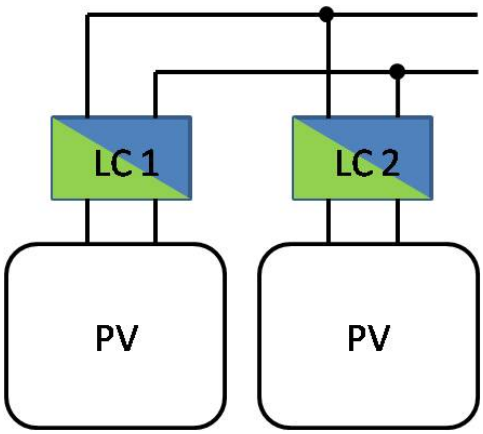

Fig. 3.6 Parallel connection of two converters

The minimal network of switches required to dynamically alter the number of active parallel-connected converters is shown in Figure 3.7. Also this can be extended to any number of local dc/dc converters.

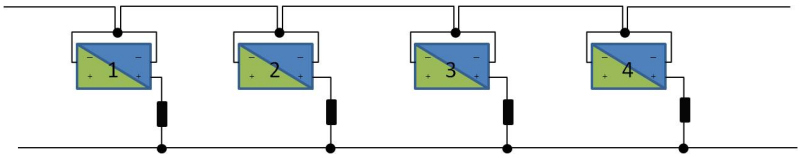

Fig. 3.7 Dynamically configurable parallel connections of the converters

Another way to have current accumulation at the converter stage is to connect the local converters in a cascaded way. A cascaded connection of two groups of cell-strings is illustrated in Figure 3.8. In the cascaded connection of the converters, the output voltage of the previous in chain converter is connected to the input of the next converter, in parallel to the group corresponding to the latter converter. The current is accumulated as the output of a converter is connected in parallel to the input of the next converter. With this type of connection between the converters, the power of each stage is reduced (depending on the efficiency of the converters). The output of each converter has to be set (by altering the duty cycle) at the voltage of the MPP of the next group of cells. The only "free converter" (in terms of value of the duty cycle) is the last one. The current produced by all cells is added, while the obtained voltage is equal to the voltage of the last group of cells (after the conversion stage). The voltage of each group (with the exception of the last group) must be able to reach the voltage of the MPP of the next group (conversion factor of the converters applied). Groups whose voltage difference is larger than the conversion factor cannot be connected.

The main advantage is the flexibility we now have in the duty cycle of the last converter. The main disadvantage of the cascaded connection of the converters is the continuous power losses due to multi-stage conversion and conversion efficiency. Furthermore, the converters must be able to both step up and step down the voltage, depending on the MPP voltage of each group and the input current of each converter increases as we move along the converter chain. So the proposal is to use this only as the very last stage in the converter chain where the added flexibility enables a better dynamic match with the optimal module or string level converter input range under different shading conditions.

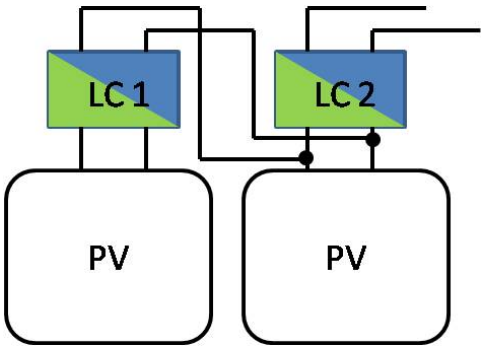

Fig. 3.8 Cascaded connection of two converters

The network of switches required to dynamically alter the number of active cascaded converters is shown in Figure 3.9.

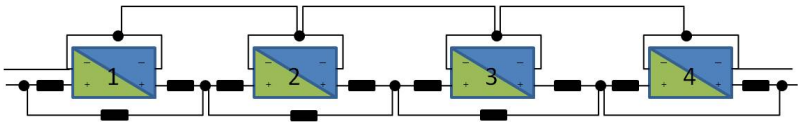

Fig. 3.9 Dynamically configurable cascaded connections of the converters

Control scheme of the converters duty cycles

As mentioned in the first part of Subsection 3.4.1, when the converters are connected in series, they are required to have the same current. The module is supplied by a current source and all converters adjust their duty cycle to extract the maximum power from their correspondent group while maintaining the imposed current at their output.

In the types of connection discussed in the second part of Subsection 3.4.1, all the converters share the same output (parallel connection) or share their output with the input of the next group (cascaded connection). In both cases, a steady voltage is applied between the

single input and output pin of the module. Each local converter is equipped with a simple MPPT. In the parallel case, each converter can operate independently and track its group MPP. However, in the cascaded case the last group's MPP affects the duty cycle of the previous converter as discussed in Subsection 3.4.1 and thus the latter will have to be readjusted.

In order to have low-cost local converters, a module converter should be used to act as a intermediate step between the local converters and the rest of the PV array. The module converter will process all the power and will likely be more expensive and complex, so that so that it can take care of both controlling the local converters output, and adapting the current/voltage level of the PV module to the string requirements.

3.4.2 Connection of cell-strings to converters

Building a network which allows all possible connections of the converters is extremely expensive and inefficient. In Subection 3.4.1 the possible connections between cell-strings are discussed and in Subsection 3.4.1 the possible connections between the converters are analyzed. An important stage which affects both decisions is how the groups are connected to the converters.

Each group of cell-strings, requires its corresponding input and output to connect to a single converter. Each choice of connection scheme of group and converter interconnection lead to a different wires required in the supporting network. In each case, the evaluation is performed by the complexity of the network and the possibility of mismatches in the converter stage. In principle, it makes sense to increase the same parameter in both stages.

Series-Series A group which is connected in series requires the input and output of the group to connect to the same local converter.If negative and positive terminals of cell-strings are connected to only one local converter this may lead to a group formation where the input pin and the output pin of a group are connected to different converters. When the outputs of the converters are connected in series, it is shown that the input of a group can bypass an inactive converter (Figure 3.5) and the input can reach the converter where the output pin is connected. If the converter which needs to be bypassed is active however, the input and the output of the group cannot reach the same converters. This necessitates multiple connections of both input (negative) and output (positive) pins to the local converters, which means a rather complex wire network. In order to prevent power loss in the converter stage, all groups must be able to reach the same current output. The overall current of each group of series-connected cell-strings is equal to the current produced by the poorest cell in that group. This mainly depends on the irradiation level, as the current is proportional to the incident irradiation. The irradiation difference within the module can surpass the conversion factor of

the converters. An option here is to use an intermediate output current value, but that leads to converter architectures which should allow both boosting and reducing of the current and that can be quite expensive.

Parallel-Parallel A group of cell-strings connected in parallel, has a number of input pins and output pins equal to the number of cell-strings in the group. The input of all cell-strings is the same and can be shared through the converter interconnections. If the output of each cell-string connects to a single converter, each group may still have potential connections to multiple converters since there are multiple instances of outputs in the group. In any case the number of connections of the output pins to the converters can be limited with no significant loss of flexibility. Lossless parallel connection of converters require the same voltage output. All groups must be able to reach a certain voltage value. The voltage of groups does not alter significantly with operating conditions [56]. This allows all groups to connect to a reduced voltage value (compared to the series-series connection) with simple converter topologies, since all converters share similar input and output voltage. So this is an attractive option.

Series-Parallel When connecting groups in series and converters in parallel, an increased danger of mismatch is present on the outputs of the converters. The number of cell-strings in a group affects the input voltage of the local converter. When this configuration is selected, one must be careful of the division of groups in the module, so the voltage difference is covered by a given conversion range. Hence, this imposes potentially undesirable limitations on the converters. It will depend on the topology and the conditions whether this is attractive or not.

Parallel-Series We believe this last case is the least promising. Parallel connections of cell-strings increase the current. Irradiation differences in combination with parallel connections of cell-strings increase the potential current differences of groups, and hence the losses.

Active Diodes

The type of reconfigurable modules which are described is this Chapter are limited in flexibility by the size of the cell-strings. Non-uniformity however can be present within the cell-strings. The objective of the a reconfigurable is, as mentioned earlier, the separation of the module into groups of cells which produce either the same amount of current or voltage (series and parallel connections, respectively). In the knob-controlled topology which was described above, the smaller component of the module which can be selected to belong or not to a specific group is a cell-string and not a single solar cell. In the case

where a smaller number of cells, belonging to the same cell-string, operate under different conditions than the rest of the module, these cells affect the operation of the entire cell-string. Instead of increasing the granularity level of the reconfigurable module by reducing the size of the cell-strings, active diodes can be placed in parallel with cells within a cell-string. Active diodes are bypass elements which use transistors to produce diode-like behavior . In comparison with a normal bypass diode, the current which is bypassed through an active diode is controllable. If an active diode is placed in parallel with those cells, the excess current will flow through the diode, allowing the rest of the cells to produce their maximum power. It is evident that there are several potential positions where active diodes can be placed in reconfigurable modules. In principle, diodes could potentially connect any two cells of the module, but it is not cost effective to have a diode in parallel to every cell of the module, as they also consume energy when they conduct.

Placing active diodes in reconfigurable modules is a design option which is compatible with the design approach described in this Chapter and can improve the performance of the module without increasing the complexity of the supporting network. However, this option has not been implemented in the application of the design method.

3.5 Run-time instantiations of the module

The division of the PV module into cell-strings and the supporting electrical network allow multiple run-time instantiations of the module. The optimal run-time configuration of the module depends on the actual operating conditions. In order to decide the best position of the switches, information about these conditions is needed. It is evident that the granularity level and the flexibility, which determine the number of potential run-time configurations, play an important role to which extent external information is needed. This information can be obtained by monitoring the PV system. The position and number of monitors required depends on the parameter selection of reconfigurable modules. Having all required information about the external conditions is not necessary. The granularity level of the necessary information depends on the granularity level of the module itself.

In a cell-string type configuration, information about the I-V characteristics is required for every cell-string at run-time. This does not mean that the voltage and the current of each cell-string needs to be monitored at run-time. The type and amount of external and internal variables we need to measure for controlling the reconfigurable topology belongs to the system identification theory. There is a minimum requirement (variables to measure) that will allow the selection of the best configuration at run-time. In the best case, no external variables (e.g. irradiance, ambient temperature, shading pattern, ...) will be needed, but

only "few" internal variables (voltages and currents)Future work is to understand which are the variables that need to be measured for selecting at run-time the appropriate position of switches and knobs. The measured variables will be fed to a controller, which through a control scheme will adjust all the knob-controlled elements to the appropriate positions.

Our first priority is to estimate the potential gains of reconfigurable topologies under different shading patterns and operating conditions, by assuming full knowledge of all external conditions. This allows an accurate estimation of the potential gains and the actual control scheme of selecting at run-time the appropriate position of switches and knobs is future work. For this purpose a simulation-based exploration framework will be proposed, which is discussed in Section 6.3.

Chapter 4

Column/Row Template of the module and Vertical Split

The concepts and principles described in chapter 3 are now applied on rectangular modules. These modules are formed by placing solar cells in a N by M layout and are encapsulated in a rectangular form. Usually, the cells within the module are connected in series along the longest direction in an alternate fashion (i.e all cells within a column are series connected), with the columns connected in series along the edges of the module with busbars. A junction box is placed on one side of the module which contains the input and output terminals of the module and the bypass diodes which protect the module from hot-spot heating and decreased performance under partial shading conditions. This type of industrial modules is not well optimized for operation under partial shading conditions; bypass diodes provide some mitigation of the shading though, so our goal is to modify them to allow the maximization of energy harvest when PV arrays are installed in non-ideal locations. The main structure of the PV module (within the encapsulation) remains the same, while modifications on the external structure allow reconfiguration of the module, depending on the external operating conditions. First, the division of rectangular modules in cell-strings and the supporting network required will be discussed in this Chapter. Next, the potential benefits of the application of reconfigurable concepts will be illustrated for shading patterns through simulation results.

4.1 Selection of cell-strings

Starting from a conventional rectangular module organized in columns and rows, an obvious choice of a cell-string would be a column of the module. From a manufacturing point of

view, it is a cost effective solution. Simply removing the busbars connecting the cells on the edges of the module creates the N cell-strings each consisting of M cells connected in series. The granularity of the PV array is equal to M, which is the number of cells in each column of the rectangular module. The division of the module in column cell-strings is shown in Figure 4.1. Each cell-string has an in and an out notation, which indicate the direction of the current flow. The current in a cell-string flows from the in pin to the out pin.

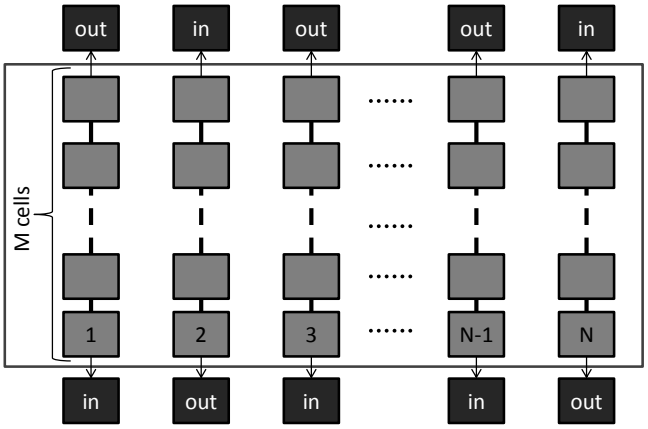

Fig. 4.1 Division of module in cell-strings comprising of the columns of the industrial module

As in the case with bypass diodes, instead of having the cells of the columns of the module interconnected, the cells can be electrically interconnected by following the rows. In that case, by removing the buslines along the edges, the module will be divided into M cell-strings of N series connected cells, as shown in Figure 4.2.

It is unlikely that N equals M, thus selecting the rows or the columns as cell-strings does not lead to the same module configuration. We will assume at this point, with no loss of generality, that $N < M$. The two potential cases of cell-strings will be examined based on the factors described in Section 3.3.

- Size of cell-string: As $N < M$, the selection of the rows of the module as cell-strings leads to a finer-grained architecture with smaller sized cell-strings. This leads to an advantage of the rows to be chosen for the basic power generating element. However it

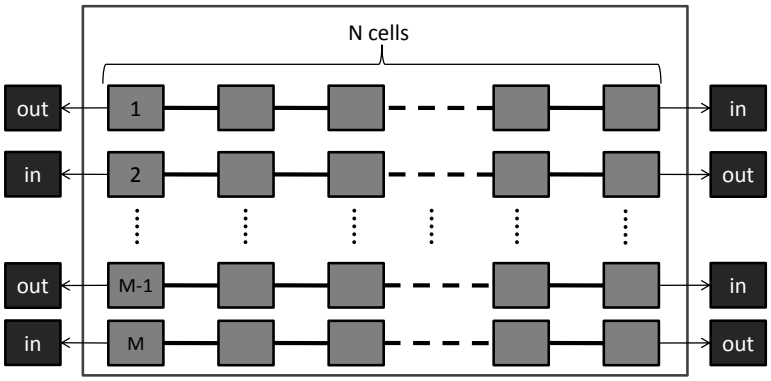

Fig. 4.2 Division of module in cell-strings comprising of the rows of the industrial module

should be noted that a finer-grained architecture requires a larger supporting electrical network to ensure flexibility, which leads to an increase of the initial cost.

- Geometry: It is assumed that the module is installed in the same space in both cases. In each case the module can optimally handle shading patterns hitting the module from one specific angle, shades whose edge is parallel to the connections within the cell-strings, as shown in Figure 4.3. Shades which come from a perpendicular angle, the edge of the shade is vertical to the connections within the cell-strings (Figure 4.4), are affecting all cell-strings of the module simultaneously, thus no reconfiguration can improve the performance of the module. According to the location of installation, the dominant direction of expected shading patterns and how they evolve over time, each division of the module can be proven to be beneficial.

- Size similarity of cell-strings. In both cases the cell-strings of the module have the same size.

Another criterion which affects the selection of cell-strings in rectangular shaped modules between rows and columns is if the number of rows and columns are odd or even. An even number of cell-strings is optimal, as in the all series connection of the module the inputs and the outputs are on the same side of the module and are easier connected to the module

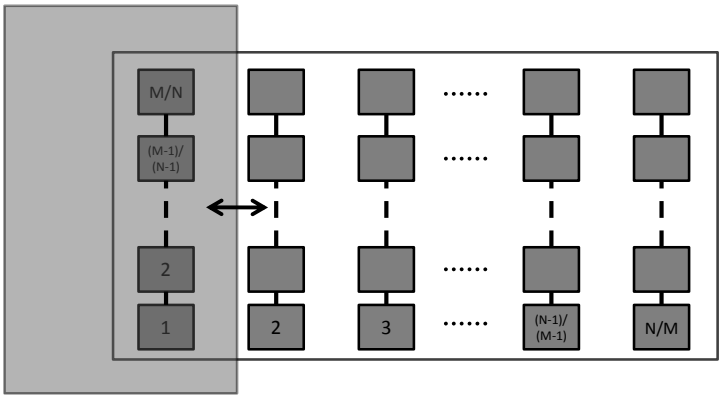

Fig. 4.3 Horizontal moving shade

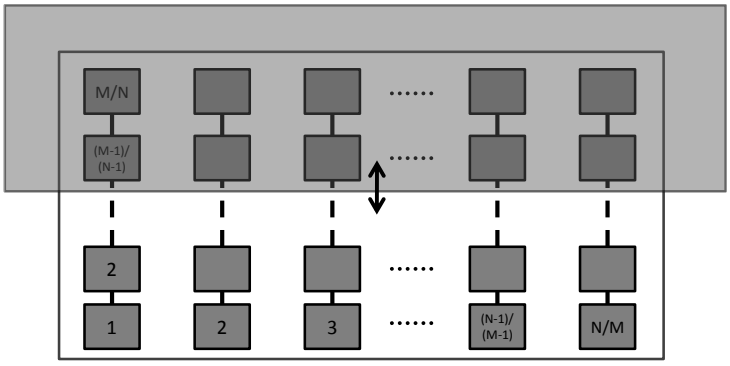

Fig. 4.4 Vertical moving shade

converter. The all in series run-time instantiation of the module is what is optimal under uniform conditions, thus it has to be the configurations with the absolute minimum resistive losses. In the case of an N by M module where $N < M$ and M is even, a pareto-optimal choice is to have M cell-strings of N cells. If M is an odd number, a trade-off (energy-wise) exists in terms of having small cell-strings or an even number of cell-strings. The case where both N and M are odd numbers is considered unlikely, though in that case the smaller dimension would be formed in to cell-strings. When both numbers are even, each selection is a different pareto point and both cases will be examined.

4.2 Supporting Electrical Network

At this point, the module is divided in cell-strings comprised of the column or the rows. All cell-strings, which are non-divisible, have their inputs and outputs located at two opposite edges of the module. This means that the supporting electrical network does not interfere with interconnections in the main body of the module, but can be placed either in the surrounding area or in the backside of the module. This is significant as not intervening in the cell matrix allows standard fabrication. The main components required to allow reconfiguration are namely switches and local converters. All interconnections between elements, except the permanent interconnections within the cell-strings are realized through the use of extra wires and switches. The interconnections between the cell-strings, the interconnections between the converters and the connections of cell-strings to the converters for this specific organization of the module into cell-strings will be described in this Section.

4.2.1 Interconnection of cell-strings

As mentioned in Subsection 3.4.1, the cell-strings can be interconnected in series or in parallel. The two basic types of connections are discussed here. Also hybrids can be created but these will be only briefly mentioned.

Series connection of cell-strings

As the cell-strings are consisting of permanently series-connected cells, the electrical orientation of each cell-string is fixed and allows only one direction of current flow. In order to maintain a minimal current path for the module under uniform conditions, the directionality of the current is the same as in a conventional module and neighboring column/row cell-strings allow an opposite direction of current flow. This is indicated in Figures 4.1 and 4.2 by in and out notations. A series connection between two cell-strings can be rendered

possible, by connecting an in pin with an out pin through the use of a wire with a switch. In Figure 4.5 all possible series connections between the cell-strings are illustrated. The continuous lines indicate wire connections which remain on the same side of the module, while the long-dashed lines and dotted lines connect an “in” pin with an “out” pin on different sides of the module.

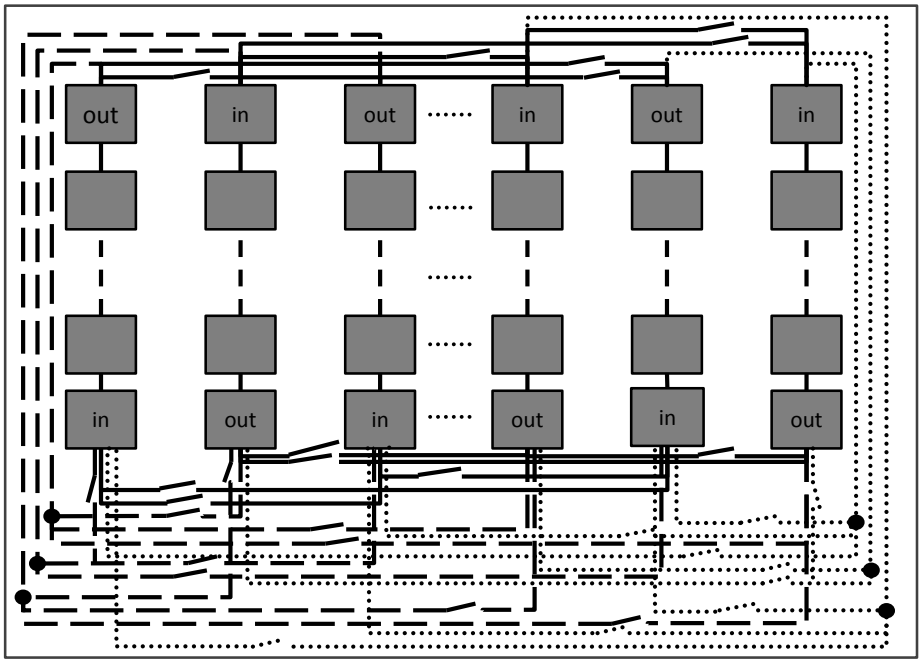

Fig. 4.5 All series connections of module (column cell-strings)

It is observed that if all possible series connections are enabled, the number of wires needed is extensive and introduces too much overhead. This is especially the case for long wires which potentially consume too much power when active without improving drastically the performance of the module; longer wires require a larger amount of metal and induce higher resistive losses.

In order to reduce the overhead, which is introduced by the presence of wires, the longest wires are removed. In series connection, the wires which are "crossing" the module, the long-dashed wires, are removed. In order to remain at the same side of the module, all cell-strings are potentially connected only with cell-strings which allow opposite current flow. Thus in a rectangular module of N by M with N (M) cell-strings, each cell-string has N/2 (M/2) connections. Depending on the number of N and M, the remaining wires can still be quite long.In that case, even more pruning will happen to remove all wires that extend beyond a user-defined threshold length. That threshold will be computed based on an analysis of

which wire length overhead cannot increase the energy-yield with a sufficient gain. This will be illustrated now in more detail.

Each cell-string is connected with all the cell-strings of opposite current flow on the same side of the module. So each cell-string has connections with N/2 cell-strings on each side of the module, as shown in Figure 4.6. This does not mean that every cell-string is connected with all N-1 cell-strings. Every cell-string is connected with N/2 cell-strings twice, once at the top of the module and again at the bottom of the module. If the cell-strings are enumerated, beginning from the cell-string which is situated on the left, then cell-string 1 is connected with cell-strings 2, 4, 6.... (with all even cell-strings). Any odd cell-string is potentially connected with all even cell-strings and any even cell-string is potentially connected with all odd cell-strings.

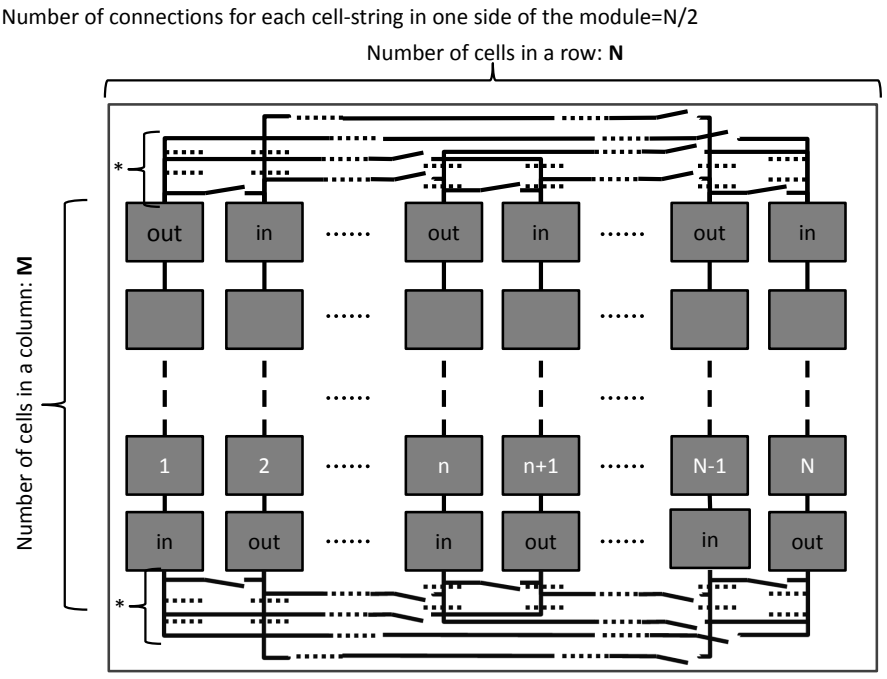

Fig. 4.6 All series connections of module (column cell-strings) which remain on the same side of the module

Although all wires that are crossing the module have been removed, the remaining wires may still be quite long, (the length of the longest wire is equal to the length of the entire module, N-1 cells long). In order to further reduce the amount of wires, a maximum length can be assigned. As an illustration, the proposed upper bound for the maximum length is selected as N/2 cells long. If x is set as the maximum length (in number of cells) and x is an odd number, the longest wires connecting cell-string number y will be with cell-strings number (y-x) and (y+x), where (y-x) and (y+x) must be between 1 and N. If x is an even

number, then the longest wires will connect cell-string number y with cell-strings number (y-x+1) and (y+x-1), where again (y-x+1) and (y+x-1) must be between 1 and N. Assuming that cell-string y is situated such that both (y-x)/(y-x+1) and (y+x)/(y+x-1) are within 1 and N, cell-string number y can be potentially connected with (x+1)/x cell-strings. If the cell-string is closer to the edge of the module, the connections are reduced, as shown in Figure 4.7.

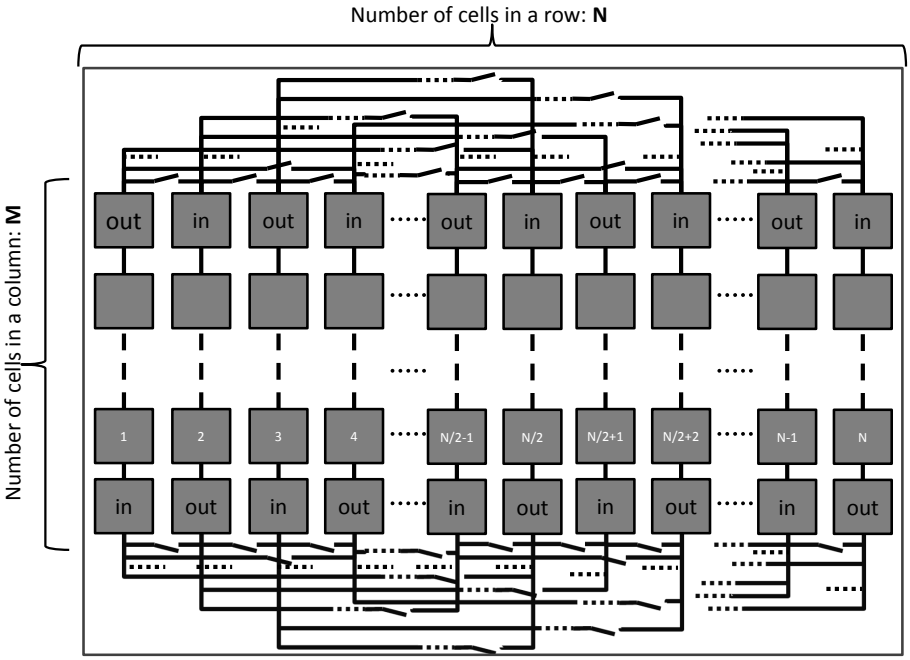

Fig. 4.7 Series connections of module (column cell-strings) which remain on the same side of the module with maximum length applied to wires

This is already a heavily pruned intermediate result which can be used as is. However, a further reduction step of the wires can be performed as described in section 4.2.2.

Parallel connection of cell-strings

In order to allow connections in parallel, an in pin should be connected with another in pin and the two out pins of the same two cell-strings must be connected as well. This means that in order to allow all possible parallel connections, all in pins should be connected to one another and all out pins with one another. In Figure 4.8, all possible parallel connections are shown. Dotted thin lines are used for connections along the same side of the module, while long-dash dot dot lines connect pins from different sides of the module. In the parallel connection, the current adds up while the voltage remains the same over all cell-strings.

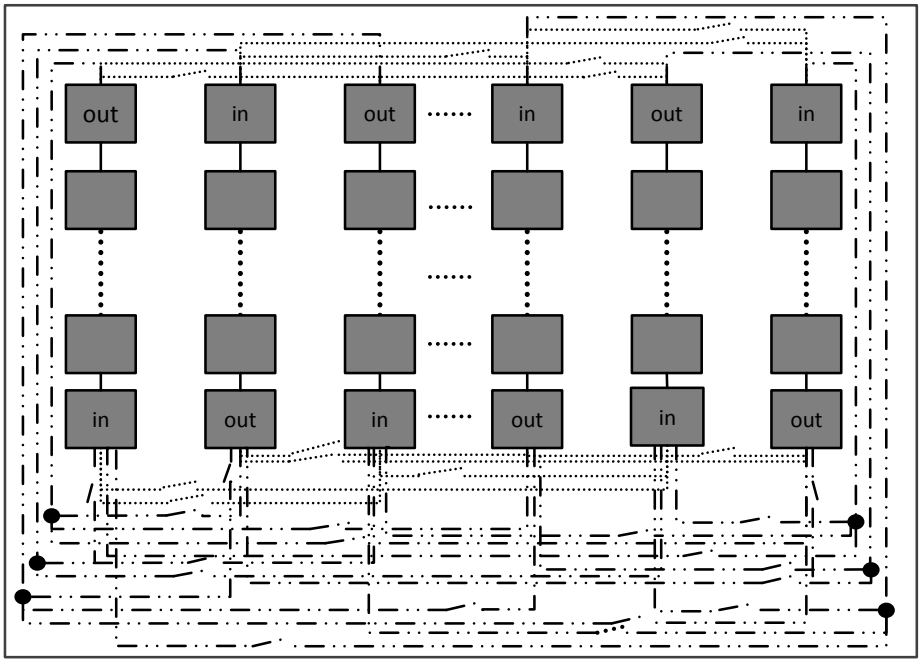

Fig. 4.8 All parallel connections of module (column cell-strings)

Once again, it can be seen that there are long wires connecting pins of cell-strings located in different sides of the module. The flexibility provided by these long connections does not compensate the extra cost and the high resistive losses they induce. These wires are removed. Elimination of wires surpassing a maximum length threshold can also be applied to parallel connections. It is not necessary to apply the same maximum length for the parallel and the series wires and it can differ due to the not identical overhead calculation.

A module where all remaining possible parallel wires are present is shown in Figure 4.9.

Hybrid connections

In the previous sections, the series and parallel connections refer to the interconnection of the cell-strings. Although the two types of connections are described separately, wires from both types of connections can potentially be simultaneously active in a run-time instance of the module. In the parameterized topology of the module all types of wires are present. Depending on the location and constraints on fabrication overhead, wires can be removed. The combination of active wires in each run-time instance suggests the number of converters which are needed and the cell-strings which should be connected to local converters, but does not affect the decision of the connections between the converters. The interconnection of the

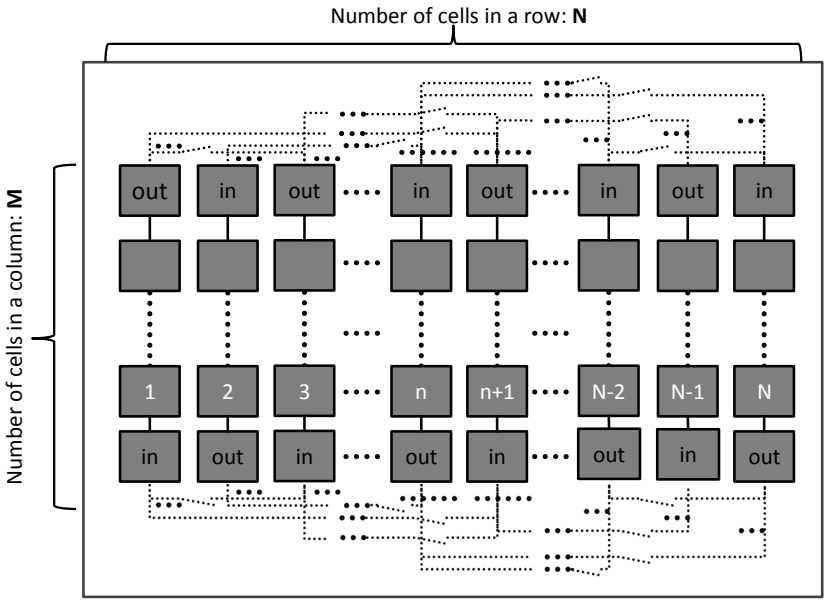

Fig. 4.9 Parallel connections of module (column cell-strings) which remain on the same side of the module with maximum length applied to wires

converters depends mainly on the characteristics of the converters used. The latter will hence be discussed next.

4.2.2 Local Converters

As stated in Subsection 3.4.1, the maximum number of dc/dc converters should be in the range of [2-X/2], where X the number of cell-strings, thus [2-N/2] or [2-M/2]. An interesting and important decision is the placement of the converters. Based on the selection of cell-strings, three potential options really present themselves. These options are illustrated in Figure 4.10 .

1. On one side of the module (blue in Figure 4.10), corresponding to a single side where half of the inputs and outputs of the cell-strings are located. By placing the converters on one side of the module, short wires can connect half the inputs and outputs of cell-strings to the converters from one side. Connections from the opposite side of the module (top in the Figure) would require long connections which introduce too much cost and thus are not suggested. This creates an asymmetry in the module which can lead to further pruning of the wires. This is accomplished by attempting to have all inputs and outputs of groups in the same side of the module. This means that all

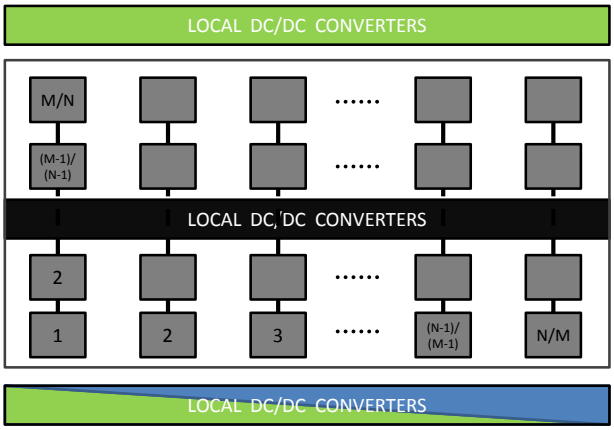

Fig. 4.10 Possible positions of placing the local converters

groups need to contain at least two cell-strings. In this case, this further supports the limit of number of available local converters to half the number of cell-strings.

2. On both sides of the module (green) where the inputs and outputs of cell-strings are located. The main advantage of having converters on either side of the cell-strings terminals is that all cell-strings can be connected via short wires to the local converters. However, the interconnections of local converters positioned on opposite edges of the module would require long wires. There are two options, namely allow some long wires between the converters placed on opposite sides, which increases the resistance of the active current path or isolate each group of converters. The isolation of each group of converters does not increase the flexibility of the module, as again each group of cell-strings needs to contain at least two cell-strings and creates an issue with the connection of the converters to the module converter and the rest of the PV array.

3. On the backside of the module (black), in the middle. The main advantage of placing the converters at the backside of the module is that in that location the converters do not take any space from potential active area. However, connecting the cell-strings to the converters requires wires which can be significantly long, depending on the size of the cell-strings. The disadvantage is the somewhat higher fabrication cost of the

module. But IBC type modules are being investigated in PV research and this is an important future potential [57].

At this stage, the first option is the most attractive as it allows sufficient flexibility and allows shorter connections to the module converter which can be placed at the same side as the local converters. Placing the converters on one side is also interesting as it creates an asymmetry and allows further pruning of the wires.

Even/Odd number of cell-strings The input and the output of a group of cell-strings, when long wires have been removed, will be on different sides of the module if the group has an odd number of cell-strings. In the best-case scenario where the whole module is operating under similar illumination conditions, all cell-strings should be connected in series. In order to avoid having long wires to the converters, the module is considered to have an even amount of cell-strings. If the module consists of an odd number of cell-strings, presence of long wires cannot be avoided. One option would be to add a long wire to one cell-string, ensuring output pins of all cell-strings are at the same side of the module where the local converters are placed. However just adding one long wire limits the flexibility of the module. The number of wires to be added depends on the location of the installation and expected irradiation conditions. Only by adding a long wire in all cell-strings would lead to a similar flexibility with a module with an even number of cell-strings. But this clearly incurs a quite large initial cost and significantly higher resistive path losses. Hence, this latter option with so many long wires will not be attractive.

Pruning of wires due to local converters placed on one side of the module

The design choice of not including long wires in the supporting network, means that a local converter cannot be used for every cell-string; a single cell-string is not possible to be isolated in the case of en even total number of cell-strings. If a cell-string is needed to be isolated from any connection, it is necessary to remove one more cell-string, which is considered an acceptable penalty given the even larger cost of adding the long wires and switches needed to enable a more flexible isolation.

The series and parallel connections of the cell-strings for a module of 10 by 6 with cell-strings of 10 cells are shown in Figure 4.11. A maximum length threshold of three cells has been applied for both series and parallel connections. The converters are located at the bottom of the module and all in and out pins of the cell-strings at the bottom side of the module are potentially connected with the converters. The dotted lines which connect the cell-strings with the converters in this illustration are switch-controlled.

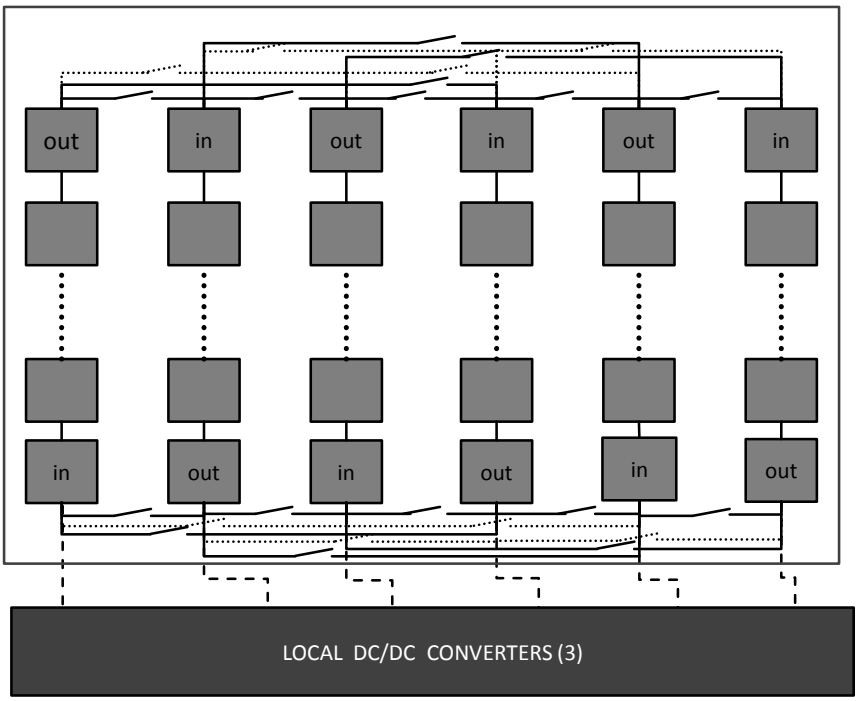

Fig. 4.11 Placement of local converters and indicative connections of cell-string to the local converters

As the converters are just on one side of the module, it is known a priori that all groups should have the input and the output at that side of the module. In Figure 4.11, the converters are located at the bottom side of the module. The bottom and the top side of the module have exactly the same connections between the cell-strings. cell-string 3 is connected with cell-string 4 both at the bottom and at the top of the module. These two connections are not equivalent as they allow different groups where the in and out will be both at the bottom of the module. For example, if one needs cell-strings 1, 2, 3 and 4 to reside in the same group, cell-strings 3 and 4 will be connected at the top side. In the case where cell-strings 2, 3, 4 and 5 belong in the same group, cell-strings 3 and 4 will be connected in the bottom side of the module (the order of the cell-strings, beginning from an "in" pin is: 5, 4, 3, 2). The fact though that the converters are situated on one side of the module, which leads to an asymmetric topology, indicates that the symmetry of the wires can be unnecessary. As all inputs and outputs should be in the bottom of the module, it means that only intermediate connections of the groups are at the bottom side of the module. If a group consists of two cell-strings, the connection between them is at the top side of the module. In the case of a group of four cell-strings, two connections are located at the top side and one at the bottom side. So the distribution of the connections at the top and bottom sides depends strongly on the specific topology instantiation.

As mentioned above, in the series connection, wires at the bottom side are used only in the case where a group of at least four cell-strings is present. As the number of converters allows all pairs of cell-strings to be connected with a local converter, some wires from the side where the converters are placed can be removed. Most run-time instances will still be realizable in the same way as before, while others will require the use of more converters.

In Figure 4.12, some wires from the side of the converters have been removed, according to the previous analysis. With the connections of Figure 4.11, cell-strings 2, 3, 5 and 6 can form a group with an ordering of the series connection from an in pin to an out pin: 3, 2, 5, 6 but a long wire is needed between cell-strings 2 and 5 at the bottom side of the module. This group would be connected to a single converter. In contrast, in Figure 4.12 this is not possible. Instead cell-strings 2 and 3 can be connected in series then and they use one converter, while cell-strings 5 and 6 use another converter.

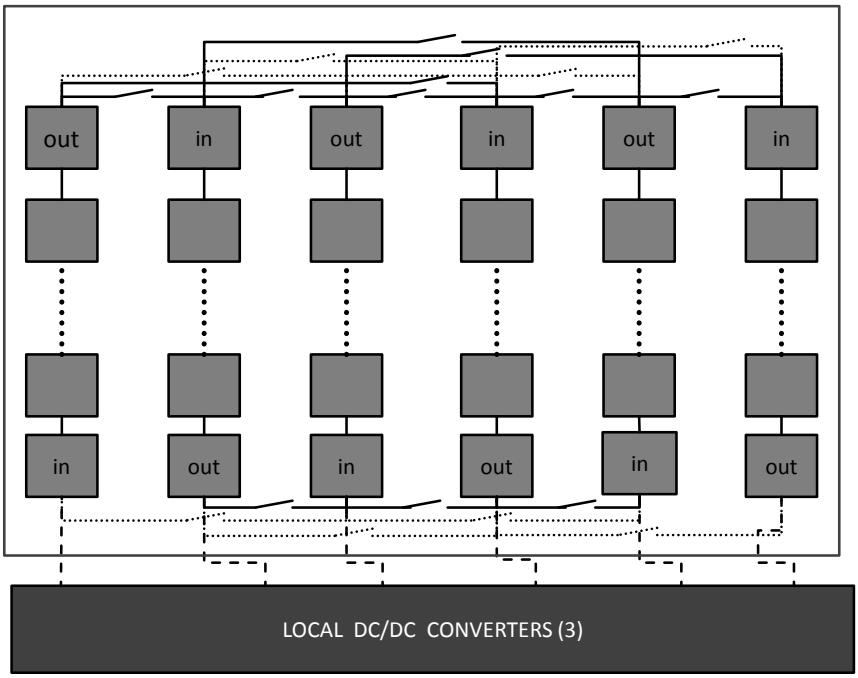

Fig. 4.12 Pruning of series connections on the side where local converters are placed

The case of a parallel connection of cell-strings is different. In order to connect two cell-strings in parallel, a pair of wires is necessary, one to connect the outputs and one to connect the inputs of the cell-strings or the set of cell-strings. It is reasonable to expect that the wires at the bottom and the top of the module will be identical, especially if it is assumed that a parallel connection is used to connect single cell-strings. The additional cost of all the wires for enabling parallel connections of the cell-strings is quite large even with the criterion of maximum length applied.

Two main factors contribute to the cost of creating a group which consists of two single cell-strings connected in parallel.

- Low voltage: A single cell-string, in a normal size module, produces a small output voltage. In a parallel connection of two cell-strings, the voltage remains the same and the current is added up and it will usually be inefficient to connect such a low voltage with a local dc/dc converter.
- Input and Output Pins: The input and output pins of the parallel connection of two cell-strings will be on different sides of the module. As the local dc/dc converters are situated on one side of the module, the connection would require the presence of long wires crossing the module.

However, in the case where four cell-strings operate under similar conditions and the voltage demand is not so high, it is not optimal to have a series connection of all four cell-strings. In that case, cell-strings 1 and 3 as well as cell-strings 2 and 4 can be connected in parallel and then 1//3 can be connected in series with 2//4 ({1//3}&{2//4}). This connection is equivalent though with connecting the cell-strings first in series and then in parallel ({1&2}//{3&4}). The second configuration has the advantage of using less wires as shown in Figure 4.13.

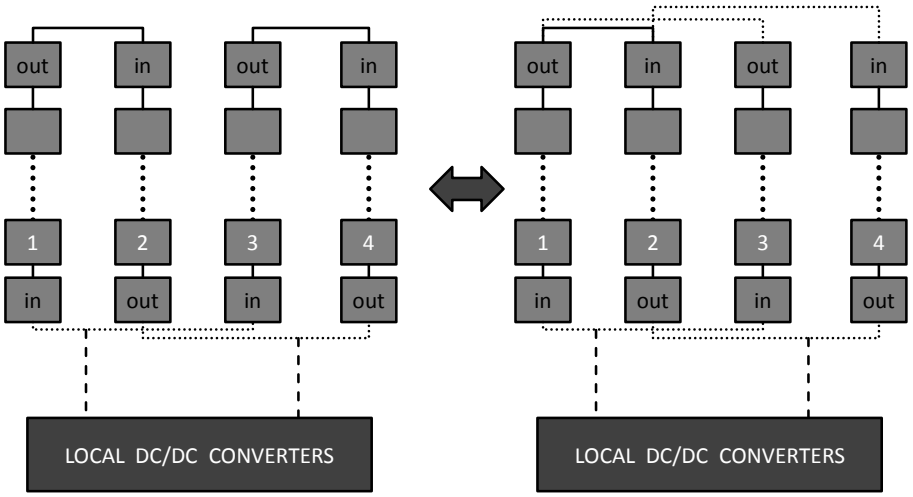

Fig. 4.13 Equivalent types of connections of a group of four cell-strings

In a parallel connection, the location of the local dc/dc converters allows all wires to be removed from the top side of the module, enabling all acceptable configurations to be realizable as before (Figure 4.14).

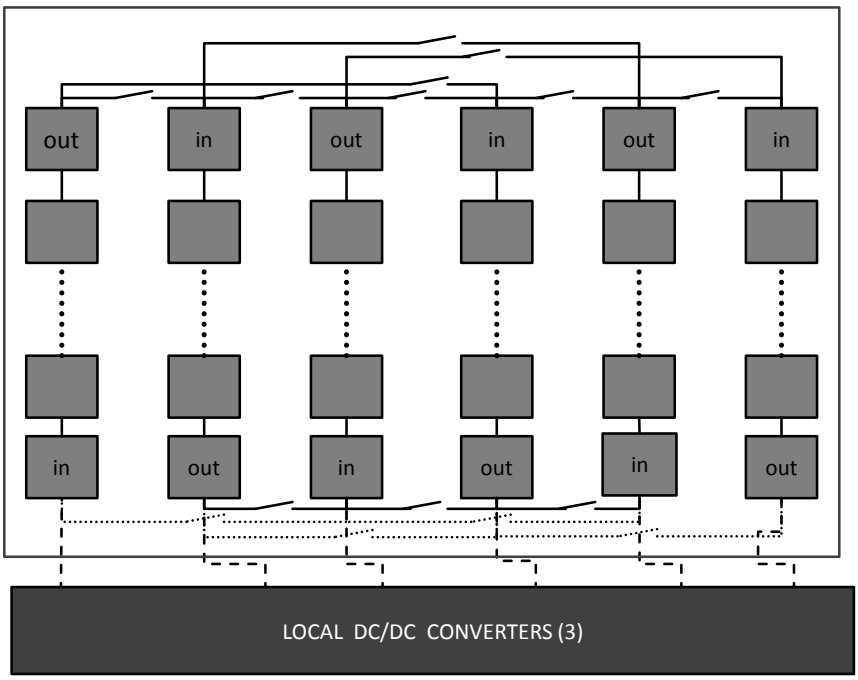

Fig. 4.14 Pruning of series connections on the side where local converters are placed, and pruning of parallel connections on the opposite side the placement of the converters

Connection of cell-strings to the converters

In the module which is described up to now, the input and output of each cell-string are located in opposite sides of the module and the local converters are placed on one side of the module. All the in pins and out pins of cell-strings located on the side of where the converters are placed are potentially connected to the converters. That does not mean that the in pin of a cell-string is connected to all in terminals of the local converters. The in pin of each cell-string at the side where the converters are placed is connected to a single converter, while the out pins of the cell-strings of the same side are connected to all converters.

Interconnection of local converters

In section 3.4.1 the possible ways to connect converters are discussed. To summarize, the three ways to interconnect the converters are:

- Series Connection: In a series connection, the outputs of all converters should reach the same current level.
- Parallel Connection: In a parallel connection, the outputs of all converters should reach the same voltage level
- Cascaded Connection: Each converter should reach the voltage of the input of the converter of the next stage.

At this point, the main focus is to divide the cell-strings into groups depending on the operating conditions of the module. Information of the outputs of the groups (in terms of optimal voltage and current) and thus the input of the local converters can help determine the best option for interconnection of the converters, as well as the required characteristics of the local converters themselves. To keep the resistive losses low, priority is given to the series connection of cell-strings. Use of parallel connections should be re-examined in case the converters cannot efficiently handle the irradiation differences between groups.

4.3 Simulation Results of Row/Column Template under static shading patterns

4.3.1 Simulation Setup

To motivate the benefits of the configurable topology, a conventional module topology has been simulated and compared against three types of configurable topologies under three representative shading patterns.The shading patterns of three representative irradiation scenarios are illustrated in Figure 4.15. Fully illuminated cells are excited by $1000W/m^2$ while shaded cells have an irradiation level of $(1-SD)*1000W/m^2$, where SD is the shading density. Nine different shading density levels were applied. A value of shade density close to 0 means that the shade is almost transparent, while a value close to 1 indicates a dense shade. The irradiation levels of partially shaded cells (Figure 4.15.c) are computed according to the shaded area of the cell.

The simulated module consists of 60 cells in a 6 by 10 mesh, which is a typical module size. As a representative conventional topology, we have used the most common configuration in the industry, which includes three bypass diodes (Figure 3.1) and is equipped with a power optimizer. For the reconfigurable topologies two cell-string sizes were selected (10 and 6 cells respectively).

As far as the solar cell is concerned, the standard steady-state two diode model for silicon cells has been used in the simulations; silicon PV cells are currently the norm. For the

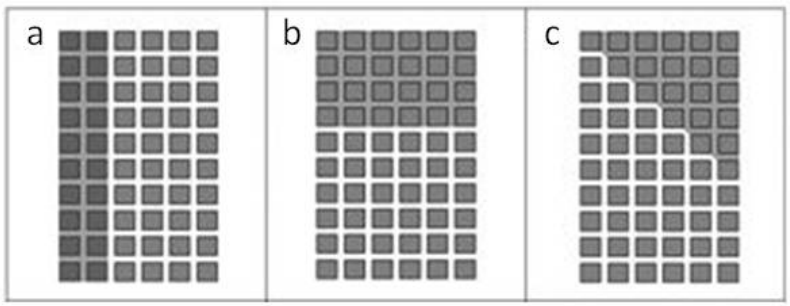

Fig. 4.15 Three representative shading patterns

simulations a 6-inch Multi-Crystalline silicon cell (IMEC cell) was used and wires and switches are included in the simulation environment as resistive elements. The on resistance of a switch is 3.6mΩ ([58]) and the resistance of the wires is 0.014Ω/m.

We assume steady state conditions, as proposed in methodologies used to compare module designs from different vendors. Transient thermal dependencies of the module operation are ignored and the ambient temperature is assumed uniform and constant at 25 degrees.

The conversion efficiency of module converters is realistically assumed to be 98%, if the voltage operating point is within the boundaries of the voltage window. The conversion efficiency of local dc/dc converters is lower and is assumed to be 95%. The input voltage window for the local dc/dc converters used in the simulations is 9-15V. The power generated by the module on each irradiation scenario is located on the P-V curve produced through HSPICE simulations and the loss due to the converters is computed based on the MPP of the configuration. Other values than the above parameters can be easily entered in our modeling framework.

4.3.2 Results

In Table 4.1 the instantaneous power for two levels of irradiation for uniform conditions are shown for the reconfigurable module of cell-strings of 10 cells, that is called Reconf.10 and cell-strings of 6 cells, that is called Reconf.6. It is seen that the module with the largest cell-strings (Reconf.10) is closest to the performance of the conventional topology, as there are fewer resistive losses in the active current path, that is all cell-string connected in series. These resistive losses depend on the current, thus on the incident level of irradiation.

In Table 4.2 the instantaneous power generated by the three different configurations of the module and a custom designed module are listed for the shading pattern of Figure 4.15.a for different shading levels. The custom designed module is a non-reconfigurable topology

Table 4.1 Instantaneous power of conventional and reconfigurable modules (Reconf.10 & Reconf.6) under uniform conditions

Irradiation Level	Conventional	Reconf.10	Reconf.6
1000 W/m^2	172.88	171.43	170.29
500 W/m^2	90.06	89.69	89.40

Table 4.2 Instantaneous power of conventional, reconfigurable modules (Reconf.10 & Reconf.6) and custom designed module for the shading pattern of Figure 4.15.a

Shading density	Conventional	Reconf.10	Reconf.6	Custom
0.1	164.76	164.69	162.49	167.78
0.2	151.96	159.57	150.15	162.40
0.3	136.74	154.30	135.34	156.87
0.4	119.96	148.89	118.93	151.19
0.5	108.96	143.34	101.28	145.39
0.6	108.92	137.67	82.59	139.46
0.7	108.89	131.89	62.97	133.42
0.85	108.85	123.09	32.04	124.25
0.9	108.84	120.17	21.39	121.20

which is designed for the specific operating conditions. This shading pattern is the best case scenario for the conventional module and the Reconf.10 topology. An entire bypass section of the module is shaded in the conventional one. In the Reconf.10 topology, the cell-strings can be successfully divided at run-time in two groups of fully illuminated and shaded cells. This configuration is the closest to a custom designed topology. The direction of the cell-strings in the Reconf.6 topology does not allow any reconfiguration for this shading pattern, so this is why the results are less good for that option and worse than the ones of the conventional module.

It is seen that the bypass diode corresponding to the shaded section is active when the shade density is high (0.5-0.9). The extra power of the Reconf.10 topology with respect to the conventional one, in low shading densities, is due to the fact the fully illuminated cells are not compromised by the shaded cells and all cells can operate at their MPP. The gains are higher when the shade density is 0.5, as the shaded cells in the Reconf.10 contribute to the shaded power while in the conventional module they are bypassed. As the shades becomes more dense, the power of the shaded cells is less and the gain drops.

Table 4.3 Instantaneous power of conventional, reconfigurable modules (Reconf.10 & Reconf.6) and custom designed module for the shading pattern of Figure 4.15.b

Shading density	Conventional	Reconf.10	Reconf.6	Custom
0.1	163.83	163.55	162.35	166.29
0.2	150.62	150.40	156.31	159.88
0.3	135.24	135.07	150.07	153.28
0.4	118.46	118.33	143.66	146.51
0.5	100.58	100.49	137.07	139.57
0.6	81.78	81.72	130.32	132.49
0.7	62.17	62.14	123.43	125.27
0.85	31.46	31.45	112.91	114.30
0.9	20.95	20.95	109.41	110.65

The power generated by the three discussed configurations and a custom topology for the shading pattern of Figure 4.15.b is summarized in Table 4.3. As all the cell-strings of the Reconf.10 topology are partially shaded, it results in slightly less energy than the conventional due to additional resistive losses. In the Reconf.6 topology, the cells can be completely divided in illuminated and shaded groups. For most shade density levels, the Reconf.6 topology outperforms the conventional module. When the shade is light (0.1) the Reconf.6 module has less power than the conventional one. This means that any power recovered due to the independent operation of shaded and non-shaded cells is lost in the extra resistive and conversion elements. However, in heavy shading, high shading densities, the gains can be over 300%.

The results for the shading pattern of Figure 4.15.c are shown in Table 4.4. The cells of the module have three different irradiation levels. The selection of cell-strings in the two reconfigurable topologies do not allow individual operation of the differently illuminated cells. The current of each cell-string is limited by its poorest performing cell. Even though a cell-string can be fully illuminated, it still may not be possible to disconnect it from shaded cell-strings. The goal is to have most of the highest irradiated cells in separate groups than the shaded cells. The conventional module and the Reconf.10 topology cannot handle this type of shade as all bypass sections and cell-strings respectively are partially shaded. The Reconf.6 topology can mitigate some of the losses by connecting the six top rows to one converter and the last four rows to another converter.

Table 4.4 Instantaneous power of conventional, reconfigurable modules (Reconf.10 & Reconf.6) and custom designed module for the shading pattern of Figure 4.15.c

Shading density	Conventional	Reconf.10	Reconf.6	Custom
0.1	165.53	164.24	161.50	165.69
0.2	153.25	152.22	153.93	158.89
0.3	138.25	137.45	145.23	151.26
0.4	121.53	120.94	135.73	143.06
0.5	103.52	103.11	125.60	134.36
0.6	84.43	84.17	114.94	125.26
0.7	64.41	64.26	103.79	115.78
0.85	32.83	32.79	86.30	101.00
0.9	21.95	21.93	80.31	95.95

The percentage of power production compared to a custom designed module for each of the three module configurations (Conventional, Reconf.10, Reconf.6) is illustrated in Figures 4.16-4.18.

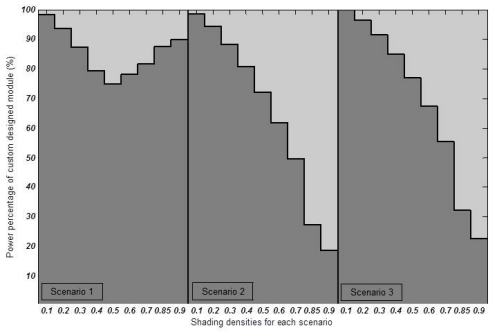

Fig. 4.16 Conventional module

In the shading pattern of Figure 4.15.a the topology with the best results is the Reconf.10 module. In the second shading pattern, the Reconf.6 module has the least power losses. In the last shading pattern, the Reconf.6 topology has a better performance than the conventional module, however the produced power is not as close to the custom designed layout.

Based on this, it is noted that the benefits of each topology heavily depend on the shape of the shading pattern. Due to the formation of the cell-strings from the rows or columns of the PV module, flexibility is limited to one dimension of the module. For this reason a division of the cell-strings is suggested, which is discussed in the next Section.

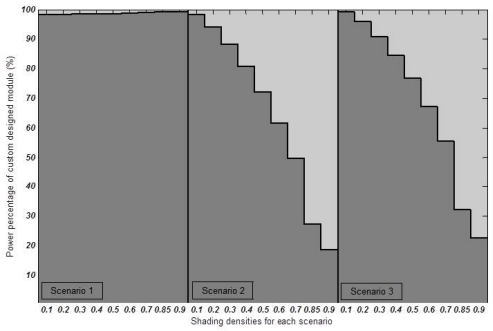

Fig. 4.17 Reconfigurable module with cell-strings of 10 cells

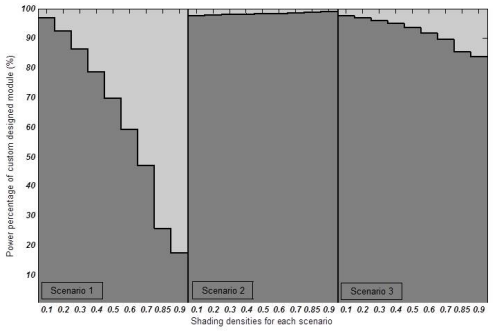

Fig. 4.18 Reconfigurable module with cell-strings of 6 cells

4.4 Vertical Split of cell-strings

Up to this point, the configuration of the module which was described allows different run-time instantiations to exploit different illumination scenarios in one direction. A configurable module, where cell-strings are either rows or columns is ideal for shadows whose edge moves in parallel to the cell-strings as illustrated in Figure 4.3. A shade which creates irradiation differences only within the cell-strings, the edge moves perpendicular to the cell-strings (Figure 4.4), causes the reduction of the short-circuit current of all cell-strings. In this case, since all cell-strings have similar I-V curves, one group is formed and the reconfigurable topology yields the same power generation as the conventional module.

This can be seen as a non-symmetrical granularity of the module, as in one direction the module has a cell-level granularity while in the vertical direction, there is no granularity at all. As mentioned above, in Section 4.1, having the shortest dimension as cell-strings allows less differentiations of irradiation within the cell-string and less power losses due to internal shading of the cell-strings. Of course this comes with the cost of a more complex electrical supporting network of wires and switches. Achieving a cell level granularity level in both directions would lead to an architecture where all cell-strings would comprise of a single cell. However, the extra hardware required to support such a granularity and the extra resistive elements in the active path render this solution non-optimal for cells producing high currents. Still some flexibility in both directions can be required when shading patterns are present which cover parts of the rows and columns, so we cannot mainly go for splitting up the module into cell-strings in 1 direction. For this purpose also a vertical split of the cell-strings is considered. The term vertical does not refer to the direction of the module, but implies the split of the original cell-strings vertically to the series connections of the cells. It should be noted that this option applies for the row/column template which has been discussed up to now. But it can also be applied equally well to the snake template which is introduced in Chapter 5. Also there the non-symmetrical granularity issue is present and the solution proposed here is valid and effective there too.

4.4.1 Division of the cell-strings and interconnections

If a module of 10 by 6 is taken to account, the optimal choice from a granularity aspect, without having a vertical split applied, is to have 10 cell-strings of 6 cells length. A vertical division of the cell-strings leads to a module which has 20 cell-strings of 3 cells length. Each cell-string of the initial 10 cell-strings is divided in 2 cell-strings of 3 cells (Figure 4.19). The module now consists of two separate sets of cell-strings, the lower (l) and upper set (u).

The current flow is indicated by in and out notations at the two pins of each cell-string. As cell-strings now comprise of 3 cells, this will be called a Reconf.3 topology.

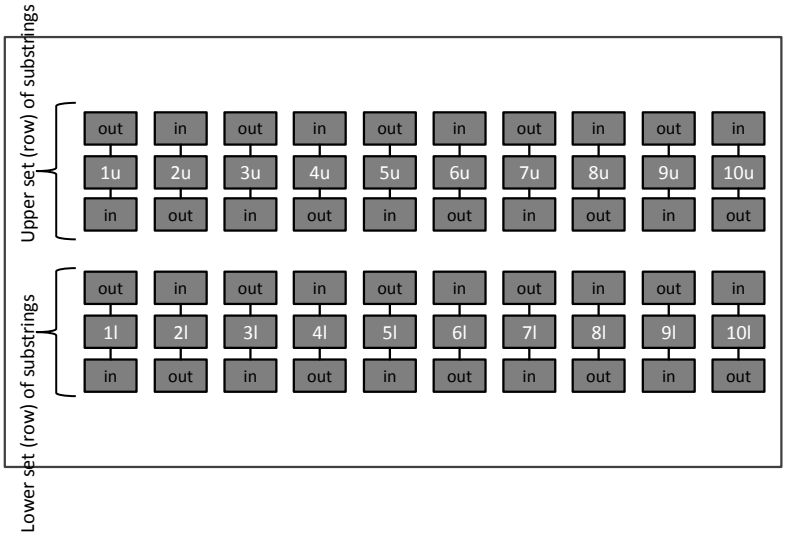

Fig. 4.19 Vertical split applied on the Reconf.6 topology leading to a Reconf.3 topology

The module can now be seen as two sub-modules of 10 by 3 cells. If each set of cell-strings is treated as a separate module on its own though, the wires required for all the connections described above (in the previous Sections of this Chapter) would be twice the amount of the ones used before the vertical split, without even having the sub-modules or sets of cell-strings interacting yet. All the wires which would be added contribute to the flexibility of the sub-module to operate under different horizontal irradiation scenarios (Figure 4.3) in which the vertical split is not necessary. When the vertical split is applied, it is hence not useful to keep all the wire connections between the two horizontal sub-modules so we will heavily prune those. In contrast, the connections on the top and the bottom of the module (the top of the upper set of cell-strings and the bottom of the lower set of cell-strings correspondingly) are left as before, both for the series and parallel cases.

Series Connections

In the middle of the module switches are added in order to allow all cell-strings to be connected in series. In the case of uniformity in the vertical direction, these switches are constantly in the closed position, allowing the module to function as a module of 10 cell-strings. Wires are also added to enable the series connections of all the cell-strings of the upper and lower set correspondingly. When the upper and lower sets of cell-strings operate

under different irradiation conditions, the two sets function independently. In order to allow some flexibility in case of a simultaneous horizontal differentiation of illumination, wires are added to connect all neighboring cell-strings in each set of cell-strings. The only interaction of the two sets is the potential connection of each nl cell-strings with the cell-string nu, where nl and nu are the cell-strings of the lower and upper sets of cell-strings respectively, corresponding to the n^{th} original cell-string. The series connections of the Reconf.3 module are shown in Figure 4.20.

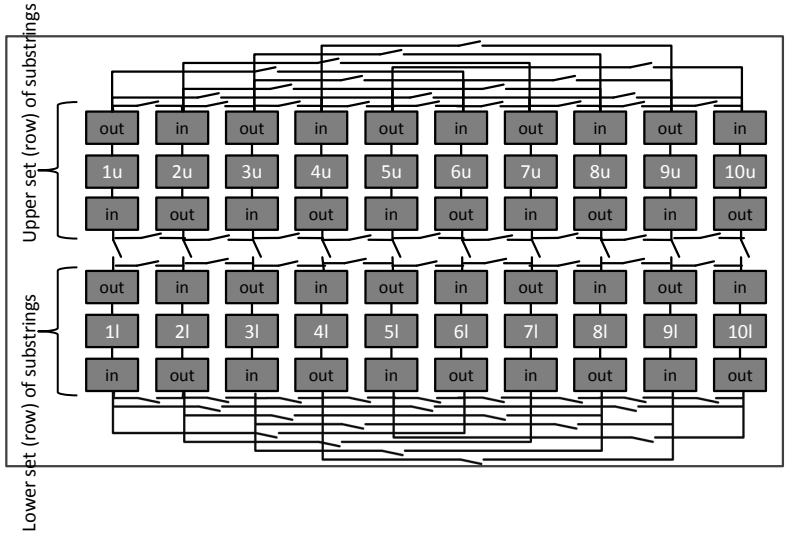

Fig. 4.20 Reconf.3 with series connections of cell-strings

Parallel Connections

The interaction of the two sets of cell-strings through parallel connections would lead to an overhead which would not be compensated by the expected gain. The only wires which are added in the middle of the module scope to the increase of the flexibility of the module in the horizontal direction, when the vertical split is in use. The cell-strings of each set can potentially be connected in parallel with the nearest cell-string of the same set which allows the same direction of current flow, this means that the threshold, in number of cells, of parallel connections in the middle of the module is 2. The Reconf.3 topology with the parallel connections of the cell-strings are shown in Figure 4.21. However, adding a lot of switches in the middle of the module can increase the cost. Limitation of the amount of enabled connections is highly recommended and parallel connections in the middle of the module can also be omitted altogether.

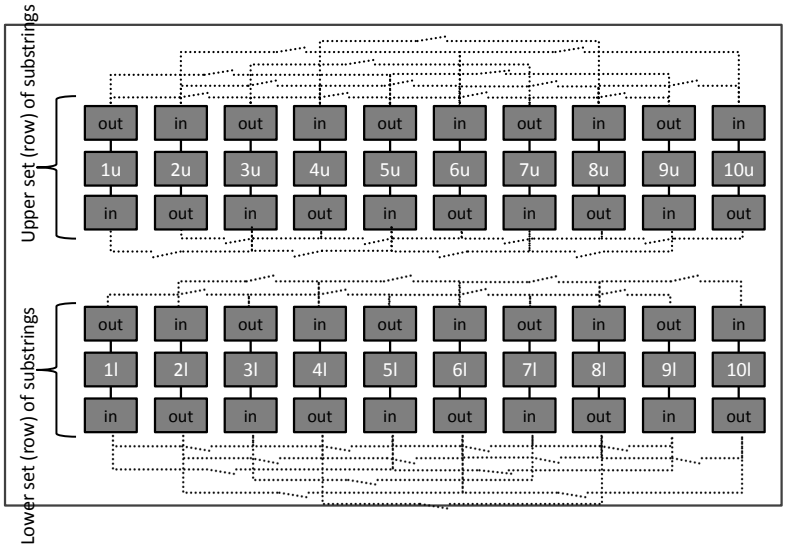

Fig. 4.21 Reconf.3 with parallel connections of cell-strings

In the example module which is used for illustration of the principles, with 10 columns of 6 cells, each column is divided in two cell-strings, leading to 20 cell-strings of 3 cells. A standard module size is considered to be 6 by 10. In the previous configurations analyzed above, we introduce either a division of the module into 6 cell-strings of 10 cells length or into 10 cell-strings of 6 cells length. In the case where the longest dimension is chosen to comprise the cell-strings, the vertical split should be applied to the longer cell-strings, which corresponds in this case in cell-strings of 10 cells. One solution is to divide the module into two sets of cell-strings each comprising of 6 cell-strings of 5 cells. A length of 10 cells however means that more irradiation differences can be present in that dimension, compared to one of 6 cells. A further split of the cells in the vertical direction could hence be applied, leading the long cell-string to be divided into three cell-strings of three, three and four cells. The module would then have three sets of cell-strings, the upper (u), the middle (m) and the lower (l) set. This is illustrated in Figure 4.22.

In conclusion, the vertical split does not necessary mean that there is a single division by two of the original cell-strings. Further divisions can be made if it is necessary or useful, depending on the dominant shading patterns and scenarios. A minimum amount of cells in a cell-string should be assigned though, in order not to have a large overhead due to the additional wires required for all the potential connections. A proposed minimum is 2-3 cells per cell-string.

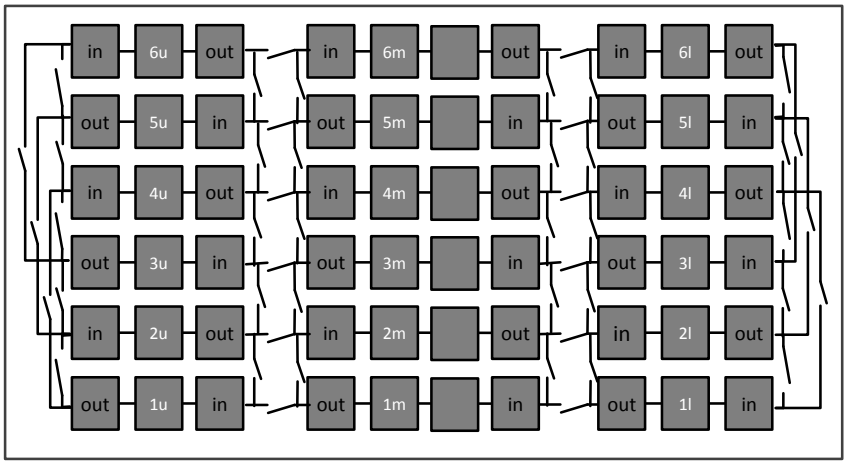

Fig. 4.22 Vertical split leading to three cell-strings with series connections of cell-strings

4.4.2 Converters with Vertical Split

It has been mentioned above in Subsection 3.4.1, that the maximum number of local dc/dc converters is half the number of cell-strings. When the vertical split is applied to a module of 6 by 10, the result is having 20 cell-strings, thus suggesting that the proposed maximum number of local dc/dc converters is 10. However having so many local converters introduces too much cost and in reality are not needed. Applying the vertical split increases the flexibility of the module by reducing the granularity level in the vertical direction. This further division of the cell-strings does not increase the horizontal flexibility of the module, thus the proposed maximum number of local converters should be computed based on the number of original cell-strings.

The converters can either be divided to be placed on both sides of the module, or be concentrated on one side of the module.

Converters on both sides of the module

It is expected to have non uniform irradiation either mainly in the horizontal direction either mainly in the vertical direction. A superimposition of both is possible, but a checkerboard irradiation scenario is considered quite improbable. As mentioned earlier on, in the case of vertical directed irradiation differences the independence of the sets of cell-strings is

necessary. If irradiation only changes in the vertical direction, the number of converters which are needed is equal to the number of sets of the cell-strings of the module. In the case of the 6 by 10 module, two converters will be used in such a scenario, one converter from the top side and the other from the bottom side of the module.This implies that each local converter should be able to handle half the power of the module. This affects the design of the local converters and their cost. In order to reduce the cost of the converters, two can be used on each side of the module. In horizontal irradiation scenarios the module will function as before the vertical split, using mainly the converters which are situated on the bottom side of the module. For that reason and in order to reduce the overhead, less converters should be placed on the top side of the module. All input and output pins (which are either at the top or the bottom of the module, not in the middle part) of the cell-strings are connected to the converters. In Figure 4.23 the connections of the module are shown and the placement of converters on both sides of the module.

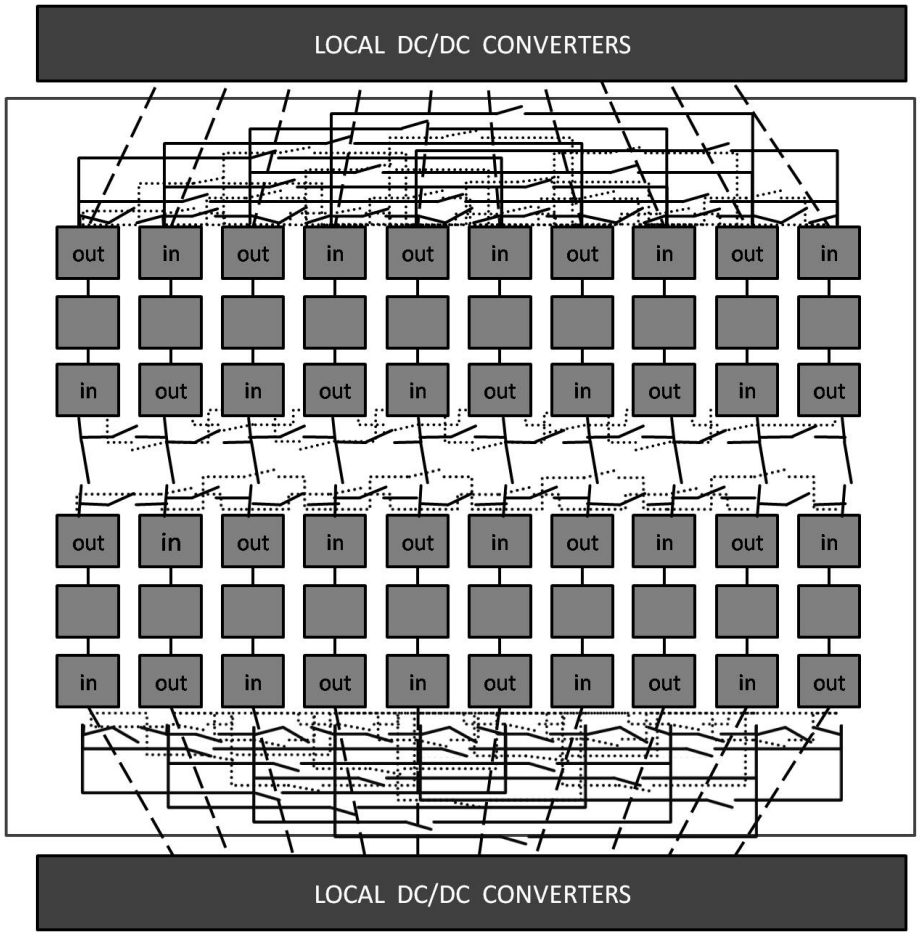

Fig. 4.23 Reconf.3 with converters on both sides of the module

Although converters are present both at the top and the bottom of the module, the input pins for each converter must be at the same side of the module, as no long wires exist. In the case where irradiation changes simultaneously both on the vertical and horizontal direction, the module can be divided in two by enabling the vertical split and then the two sets of cell-strings can be treated independently to taking into consideration the differences of horizontal operating conditions. Each set of cell-strings uses the converters on the corresponding side of the module. Another option in such a scenario is to apply the vertical split only at the part of the module which is affected by vertical irradiation changes, if that is possible. If for example, irradiation changes vertically just at the 4 first columns of the module, then the vertical split can be applied just there, while the other columns of the module (5 to 10) are not divided as the irradiation in the vertical direction is uniform.

It was mentioned above that each set of cell-strings is connected to its "own" converters on one side of the module. In the case where the rows or columns of the module are divided by 3, the result is 3 separate sets of cell-strings: the upper, the middle and the lower set. Each set shares equal number of cell-strings, but only the cell-strings which belong either to the upper or lower part of the module have pins on the edge of the module where local converters are potentially located. Placing converters to the middle part would require a much higher technological effort, increase cost and will probably not lead to the desired results. If it considered necessary to have the option of connecting cell-strings which belong to the middle set of the module with a converter, it is better to add some long wires. If no such option is required, the cell-strings in the middle part will directly be connected to the upper part or the lower part of the module.

Converters on one side

The extreme case of reducing the local converters at the top of the module is to have converters just on one side of the module, the bottom side. The horizontal irradiation differences would be treated in the same way, as explained earlier on, with no additional wires needed. If their are irradiation differences in the vertical direction though, input and output pins of groups are situated on both sides of the module. Each set (upper and lower) will form a separate group. This can be compensated by allowing the existence of some long wires which are crossing the module, thus allowing the pins of the cell-strings on the top side of the module to connect to converters at the bottom side of the module. This configuration is no longer symmetrical at all in the vertical direction and it leads to a highly non uniform module. Not all the in and out pins of the cell-strings on the top of the module will be potentially connected to the converters. The input and output pins which are close to the edges (left and right) should be connected to the converters. An issue is raised here though, namely whether in this case the

wires should be added to connect the in and out pins of the upper cell-strings on the top of the module (Figure 4.24) or the middle of the module (Figure 4.25) with the converters. If the wires are added on the top, the functionality of the module is the same as described before (converters on both sides of the module), otherwise the functionality slightly differs. In the first case, the top pins of the upper set of cell-strings, which also have the most possible series connections between cell-strings, are connected to the converters.In the second case the bottom pins of the upper set of cell-strings, which have less number of possible series connections between the cell-strings, are connected to the converters. As analyzed before, series connections can be reduced on the side where the local converters are placed. This means that the connection of the bottom pins of the upper set of cell-strings to the local converters increases the flexibility of the module. However, a hybrid of the addition of wires can be considered as well.

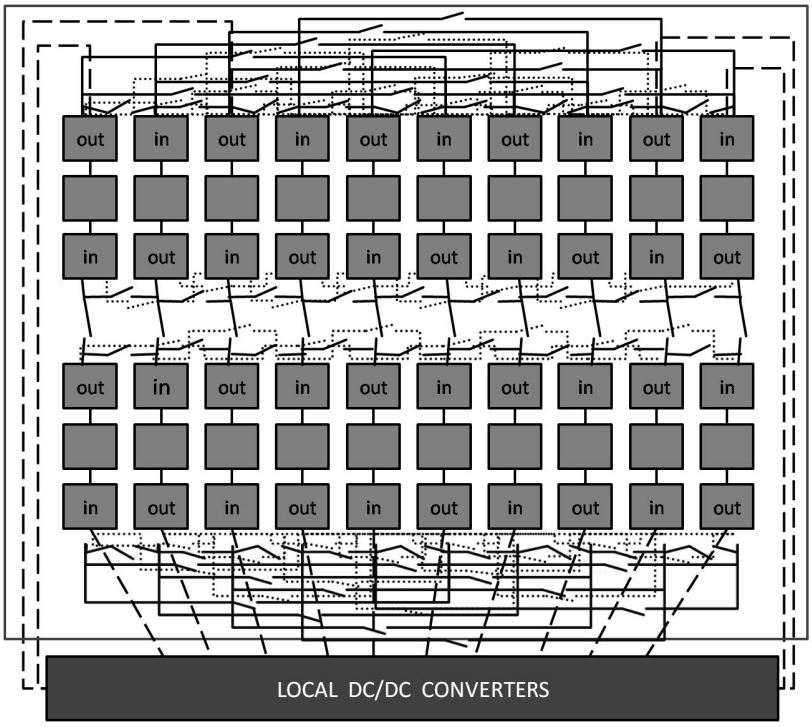

Fig. 4.24 Reconf.3 with converters on one side - Top pins of cell-strings of upper set connected to the local converters

The long wires that are shown in Figures 4.24 and 4.25 are chosen arbitrarily and just indicate how the wires will be placed if the wires connect the pins on the top of the module and the middle of the module correspondingly. Which pins will be connected depends mainly on the cost requirements and on the frequency of each irradiation scenario. The dashed wires

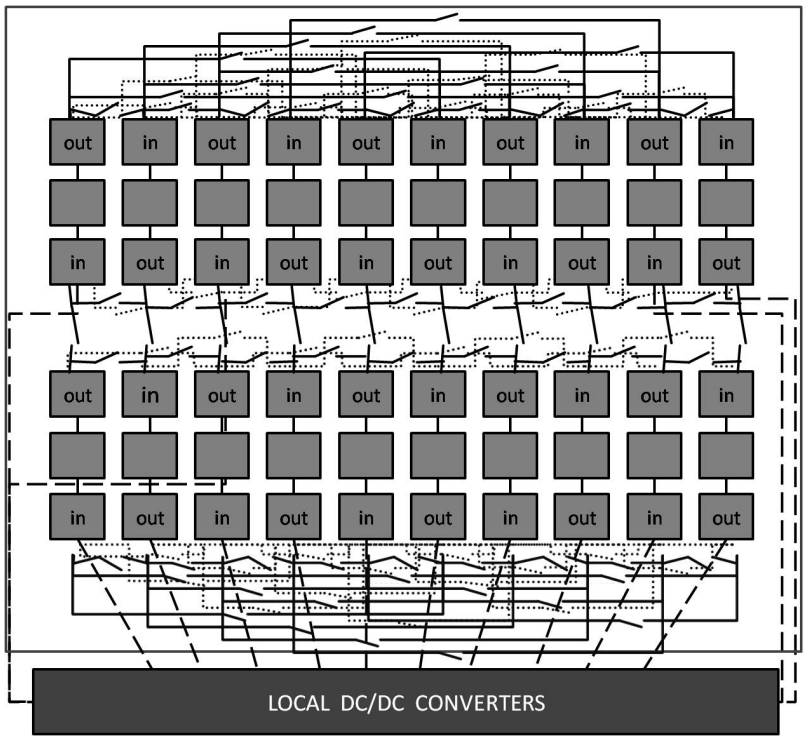

Fig. 4.25 Reconf.3 with converters on one side - Bottom pins of cell-strings of upper set connected to the local converters

which are shown in Figures 4.24 and 4.25 indicate that on that position a switch is present which is not shown.

4.4.3 Simulation Results

A module of 10 by 6 was simulated for the shading patterns of Figure 4.15 for various shading densities. The simulation results for the three shading patterns are shown in Tables 4.5- 4.7. For the shading patterns of Figure 4.15.b and 4.15.c, the Reconf.3 topology, outperforms the conventional module for most shading densities. The division of the module for the shading pattern 4.15.c is shown in Figure 4.26.

For the shading pattern of Figure 4.15.a, which is the best shading scenario for a conventional module, the conventional module outperforms the Reconf.3 topology, but it can be seen that the losses are not as severe as in the case of Reconf.6 (Table 4.2).

The performance of the Reconf.3 module for uniform conditions is shown in Table 4.8. It can be seen that the losses of this topology exhibits more losses than the other two reconfigurable modules examined (Table 4.1). This is expected as more resistive elements are added in the active path of the series connection of the cell-strings in the Reconf.3 topology.

Table 4.5 Instantaneous power of conventional, Reconf.3 and custom designed module for the shading pattern of Figure 4.15.a

Shading density	Conventional	Reconf.3	Custom
0.1	164.76	161.08	167.78
0.2	151.96	149.66	162.40
0.3	136.74	142.63	156.87
0.4	119.96	135.09	151.19
0.5	108.96	127.09	145.39
0.6	108.92	118.69	139.46
0.7	108.89	109.92	133.42
0.85	108.85	96.19	124.25
0.9	108.84	91.50	121.20

Table 4.6 Instantaneous power of conventional, Reconf.3 and custom designed module for the shading pattern of Figure 4.15.b

Shading density	Conventional	Reconf.3	Custom
0.1	163.83	160.31	166.29
0.2	150.62	154.41	159.88
0.3	135.24	148.32	153.28
0.4	118.46	142.02	146.51
0.5	100.58	135.54	139.57
0.6	81.78	128.89	132.49
0.7	62.17	122.08	125.27
0.85	31.46	111.67	114.30
0.9	20.95	108.19	110.65

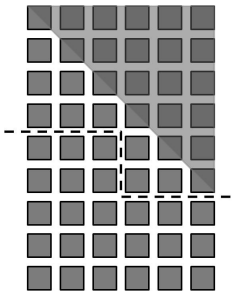

Fig. 4.26 Division of the module in the reconfigurable 3 topology for the shading pattern of Figure 4.15.c

Table 4.7 Instantaneous power of conventional, Reconf.3 and custom designed module for the shading pattern of Figure 4.15.c

Shading density	Conventional	Reconf.3	Custom
0.1	165.53	159.58	165.69
0.2	153.25	153.32	158.89
0.3	138.25	146.24	151.26
0.4	121.53	138.57	143.06
0.5	103.52	130.40	134.36
0.6	84.43	121.78	125.26
0.7	64.41	112.78	115.78
0.85	32.83	98.64	101.00
0.9	21.95	93.80	95.95

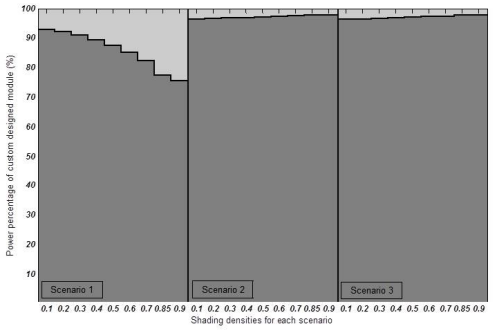

Fig. 4.27 Reconfigurable module with cell-strings of 3 cells

Table 4.8 Instantaneous Power of Reconf.3 under uniform conditions

Irradiation Level	Conventional	Reconf.3
1000 W/m^2	172.88	168.67
500 W/m^2	90.06	88.98

4.5 Conclusions

It is shown that the three design instantiations of reconfigurable topologies exhibit promising results when operating under non-uniform conditions, especially under partial shading conditions. The row/column templates (Reconf.10 and Reconf.6) are limited by their one-dimensional granularity and the template where the vertical split is applied (Reconf.3) exhibits larger power losses when operating under uniform operating conditions. As uniform conditions are still expected to be present quite frequently, a topology is needed which allows has a similar granularity and flexibility as the Reconf.3 template, but which has less power losses under uniform conditions. This is explored in Chapter 5.

Chapter 5

Snake Topologies

In Chapter 3, the main concepts of reconfigurable topologies were discussed and in Chapter 4 these concepts were applied in rectangular modules where the main objective was to interfere as little as possible with the preexistent connections of conventional modules. It is observed however that in order to obtain some degree of flexibility in both direction of a PV module, switches need to be added in the middle of the module. The purpose of a snake topology is to avoid any type of switches and dynamic elements within the cell matrix of the PV module and to reduce the resistive losses of the module under uniform conditions.

A different layout of cell-strings and a supporting electrical network are proposed in this Chapter which enable reconfiguration of the module. Granularity is present in both directions of the module. First, the division of the module into cell-strings is presented. Next the required supporting network is described and the two main run-time instantiations of the module are shown. Finally, simulation results illustrate that the performance of snake topologies under uniform conditions have very few losses.

sectionSelection of Cell-strings

As discussed in Section 3.3, the module must be divided into series-connected cell-strings to reduce the overhead of component cost but also of wiring, converter and switching losses. The goal is to find a Pareto optimal size of the cell-string. Apart from the trade off between architecture complexity and run-time flexibility, the decision of the layout of the cell-strings depends on

1. The initial manufacturing cost. Adding switches in the middle of the module is more expensive and thus all dynamic elements in the proposed template are restricted to the edges of the module.

2. The performance of the module under uniform conditions. An all series connection is known to be the optimal configuration under uniform operating conditions because it

allows to restrict the current and hence to reduce the important resistive losses. When all cells have similar electrical response at run-time, the module performance should deviate from the conventionals as little as possible.

A proposed cell-string template is depicted in Figure 5.1 for an M by N module. Once again, without loss of generality, it is assumed that $N < M$. Factors of selecting the cell-strings:

- Size of cell-strings: To increase the granularity level of the module the largest dimension is selected to have more divisions.
- Geometry: The majority of the cell-strings are U-shaped to allow a better split of the module for both vertical and horizontal moving shading patterns.
- All cell-strings consist of the same number of cells to allow both parallel and series connections of cell-strings.

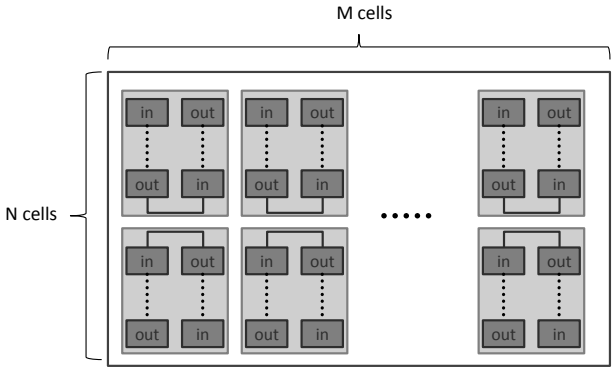

Fig. 5.1 Layout of the cell-strings for a M by N module illustration (U-type template)

The cell-strings of the proposed template consist of N cells connected in series. In the template of Figure 5.1, the module is symmetrical and all the strings are U-shaped. This geometry of the cell-strings allows a better split of the module in all directions.The granularity level of the module in one direction is of two cell-strings, while in the other direction of N/2 cells. The extra factor of minimizing the losses of the module when operating under

uniform/near uniform operating conditions requires to have an active path with minimal addition resistive losses due to added wires and switches. This is achieved by having an all-series connections of the cell-strings. In Figure 5.2 the wires and switches required for the series connection of the cell-strings are shown for a module of 10 by 6 cells. Due to the electrical orientation of the cell-strings, a long wire is needed to connect two of the cell-strings located on the left edge of the module. Furthermore, the general input and output of the module are located on two opposite sides of the module, necessitating long wires to connect to the module converter.

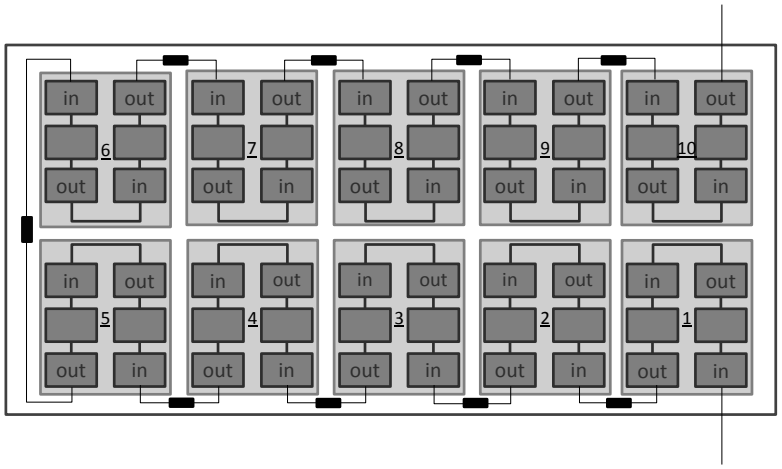

Fig. 5.2 Layout of the cell-strings and series connection of cell-strings for a 10 by 6 module illustration (U-type template)

In order to reduce the resistance on the active path for uniform conditions, a modified layout of cell-strings is considered as shown in Figure 5.3. The two cell-strings on the edges of the module of the template are straight. The granularity of N/2 cells in the vertical direction is not present for the entire module. This allows less active wire length under uniform irradiation conditions, as shown in Figure 5.4, but limits the flexibility of the module for shadows moving vertically to the direction of the columns. In order to distinguish the two templates, they will be referred to as U-type template and I-type template respectively. The connection of the cell-strings in series resembles a snake-like configuration, thus the name of snake topologies.

5.1 Supporting Electrical Network

The proposed configuration consists of the layout of cell-strings as depicted in Figures 5.1 and 5.3. In order to improve the performance of the module under different operating

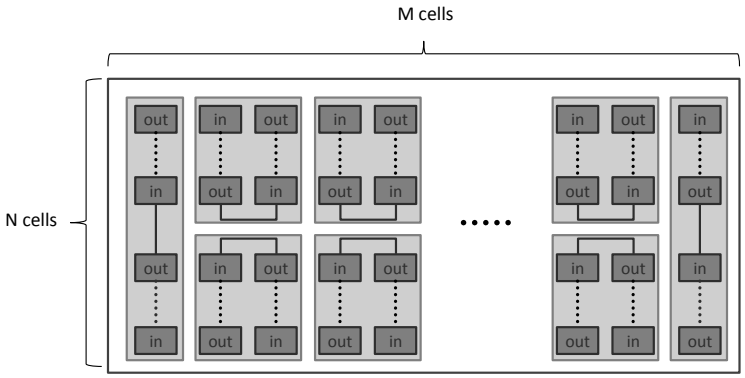

Fig. 5.3 Layout of the cell-strings for an M by N module illustration (I-type template)

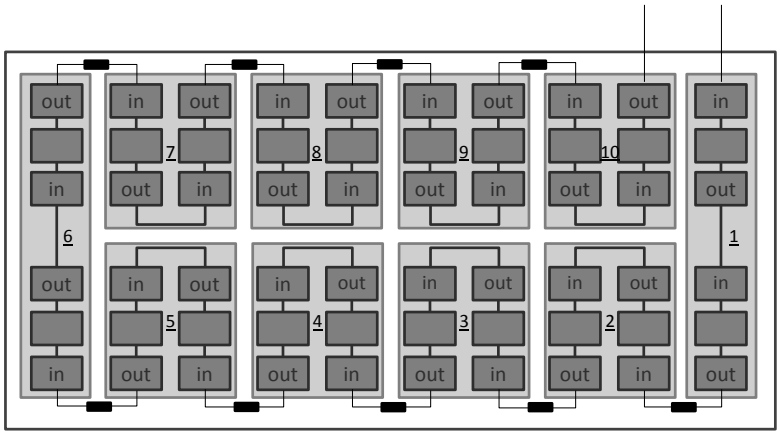

Fig. 5.4 Layout of the cell-strings and series connections of cell-strings for a 10 by 6 module illustration (I-type template)

conditions, different options are available for the interconnection of the cell-strings which is aided by the use of local converters. The proposed supporting network snake type topologies is presented here.

Series Connections The series connections of cell-strings are necessary for operation of the module under uniform irradiation conditions. As seen in Figures 5.2 and 5.4, all cell-strings are connected via a wire and switch with the neighboring cell-string. As mentioned in Chapter 3, a series connection of two cell-strings requires one switch. The number of wires and switches required for the all series connection of the cell-strings is X-1, where X the number of cell-strings. In the general case described above, this is equal to M-1. In order to keep the added hardware to a minimum, no other potential series connections of cell-strings will be added.

Parallel Connections In section 3.4.1, the parallel connections of cell-strings are described. It is noted that the parallel connection of two cell-strings is optimal when they share a similar voltage around their optimal operating point. All the cell-strings have the same number of cells and thus when they operate under similar conditions, the voltage of the cell-strings is similar. Under different irradiation conditions, the voltage point of the MPP does not shift so much [56]. This means that mismatch occurrences between cell-strings with different irradiation conditions in a parallel connection are not often. However, having all M cell-strings connected in parallel in one large group would increase the current to the extent that the resistive losses would be a dominant factor. Furthermore, the current may be too large to be handled by the module converter. At this point, no direct parallel connections of cell-strings are added. Parallel connections will be introduced with the inclusion of local converters to the template.

5.1.1 Local Converters

In section 3.4.2 the possible combinations of type of connections within a group of cell-strings and the type of connections between the converters is described. Here, the selection is to have groups of parallel connected cell-strings connected to groups of parallel connected local converters. The parallel connection of the cell-strings ensures the limitation of mismatch losses, but increases any resistive losses in the active current path. The goal here is to reduce the parts of the active path where high current flows.

In order to connect two cell-strings in parallel, two switches are needed. One for connection of the in pins and another for the connection of the out pins. To connect the group of these two cell-strings to a local converter, two more connections are required, one

to the positive terminal of the converter and one more to the negative terminal. The wires connecting the cell-strings to the converters have the disadvantage of carrying the sum of the currents of the two cell-strings. Another equivalent option would be two connect the pins of each cell-string directly to the terminals of the converter. In the case of two cell-strings both options have four switch-controlled connections, but the second one has the advantage that current is accumulated only when it reaches the local converter. The two options are illustrated in Figure 5.5.

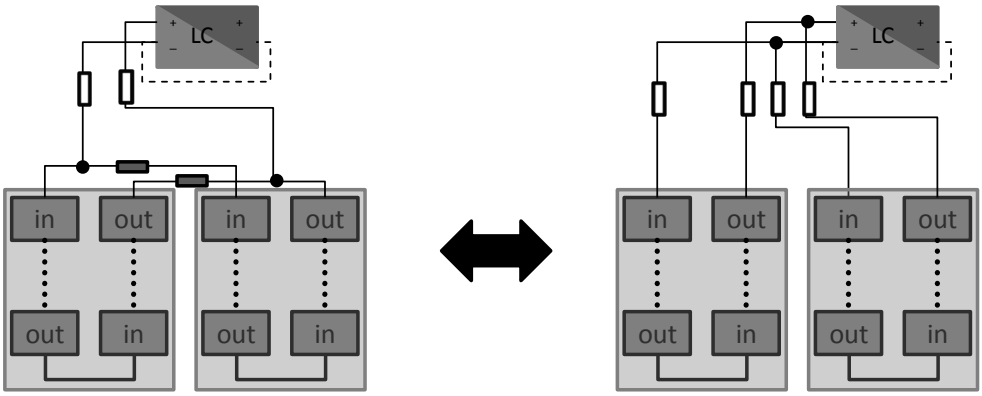

Fig. 5.5 Equivalent options of connecting a group of two parallel connected cell-strings to a local converter

Connection of cell-strings to local converters

In the snake topologies, under non-uniform conditions, the cell-strings are connected in parallel to form groups, where each group is connected to a local converter. The division

of the cell-strings in groups is not based on the run-time conditions of the module, but is determined at design-time. Parallel connections of the cell-strings ensure that the cell-strings are not so affected by partial shading; Vmpp is not so strongly affected by irradiation. However, the parallel connection of the cell-strings increases the current level of the group; the maximum current of each group which reaches a local converter is equal to the sum of currents of the cell-strings in the group and can be equal to the number of cell-strings in a group times the current of a fully illuminated cell.One of the main roles of local converters in the snake topology is to boost the voltage and reduce the current. The current reduction is needed to keep the resistive losses after the conversion stage as low as possible and to meet the module converter requirements in terms of maximum input current. The voltage boost is also needed to reduce the module converter requirements in terms of input voltage range.

Interconnection of local converters

Under partial shading conditions, where local converters are active, all groups are formed by parallel-connected cell-strings. As all cell-strings have the same number of cells, the voltage of each group does not differ significantly. The simpler and most cost-/complexity-effective solution, when groups of cell-strings with similar MPP voltages are considered, is a parallel connection of the outputs of the converters. In parallel converter connection with parallel grouping, it is optimum to activate all converters to ensure that the current of no group is too high. Thus no bypass scheme is required to bypass local converters in this topology. Two accumulative bus lines, which are not switch-controlled are utilized to collect the current out of the converters; a groundline and an accumulative bus. These are the only large wires where more than the current of a single cell-string flows.

The groundline and the accumulative bus are connected to the module converter which regulates the voltage and current and can be used to connect to other elements of the PV array. The connection of the local converters to the module converter is a cascaded type connection. The interconnections of the converters are shown in Figure 5.6. The dashed line is the groundline, while the continuous black line represents the accumulative bus. The accumulative bus may also be split in two different buses, which would have the advantage of less metal, less current per bus and less differences in the local converters' output voltages.

5.1.2 Hardware Requirements

The cost of the proposed PV module topologies in hardware terms is summarized in Table 5.1. A distinction is made between the different types of switches and converters. Each type of switch needs to withstand a different voltage, thus leading to a different cost. Three different

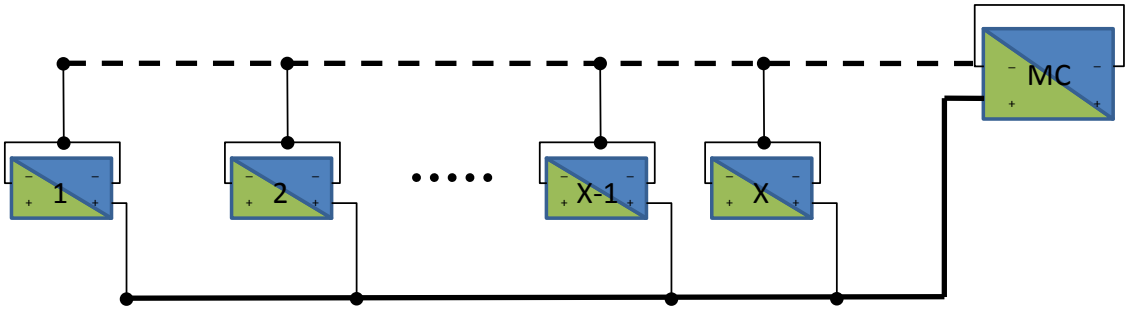

Fig. 5.6 Interconnection of local converters and module converter for snake topologies

types of switches are present in the table. The distinction is made based on their use and the conditions that they should withhold when they are active or inactive.

Switches between cell-strings are used to connect the cell-strings in series. The number of switches required for this is X-1, where X the number of cell-strings of the module. When these switches are active they maximally carry the current of a single cell. When they are inactive, if only the two main classes of run-time instantiations are considered (all in series and groups of parallel connected cell-strings, Section 5.2), the voltage across them is the operating voltage of a cell-string.

Switches between cell-strings and the ground line connect the in pin of a cell-string to the ground line. As one cell-string is connected to the ground line both in the series connection of the cell-strings and in the parallel connection in groups, X-1 switches are needed and the common connection of the cell-string to the ground is a permanent one. When active, these switches carry the current of a single cell. However, when they are inactive, the voltage across them is higher and depends on their position in the module, maximally reaching the operating voltage of the entire module.

The other type of switches is the one connecting the cell-strings to the converters. In the series connection, one cell-string is connected to the module converter. In the parallel case, all cell-strings are connected to local converters. This leads to (the number of cell-strings plus one) potential connections of cell-strings to converters. This illustrates that the number of switches is not related to the number of local converters, but solely on the number of cell-strings in the module (granularity level). Once again, the current flowing through these switches never exceeds the current of a single cell. As the converters are also inactive when the switches are inactive, the voltage across them when they are inactive is not really determined as it also depends on the actual design of the converters.

Two types of converters are applied as well. The distinction in the converters is based on the width of the voltage window. The four local converters require a small voltage window; when active, they are always connected to groups of parallel cell-strings. The module converter requires a larger voltage window. Under uniform conditions, it is connected to the entire module, while under partial shading it boosts the voltage of the four parallel converters. Neither type of converter requires a complex MPPT algorithm, as the absence of bypass elements eliminates the possibility of local maxima.

5.2 Run-time configurations of the module

The proposed template along with the supporting network is illustrated in Figure 5.7, for a module of 10 by 6 cells. To avoid redundancy, the complete configuration is illustrated only

Table 5.1 Additional components required for the snake topologies

Component	X cell-strings
Switches between cell-strings	X-1
Switches between cell-strings and ground line	X-1
Switches between cell-strings and converters	X+1
Local converters	n
Module converter	1

for the template utilizing I-type cell-strings. The proposed reconfigurable topology has two main types of run-time instantiations which are better suited for uniform and non-uniform conditions respectively. It should be noted here that uniformity is not only related to shade. Other factors like defective cells or bird droppings can create significant non-uniformities which can be handled in the proposed reconfigurable topologies.

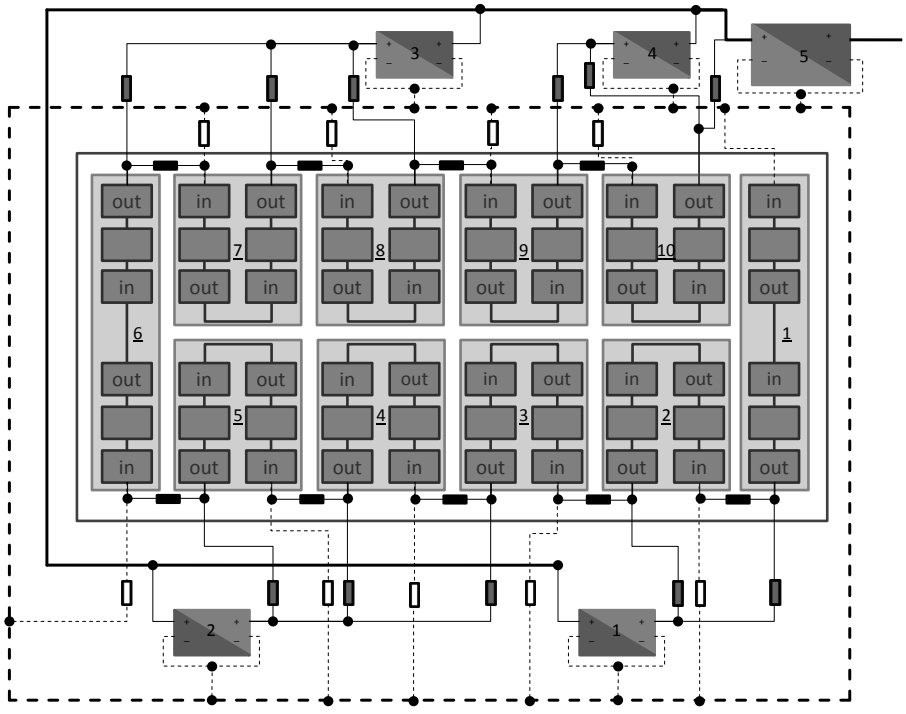

Fig. 5.7 I-type template of the reconfigurable module

5.2.1 All-series connection

An all series connections of the cell-strings, which is optimal when the module operates under uniform conditions. Under uniform conditions, there is no real issue for mismatch occurrences between the cell-strings and a single configuration is available. The all series connection of the cells is optimal as the current level is equal to the current produced by a single cell and the resistive losses are kept minimal. The cell-layout of the I-type is better as shorter wires (than in the U-type) are active when all cell-strings are connected in series (Figures 5.2 and 5.4). The active components of this configuration for the I-type template are depicted in red in Figure 5.8.

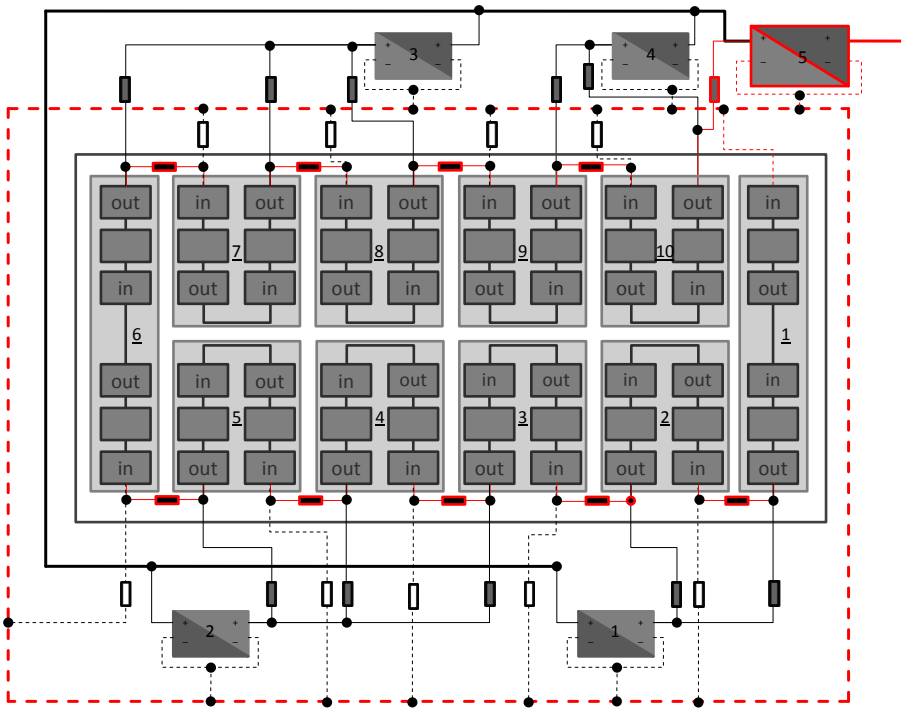

Fig. 5.8 Active components of the template for the all series connection (I-type template)

5.2.2 Parallel connection of cell-strings

A configuration of groups of parallel connected cell-strings to local converters optimal for operation under partial shading conditions. Under non-uniform conditions, the cell-strings are connected in parallel to avoid large mismatch losses. (Voltage is not so sensitive to the incident irradiation level). However, the parallel connection of cell-strings increases the current level and thus the resistive losses. The number of parallel-connected cell-strings in a

group should not exceed a certain number (depending on the electrical characteristics of the cells), as the gain from avoiding mismatch losses would not compensate for the increased resistive losses. Local converters are placed to reduce this current and to keep the resistive losses low, as stated in Section 5.1.1. However, local converters are likely to show lower efficiency at high current. Furthermore, the higher the input current, the more complex and expensive the local converter. This represents additional limitation to the maximum number of parallel-connected cell-strings. The output ports of the local converters are connected in parallel. The input port of the module converter is connected to the outputs of the local converters to further boost the output voltage for connection of with the rest of the PV array. In this configuration, the U-type module has a a better division of the cells (than the I-type) in the vertical direction for the entire length of the module. The active path of the this run-time instantiation is illustrated in Figure 5.9 for the I-type template.

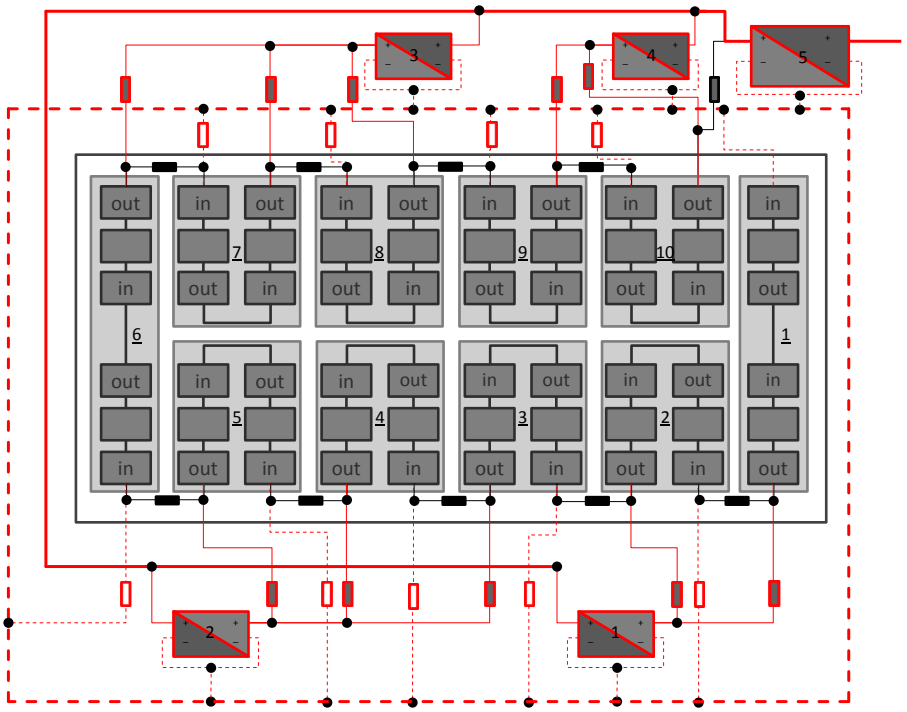

Fig. 5.9 Active components of the template for the parallel connection of cell-strings (I-type template)

Hybrid types of run-time instantiations are also possible. Depending on the operating conditions, the cell-strings within a group can be connected in series, cell-strings can be isolated or local converters can be bypassed. Thus, several configurations are available, but their similarity allows to treat them as one of the above configurations.

Reliability of the reconfigurable module The reliability and the lifetime of PV modules are important factors in the market of PV systems. The lifetime of the cells themselves should not be affected by the presence of extra components. The smaller size of cell-strings compared to the bypass sections of the conventional module protect cells from mismatch effects and degradation. The reliability of switches and converters is not the focus of this work. Another community is working on this issue ([59], [60]). The topology exploration performed in this work is believed to be compatible and complementary to the solutions provided for the extra components.

5.3 Results for Uniform Conditions

Under uniform conditions the conventional module performs slightly better than the reconfigurable. The only extra components in the reconfigurable topology are the switches enabling the series connections of the cell-strings. These switches add a resistance in the active current path which result to some power losses as the current increases. The power performance of the conventional module and the reconfigurable topologies with I-type and and U-type cell-strings are shown in detail in Table 5.2. As expected, the reconfigurable module with a U-type cell-strings, has slightly larger resistive losses. The module in test has a short-circuit current of 5A under uniform irradiation of 1000W/m^2 intensity. It has to be mentioned here though, that even under high irradiation, where the current is higher, the power loss of the reconfigurable module does not exceed 0.4% and 0.6% for the I-type and U-type cell-strings respectively.If the current of a module is larger, the resistive losses are expected to be higher as well. The wires, switch and cell characteristics are described in detail in Section 6.2.

5.4 Performance under static shading conditions

The performance of each of the proposed templates for the shading pattern presented in Section 3.1 (Figure 5.10) is listed in Table 5.3, along with the power generated for a conventional topology.

The notations (S) and (P) next to the power generated by the two proposed reconfigurable topologies denote whether the best performance of the reconfigurable module is an all series connection of the cells (S) or a parallel grouping of the cell-strings (P).

This shading pattern, as stated earlier on, is an ideal case for the conventional module utilized in this work as the shade affects only one bypass section. Furthermore, all the cells of that bypass section are shaded and thus there are uniform conditions within all bypass sections of the conventional module. The specific shading pattern is selected as the MPP,

Table 5.2 Performance under Uniform Irradiation Conditions

Level of Irradiation (W/m^2)	Power of Conventional Module (W)	Power of I-type Snake (W)	Power of U-type Snake (W)
1000	109.2	108.8	108.5
900	99.9	99.6	99.4
800	91.3	91	90.8
700	82.4	82.2	82
600	72.9	72.7	72.6
500	62.6	62.5	62.4
400	51.3	51.2	51.2
300	39.2	39.1	39
200	26.1	26	26
100	12.4	12.4	12.4

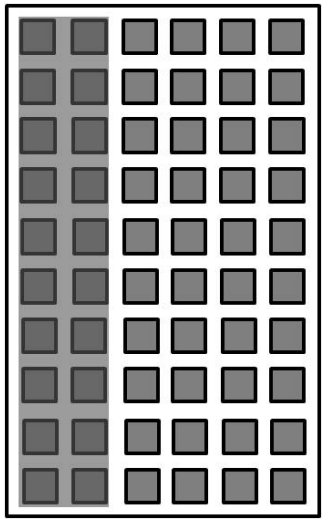

Fig. 5.10 Shading pattern of Section 3.1

depending on the shade density, lies either in region I (the bypass diode is active) or in region II (the bypass diode does not conduct). This allows to analyze the performance of reconfigurable topologies in both cases. The fully illuminated cells receive $1000W/m^2$ while shaded cells have an irradiation level of $(1-SD)*1000W/m^2$, where SD is the shading density.

Table 5.3 Performance for the shading pattern of Figure 5.10

Shade density	Power of Conventional Module (W)	Power of I-type Snake (W)	Power of U-type Snake (W)
0.1	105.0	104.8 (S)	104.5 (S)
0.2	99.0	98.7 (S)	98.5 (S)
0.3	91.0	90.7 (S)	91.2 (P)
0.4	81.2	84.1 (P)	86.8 (P)
0.5	71.0	78.0 (P)	81.9 (P)
0.6	71.0	71.0 (P)	76.4 (P)
0.7	71.0	63.9 (P)	70.5 (P)
0.8	71.0	56.3 (P)	64.2 (P)
0.9	71.0	48.2 (P)	57.3 (P)

It can be seen that in the conventional module, the diode corresponding to the shaded section is active when the shading density is over 0.5 and for the range of shading density [0.5-0.9] the power of the conventional module is the same. When the shading density is low, thus the non-uniformity degree within the module is low, the best run-time instantiation of the reconfigurable topologies is the all-series connections of the cell-strings. As the shade becomes denser, the parallel connection of the cell-strings has better results.

For this shading pattern, 6 cell-strings of the I-type snake module and 5 cell-strings of the U-type snake module are partially shaded. The portion of the module in reconfigurable topologies which is affected by shade (60% and 50%) is quite larger than that of the conventional module (33%). Despite this fact, the reconfigurable modules still have some gains for the shading densities 0.4-0.6 (0%-15%).

It is a different case however when only part of the bypass section of the conventional module is shaded, i.e four shaded cells as shown in Figure 5.11. The results of this shading patterns are shown in Table 5.4. The same portion of the conventional module is affected by the shade and the results of the conventional module are the almost the same as those before. The portion of the reconfigurable modules which is affected however changes quite a lot. The finer granularity level means that this shading pattern affects two cell-strings (20%) of the I-type module and one cell-string (10%) of the U-type module.

For this shading pattern, both reconfigurable topologies have power gains when the shading density is over 30%. It can be seen that the percentage of gain increases up until the shade density reaches 0.7 and for denser shades, the gain starts dropping. When the shade density is light, the recovered power comes from the fully illuminated cells; in the conventional module these cells operate with a reduced current as the diode is not conducting.

Table 5.4 Performance for the shading pattern of Figure 5.11

Shade density	Power of Conventional Module (W)	Power of I-type Snake (W)	Power of U-type Snake (W)
0.1	108.2	107.8 (S)	107.5 (S)
0.2	104.5	104.2 (S)	103.9 (S)
0.3	97.2	98.0 (P) [0.82%]	99.5 (P) [2.37%]
0.4	87.4	95.8 (P) [9.61%]	98.5 (P) [12.70%]
0.5	75.7	93.5 (P) [23.51%]	97.4 (P) [28.67%]
0.6	71.0	91.0 (P) [28.17%]	96.2 (P) [35.49%]
0.7	71.0	88.5 (P) [24.65%]	95.1 (P) [33.94%]
0.8	71.0	86.1 (P) [21.27%]	93.9 (P) [32.25%]
0.9	71.0	83.6 (P) [17.75%]	92.7 (P) [30.56%]

When the shade becomes denser and the bypass of the conventional module conducts the extra current of the fully illuminated cells, the power is recovered from the shaded cells which are bypassed. As the shade becomes even more dense, the irradiation received by the shaded cells becomes less, the contribution of the shaded cells is not so significant.

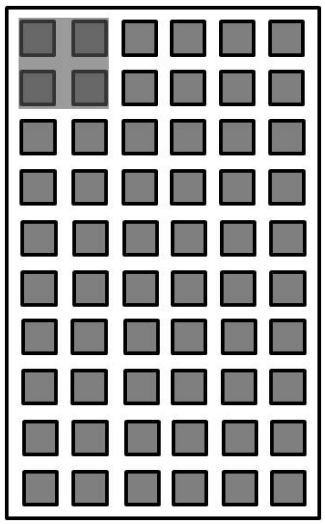

Fig. 5.11 Shading pattern with four shaded cells

When the shading pattern affects all bypass diodes, as the shading patterns shown in Figures 4.15.b and 4.15.c, the gains of the reconfigurable topologies w.r.t the conventional module always increase as the shade density becomes denser. In this type of shading patterns, the overall current of the conventional module is always limited to the current produced by the shaded cells (no local peaks in the Power-Voltage curve of the conventional module)

and the overall current of the conventional module becomes smaller as the shade density increases.

5.5 Conclusions

It can be seen that the two snake templates have significant less power losses w.r.t the conventional module under uniform operating conditions than the Reconf.3 topology described in Chapter 4. The power loss of I-type and U-type are 0.4% and 0.6% at a irradiation level of $1000W/m^2$, while the Reconf.3 topology had a power loss of 2.44%. There are two reason for this reduction of power losses. Firslty, each cell-string of the snake templates comprises of twice as many cells as the cell-strings of the Reconf.3 topology. This means that in the all series connection of the cell-strings less extra elements are present. Secondly, a smaller cell was used for the snake topologies, 5-inch cell instead of 6-inch cell. A smaller cell in area produces a smaller current and the module requires shorter wires for the interconnections of the cell-strings. This means that the additional resistive losses are futher reduced due to smaller resistances and less current. The losses of the snake-templates, under uniform conditions, when 6-inch cells are used are 1.41% and 1.59% for the I-type and the U-type respectively. These losses are closer to the Reconf.6 topology (1.50%) as the three templates have the same number of cells per cell-string. For this reason, smaller-sized cells (in area) are better-suited for reconfigurable topologies.

The snake topologies, in contrast with the row/column topologies of the module have a granularity level in both directions of the module and have lower power losses in uniform conditions than a topology where a vertical split is applied. Furthermore, the reduction of run-time instantiation of the module to two main classes (all series and parallel connection of cell-strings) will potentially allow a simpler implementation of a control scheme. In order to further explore the potential gains of reconfigurable topologies, the performance of different module types need to be compared for dynamic conditions. For this, a simulation environment is needed which allows an accurate estimation of the energy yield of PV modules. This is discussed in Chapter 6, along with a more detailed analysis of the cost.

Chapter 6

Design Time Instantiations of Snake Topologies / Performance under dynamic shading

In the previous Chapter, the concepts of the snake topologies are introduced. The templates presented were parameterized and the role of each component was analyzed. For specific values of the parameters, a design instantiation of the PV module is created. Each design time instantiation allows two main classes of run-time instantiations of the module. Once a design instantiation has been decided, a more analytical energy-yield evaluation and fabrication cost can be calculated. In this chapter the energy-yield of the two main instantiations is analyzed. A cost model is presented for the general case and the cost is calculated for a specific design time instantiation of a snake topology. Furthermore a simulation environment is presented which is used to evaluate the performance of a reconfigurable module under dynamic shading conditions caused by static objects. Finally simulation results are presented for these dynamic scenarios and the performance is compared to that of conventional modules.

6.1 Energy Yield Overhead of Snake Topologies

As stated earlier, snake topologies have two main run-time instantiations which are active under different operating conditions of the module. The active components, the power losses they induce and the reason of their presence are discussed separately for the different active current paths in this section.

6.1.1 All series connection

The additional components are placed to enable a different configuration for non-uniform operating conditions and to improve the performance under partial shading. Under uniform conditions, some of these added components are active and increase the resistive losses of the module, compared to an industrial module with the same number of cells.

Added active components under uniform conditions include:

1. Switches which connect the cell-strings in series (the number of switches depends on the number of cell-strings). These switches do not have to withstand a large voltage difference.

2. Switch from the output to the module converter

3. Additional wiring required for the edge connections of the cell-string. The cost and the resistance of such additional wiring depend on:

    - Material that they are made of (copper or aluminum)
    - Wire dimensions. The length of the wires is strictly related to the design-time instantiation (position of wires, switches, converters and cells) as well as to the dimensions of the cells. The cross-section of the wires can be changed instead to balance additional cost (amount of material) and wire resistance.

All these losses depend on the current that flows through the wires. Under uniform conditions, the current flowing through the module is equal to the current produced by a single cell. This current depends on the level of incident irradiation and the cell's technology. Thus it should be noted here that the cell's characteristics have a significant impact on instantiating a reconfigurable topology. The instantiation of the snake template is optimized for a 10 by 6 rectangular module with a 5 inch cells where the short-circuit current under Standard Test Conditions (STC) is around 5A [61]. The simulation results of this module are shown in section 6.4 and it can be seen that the losses for uniform cases are reasonable due to the heavy emphasis that has been put in our design template to reduce these (see section 5). However, the location of installation should be characterized by periods of partial shading in order to compensate for these losses and finally gain in the overall energy production. Larger cells (in area) produce more current and thus the resistive losses can become more dominant. In that case, the total resistance in the active path for uniform conditions should be decreased. A first option would be to remove some switches and increase the size of some cell-strings. However, when doing so it is recommended that cell-strings which are assigned to a certain

converter should have the same size. In case of larger modules, i.e. a module of 12 by 6 cells, the same principles are applied. There are mainly two options, one is to have the cell-strings with the same size and increase the number of switches or to allow the presence on some longer cell-strings. Depending on the size of the module, extra local converters can be placed. On the other hand, use of half cells, as proposed in some recent industrial trends [62], would reduce the amount of current produced by a single cell, thus the resistive losses would be even less. That last option is hence a very attractive one.

6.1.2 Groups of parallel connected cell-strings

Active components under non-uniform conditions:

1. Switches which connect the input and output of cell-strings to the local converters
2. Local converters
3. Additional wiring required for the interconnection of all the components

The switches and the additional wires required for the interconnection of the cell-strings and groups increase significantly the resistance on the active path of the current in this configuration. Under uniform conditions, although no mismatch phenomena are present, this configuration has big resistive losses, due to bigger currents and longer paths. The level of non-uniformity, thus recovered power due to mismatch effects, should be significant to justify a switch to a parallel configuration of the cells. The number of switches are the minimum required to enable both types of the main run-time instantiations and are placed in such a way to carry the current of a single cell.

The main parameter to decide on at design-time is the number of parallel stubs (with each one local DC converter) and which of the neighboring cell-strings are grouped into each parallel group. The number of cell-strings corresponding to each converter, the number of the local converters and the exact placement of the converters are decided at design time. All these parameters have an impact on the resistive losses of the current path. In this configuration, all local converters are operating in a boost mode in order to reduce the output current of each group and keep the resistive losses along the accumulative bus and ground line minimal. This is illustrated in Figure 6.1.

The wires and switches which connect the input and outputs of each cell-string to the corresponding converter carry the current of a single cell-string. The resistance of the wire depends on its length, thus the location of the converters determines the total resistance of these connections.

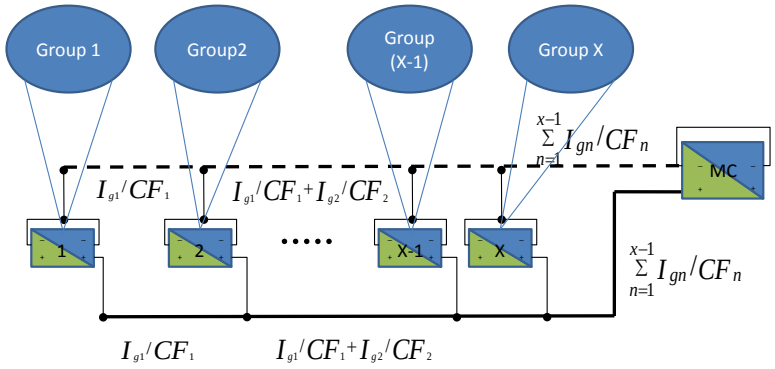

Fig. 6.1 Current flow when the local converters are active, I_g: input current of a group, CF: conversion factor

6.1.3 Other types of connections

The additional hardware described in Section 5.1 enables also other types of run-time instantiations of the PV module. Other types of connections are relevant only under non-uniform conditions as it has been demonstrated that the best configuration for uniform conditions is an all series connections of cells.

Under conditions of partial shading, instead of connecting the cell-strings of each group in parallel, the cell-strings of a group can be connected in series. The main advantage of the series connection of cell-strings is that it does not increase the current and thus parasitic losses are minimized. Of course it has to be noted here that in order to connect a group of cell-strings in series, the current of all cell-strings needs to be similar to avoid mismatch losses. This would necessitate information about the run-time electrical characteristics of each individual cell-string, thus use of more monitors. Another disadvantage of allowing this type of run-time instantiation is that the voltage which will be imposed in inactive switches is increased and a larger subset of switches should be able to withstand higher voltages. Still, also that can be prevented with the use of monitors because an attractive hybrid case would allow to use the series option only for situations with quite low power where the max voltage is still low enough, and to switch to the parallel option as soon as the total voltage increases above a threshold. The potential gain of these configurations should be evaluated to determine if the overall gain in energy-yield would compensate for the extra cost needed.

It is not necessary to have either all groups of cell-strings in parallel or in series connection; some of the groups internally can be connected in series and others in parallel. The local converters however are all connected in parallel and the output of all local converters should be able to reach a common voltage. If a group is internally connected in series, the voltage at the input terminal of the converter is almost equal to $x * V_{cs}$, where x the number of cell-strings in the group and V_{cs} the operating voltage of a cell-string. Thus the ability of reaching a common voltage when all groups are internally connected in series depends on the number of cell-strings within all groups and the available conversion factors of the local converters. If hybrid connections are allowed to take place as well, the voltage of a single cell-string should be able to reach the voltage of a series connected group, through the proper run-time selection of the conversion factor.

6.2 Investment cost and fabrication cost

In Section 5.1.2 the hardware requirements of a snake topology with X cell-strings is discussed. In this chapter the focus is on a design instantiation of a PV module with 10 cell-strings. The number of added discrete elements are shown in the following table for a PV module with a snake topology design and 10 cell-strings. These elements apply for both a U-type and I-type module.

Three different types of switches are present in the table. The distinction is made based on their use and the conditions that they should withhold when they are active or inactive. The ON resistance of all switches in considered to be 3.6mΩ [58].

Table 6.1 Additional elements for snake topologies with 10 cell-strings

Component	10 cell-strings
Switches between cell-strings	9
Switches between cell-strings and ground line	9
Switches between cell-strings and converters	11
Local converters	4
Module converter	1

The additional wires needed for the interconnections of the elements of the reconfigurable module cannot be addressed with number of connections, as the extra metal required depends on the design of the module. In this work, the module template is optimized to reduce the additional power losses, while maintaining the investment cost in reasonable levels. This is achieved by selecting appropriately the placement of the local converters. The wires

Table 6.2 Wire Dimensions for Snake modules

Type	Material	Width	Thickness
Accumulative Bus	Copper	5mm	0.5mm
Ground Line	Copper	10mm	0.5mm
Cell-strings to Cell-strings	Copper	4mm	0.3mm
Cell-strings to Converters	Copper	4mm	0.3mm
Cell-Strings to Ground Line	Copper	4mm	0.3mm
Converters to Ground Line	Copper	10mm	0.5mm
Converters to Accumulative Bus	Copper	4mm	0.3mm
Perpendicular connections within a U-shaped cell-string	Copper	4mm	0.3mm
Long wire in U-type module	Copper	5mm	0.5mm

dimensions and material are designed to keep the resistive losses minimal with consideration of the investment cost they impose.

The dominant added wires in the reconfigurable module are the accumulative bus and the ground line which surround the module as seen in Figure 5.7. Shorter wires are needed to connect cell-strings to cell-strings, cell-strings to converters, cell-strings to the ground line, converters to ground line and converters to the accumulative bus. Additional metal is also used for connecting cells perpendicularly within a U-shaped cell-string and for the long wire required to connect "neighboring" cell-strings in the U-type module. For each category of connections, different cross-sections of wires are used. In order to keep the resistance and the area low, the metal that is used is copper. If needed, aluminium can be used to reduce the fabrication cost, but as aluminium has a larger resistivity the amount of metal should be increased to have the same total resistance. Still, because the cost of aluminium is so low, the material cost will still outperform the copper for an equivalent total resistance. So the main decisive factor will be the ease of connections which requires some form of soldering or an alternative interconnect approach. Another option, as discussed in 4.2.2. would be to place the wires and added components on the backside of the module, but this is costly with today's standard modules and constitutes future work.

The thickest and wider wires are used for the accumulative bus and the ground line. These wires surround the entire module, thus are the longest and carry the highest current. Cross-section of the shortest wires and of all wires that are subjected to a maximum current level equal to the cell current, is kept equal to that of wires in the edges of industrial/conventional PV modules interconnecting the columns, that is width 4mm and thickness 0.3mm. To estimate the total amount of metal needed for a specific design instantiation of a PV module,

some other dimensions are needed as well. The cell size, that is 12.5x12.5cm^2 for the selected cells and the cell spacing, that is kept to 2mm, as in current standard modules. Two-busbars cells are considered, where the distance between the busbars is 6.2cm and the distance between a busbar and the edge of the cell is 3.15cm [61]. The exact location and placement of the local converters and the module converter are needed to calculate the length of all wires. Once the length of the wires is calculated, based on the dimension of the cells and the spacing, and by taken into account the dimensions of the cross section of wires depending on the type (see Table 6.2), the total volume of required metal can be computed. By converting the volume to mass, and by using the price of metal per kilogram the cost of the extra wires can be calculated.

As an illustration for a placement of the four local converters in the middle of their corresponding groups and by using a price of 4.25 euros per kilogram of copper (June 2017) the extra cost for wires for the U-type and I-type is 1.65 euros and 1.62 euros respectively. The cost of each switch is considered to be 0.10 euro [58]. Thus the extra cost introduced by the switches in both configurations is 2.90 euros. The cost of the converters depends on their design and their characteristics. For the moment the price of each converter will be symbolized by y. Thus the additional manufacturing cost of the two templates compared to a conventional module is:

- Itype=4.52 euros + $4 * y$
- Utype=4.55 euros + $4 * y$

The cost of the module converter is not considered extra cost, as the price is expected to be close to the power optimizer which is used in the conventional topology.

6.3 Energy-yield evaluation under dynamic conditions/Simulation Environment

In order to evaluate the best setup and/or topology for a PV system, an experimental setup or a simulation environment is required. In the design phase, building many variants of a PV installation is unrealistic as the available investment cost will heavily limit the number of configurations that can be examined. This motivates the need of an accurate simulation environment to compare different alternatives for the PV system. Most models which exist in literature are suitable for analysis under uniform steady operating conditions, but are not as detailed and not sufficiently accurate for simulating the modules performance under dynamic non-uniform conditions.

The necessary elements (characteristics) of an accurate model for the above purpose, are a fine-granularity level , inclusion of the non-ideality of all components in a realistic matter, transient effects and the availability of realistic input data. Moreover, the model should be evaluated in a quite fast way to enable the exploration of many variants (preferably hundreds or even thousands). The simulation environment which is used in this work meets these requirements and allows an accurate but still relatively slow estimation of the performance of the different PV module's configurations.

A speed-up of the simulation environment needed to handle these other cases requiring faster execution speed will be discussed in Chapter 7.

6.3.1 Simulation Environment

The evaluation of the performance of the module topologies is done through simulation. This allows the comparison of different configurations of the module under the exact same external conditions. In order to simulate the electrical output of a PV module, a detailed model is needed. As the solar cell is the basic structure of any PV module, and the goal is to explore different configurations within the module level, the simulation environment requires a cell level granularity. The simulation environment is built on top of the physics-based energy simulation framework which is presented in [63]. The Electrical-Optical-Thermal (EOT) model is constructed in Verilog-AMS and allows an accurate SPICE-level simulation of a PV module (simulation error in energy<2%). This model takes into account the optical, thermal and electrical behavior of each individual cell. Furthermore it considers the thermal and electrical interactions among neighboring cells. The extra wires and switches which are needed in reconfigurable topologies are included in the simulation environment and are implemented by electrical resistances. Depending on the cell-string layout of the reconfigurable topology which is simulated the appropriate thermal connections among the cells are instantiated.

The final simulation environment is Cadence Spectre which is a circuit simulator, supports the Verilog-A modeling language and allows modeling of transient effects. The simulation environment is fully parameterized and can support different solar cell technologies and different types of wires, switches and converters. This enables the instantiation of the module to satisfy different module topologies. Furthermore, given degradation models of components, degradation effects can be included. The required inputs of this simulation environment are:

1. Irradiation: To evaluate the performance of different cell configurations within the module, the irradiation input has a cell granularity and each solar cell can be potentially excited by an individual irradiation level.

2. Ambient Temperature

3. Wind Velocity

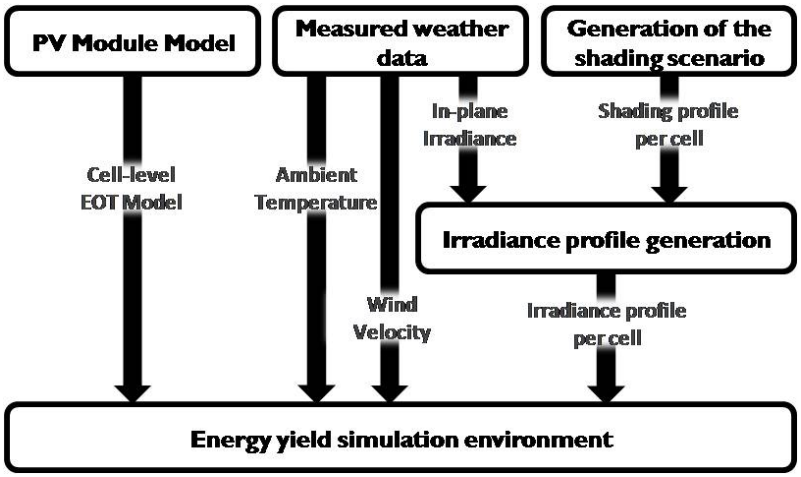

Fig. 6.2 Block Diagram of Simulation Environment

The aforementioned simulation environment does not include an analytical model for converters. The converters are modeled in a behavioral way. Local converters are considered to have a different conversion efficiency than the module converter, although all converters have a constant efficiency which does not depend on the operating point. The efficiency is a parameter in the simulation framework. In the specific simulation results discussed in Section 6.4,the local converters are considered to have a constant 95% efficiency, while the module converter is assumed to have an efficiency of 98%.

Simulations of the module can either be dc sweeps, where the output is the current-voltage (I-V) curve of a group of cells for specific external conditions. This I-V curve corresponds to the input port of a converter. Transient simulations can be performed as well, where the operating voltage point is determined at run-time, through a simple MPPT algorithm. Again, the voltage point corresponds to the input port of a converter.

Simulation of the all-series topology and conventional modules In industrial modules and in the all-series connection of the cells of the reconfigurable snake topologies, only one converter is active, the module converter. Since the goal is to maximize the energy yield of the module, a transient analysis with a MPPT algorithm at the module converter is the best solution. The module converter for the reconfigurable topologies and the conventional module should be differentiated and can potentially take different efficiency values.

Simulation of the groups of parallel cell-strings topology In the group configuration of parallel cell-strings, all local converters and the module converter are active. The model includes all elements up to the input ports of the local converters. Ideally, having all potential operating points for each converter (I-V curves) would allow a better exploration of the combination of operating points which maximize the module's instantaneous power. However, the increased simulation time required and the lack of an analytical model of a converter constitute this unrealistic. A transient analysis is performed and the voltage of each converter is determined by a distributed MPPT algorithm: each local converter performs the MPPT of the group of parallel cell-strings connected at its input. The voltage at the input of the module is fixed and, for the moment, a local converter is assumed to have a fixed efficiency (independently of the operating point). The MPP of each group allows an estimation of the gain of reconfigurable modules under realistic dynamic operating conditions, which is the goal of this work.

6.3.2 Input Files

The meteorological data that are needed as stated earlier are level of irradiation, ambient temperature and wind velocity. Two requirements are needed for the input data. The second requirement applies specifically for the irradiation level.

1. Temporally fine-grained data (temporal difference between measurements should be in the second-level)

2. Spatially fine-grained data (information of the different irradiation levels in cells within the module)

The first requirement can usually be met. In most PV installations and locations, irradiation and other meteorological data are measured every 10-15 minutes. However it has become a trend to reduce the time space between two consecutive measurements. Meteorological data per second are available for a location in Oldenburg, Germany where a setup is installed to measure direct irradiation, diffuse irradiation, ambient temperature, wind speed and wind direction [64]. It is expected in the near future to have similar data for locations in Ghent and Genk, Belgium.

The second requirement however is more difficult to get through real data and a different approach was used.

Creation of shading tables Shading tables are created by using the SketchUp software [65] and image processing. The SketchUp software enables creation of oriented 3D geometries,

takes into account the geo-location of the model and allows date and time specification. Thus, the real sun path and the orientation of the module and the surrounding objects are taken into account in the casted shades.

Fig. 6.3 Model in SketchUp, Location: Oldenburg, Date: September 17th, 2014, Time: 09:44:20

A house model was built and the location of the house was set at the exact same location of the measurement setup in Oldenburg. Modules were placed on the rooftop with a 45 degree south orientation (Figure 6.3). Depending on the location of the available data, the model can be set in different geographical coordinated with a different orientation. Images can be extracted from SketchUp for a specific time (Figure 6.4). Image processing can be performed to calculate the shading percentage of each cell. By extracting images for the entire day, daily shading tables can be created.

Calculation of incident irradiation With the use of these shading tables and given the Direct Normal Irradiance ($DNI(t)$) and the Diffuse Horizontal Irradiance ($DHI(t)$), which are available for this location (Oldenburg) with a 1 second resolution, the global in-plane irradiance of each cell N can be computed.

The objects which cast the shade are opaque and near the module, thus direct irradiation is considered to be completely blocked by shade. However, how the shade affects diffuse irradiation has some uncertainty [66]. In order to cover the entire range, three possible options were taken into consideration.

1. Diffuse Horizontal Irradiance is completely blocked by shade ($x = 1$).

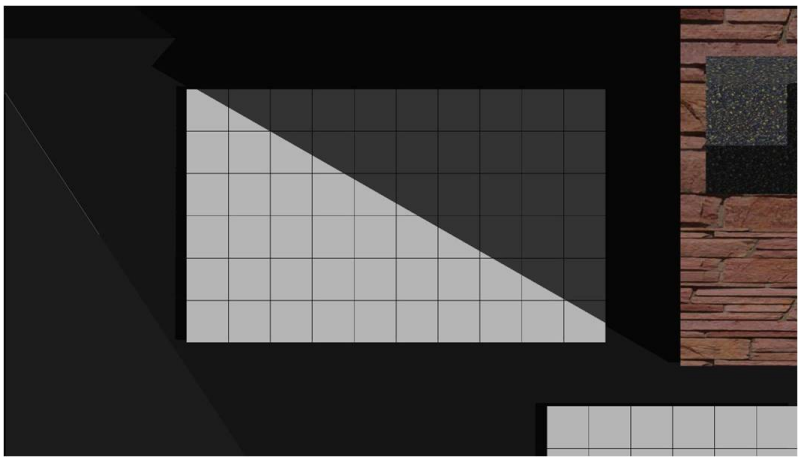

Fig. 6.4 Extracted image from SketchUp, Location: Oldenburg, Date: September 17th, 2014, Time: 09:44:20

2. Half of Diffuse Horizontal Irradiance is affected by shade ($x = 0.5$)

3. Diffuse Horizontal Irradiance is not affected at all ($x = 0$)

The irradiation of the illuminated part of the cell is calculated based on 6.1, while the incident irradiation of the shaded part depends on the value of x as shown in 6.2. The total irradiation of each cell is the sum of 6.1 and 6.2, as shown in 6.3.

$$G_{N,ill}(t) = (1 - SP_N(t)) * (DNI(t) + DHI(t)) \tag{6.1}$$

$$G_{N,sh}(t) = SP_N(t) * (1 - x) * DHI(t) \tag{6.2}$$

$$G_N(t) = G_{N,ill}(t) + G_{N,sh}(t) \tag{6.3}$$

6.4 Simulation Results

Dynamic shading patterns were calculated for modules placed at three different locations of a house rooftop (Figures 6.5 and 6.6). In two of the locations, the shade is casted by static objects (chimney/roof), while in the other location the module is shaded by a nearby tree. These three potential placements of the module were chosen as in each of them, different shapes of shade are present for different periods of the day.

In the first scenario, the module is shaded by a tree. The tree creates irregular shading patterns on the surface of the module which causes partial shading of the module for part of the afternoon. Since the object causing the shade is a tree, which is an obstacle affected by wind, no wind is considered in this shading scenario.

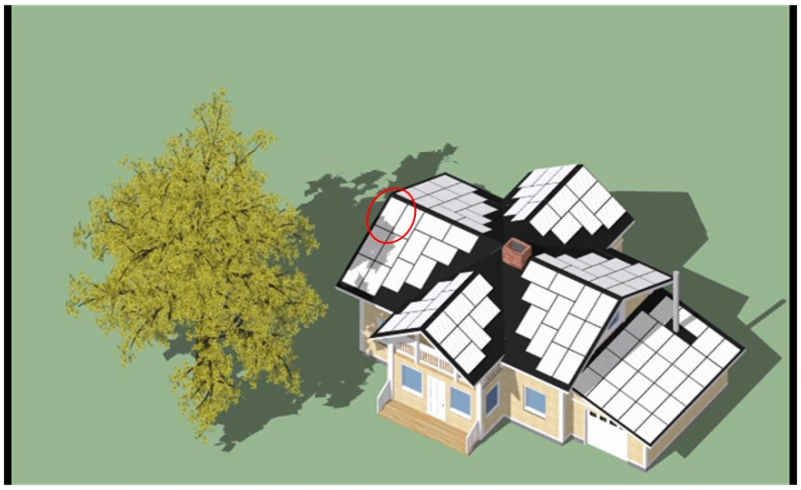

Fig. 6.5 Shading scenario 1

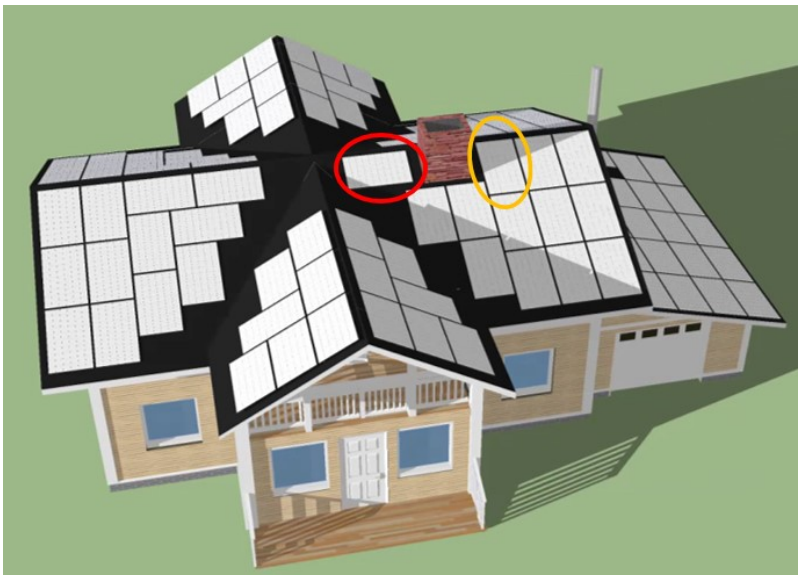

Fig. 6.6 Shading scenario 2 (red) and 3 (orange)

In the second shading scenario, the module is shaded by a chimney in the morning and part of the roof in the evening. The shade moves mainly along the long edge of the module.

In the third shading scenario, the module is partially shaded by a chimney in the afternoon. The orientation of the module and the chimney cause a shade which moves mainly parallel to the short edge of the module.

The last two shading scenarios create shades which have clean cut edges. Due to the different positions of the module in the rooftop, the casted shade moves mainly in a horizontal direction in shading scenario 2 and in a vertical direction in shading scenario 3. It has to be reminded here that horizontal and vertical direction refer to the movement of the shade w.r.t the connections of the cells as described in Figures 4.3 and 4.4. This makes these two shading scenarios complementary, as a plethora of shading scenarios will have casted shading patterns moving between these two edge shading scenarios.

The first scenario is more of an outlier. The object casting the shade (tree) is further away from the module. This means that for some period of the year no shade is cast on the module (due to the change of the sun path). Moreover, the casted shade is highly irregular and because of the size of the tree covers the entire module, leading to more frequent uniform conditions of the module.

The input files for uniform conditions, along with the active wind speed and ambient temperature for the 17th of September 2014 are shown in Figure 6.7. This day is selected to illustrate the performance of the reconfigurable topologies as it is mostly sunny (no long presence of clouds) and the shading patterns are due to the static objects located nearby. The conventional module, the I-type and U-type modules are simulated for these uniform external conditions. These irradiation and temperature inputs were simulated for wind and no wind conditions. The results are shown in Table 6.3.

Table 6.3 Energy for Uniform Conditions on 17th September 2014

Type of Module	Energy with Wind (KWh)	Energy with No Wind (KWh)
Conventional	0.8208	0.8099
I-type	0.8159	0.8048
U-type	0.8145	0.8033

As expected, under uniform conditions the conventional module outperforms both types of snake topologies. The I-type snake module performs 0.6% worse than the conventional while the U-type module has 0.75% losses for the entire day. It is also seen that the performance of all topologies is slightly better when wind is present. This is expected, as wind cools down the module and the cells operate at lower internal temperatures.

In order to have the performance of a reconfigurable modules for the day, the two main types of run-time instantiations of the module are simulated for the entire day (the all series

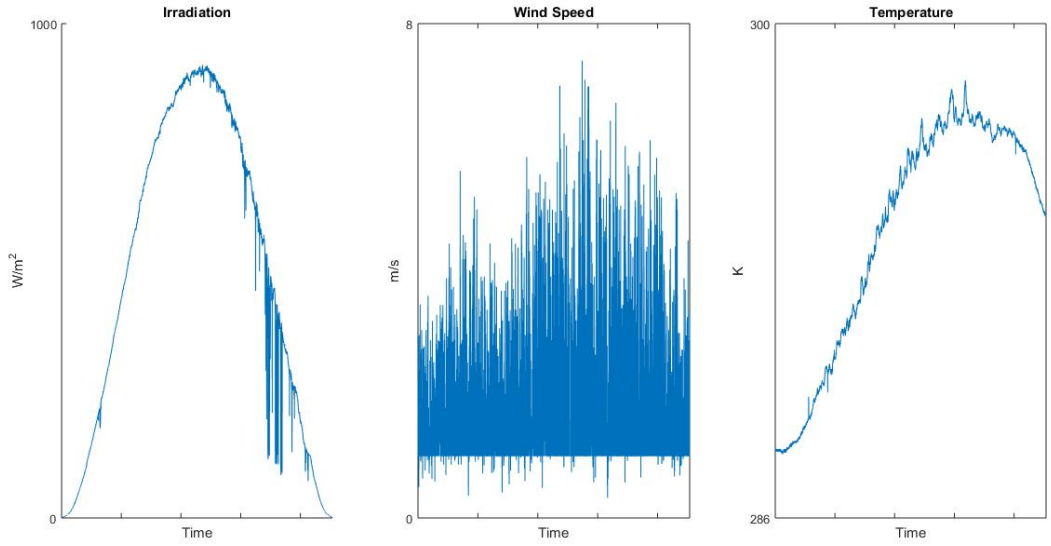

Fig. 6.7 Operating Conditions for 17/09/14

connection of cell-strings and the groups of parallel cell-strings). The two curves are then compared and the configuration which yields the better results is selected for each time period. This is shown in Figure 6.8. For the parallel configuration of the groups, the range of the conversion ratio of the local converters is set to [3,5] and the input of the module converter is 12V. The local converters have a constant efficiency of 95%, while the module converter has an efficiency of 98% for both the conventional and reconfigurable topologies.

The irradiation files for Scenario 1 (for all values of x), which is shaded by a tree for part of the day, are shown in Figure 6.9. The irradiation files were computed based on the direct and diffuse irradiation measurements for that day (Figure 6.10) and the shading tables which were extracted in SketchUp for different values of x. In this location the module is shaded for part of the day in the late afternoon. As stated above, because the shade is casted by a nearby tree, the wind is set to the lowest value.

When the diffuse irradiation is completely blocked by shade, the irradiation differences within the module are larger and the degree of non-uniformity within the module is highest, out of all the three cases. As fully shaded cells do not receive any irradiation, they do not contribute to power generation. In industrial modules this means that when not all bypass sections are affected, the bypass diodes of the shaded sections are active as to not compromise the operation of the rest of the module. Recovered energy in reconfigurable modules is attributed to illuminated cells which do not compromise their operation due to series connection with shaded cells.

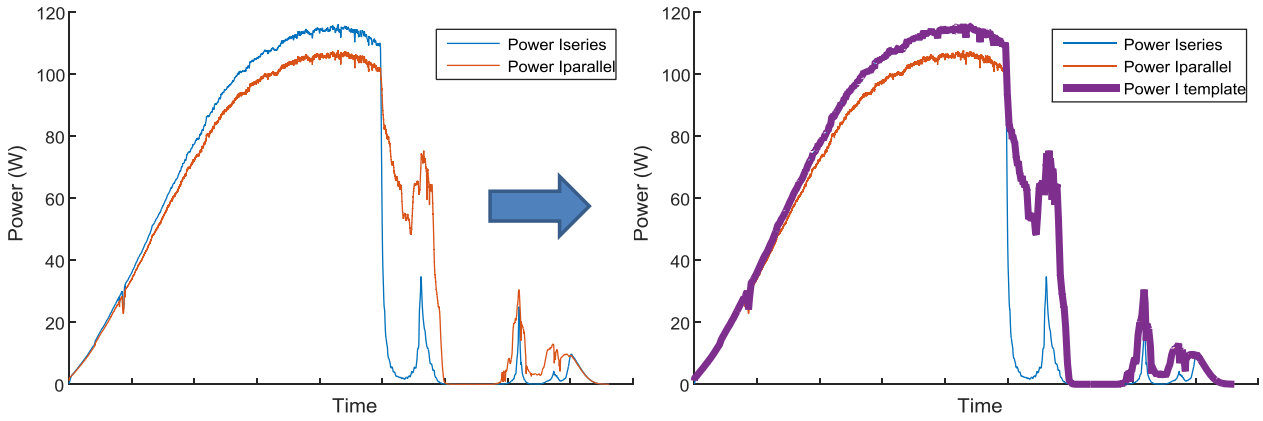

Fig. 6.8 Example of how power curve of reconfigurable module is calculated

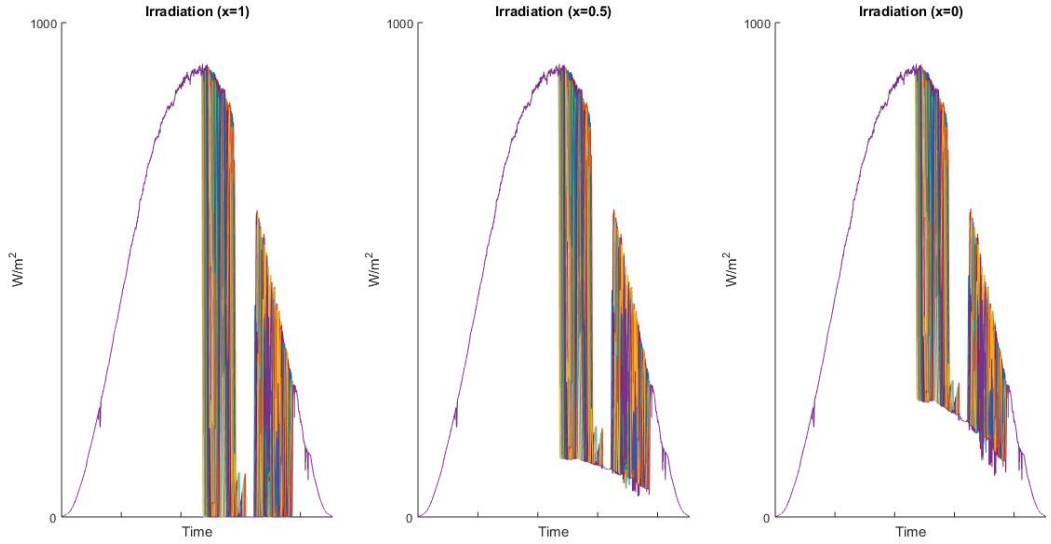

Fig. 6.9 Irradiation values for shading scenario 1 for 17/09/14 for all values of x

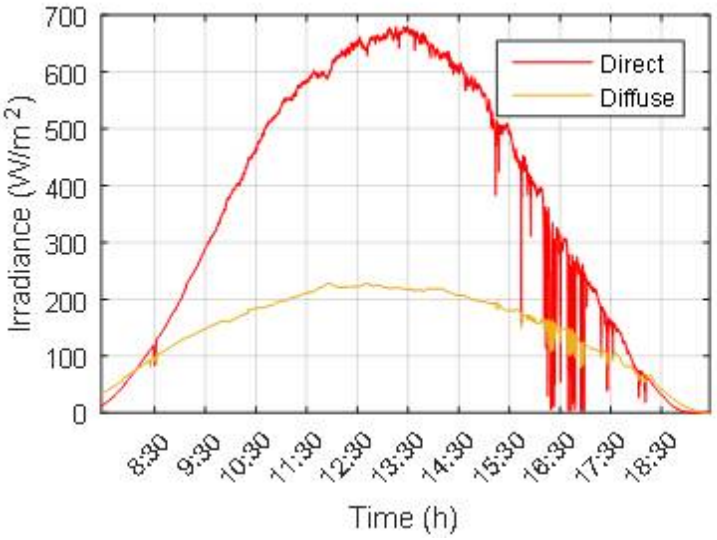

Fig. 6.10 Direct and Diffuse irradiation for 17/09/14

In the second case, where only part of the diffuse irradiation is affected by shade, shaded cells receive some irradiation and thus can partly contribute to power generation. Similarly, in the third case, the shaded cells have a higher irradiation level as the diffuse irradiation is not affected at all and their contribution to power generation is higher. The Maximum Power Point of industrial modules can either lie in the region where shaded sections are bypassed or in the region where the overall current of the module is reduced, depending on the level of the irradiation differences. Recovered energy in reconfigurable modules is both due to independent operation of fully illuminated cells and extraction of power from shaded cells.

The power curves of the three types of modules, when diffuse irradiation is completely blocked by shade (x=1), are shown in Figure 6.11 for Scenario 1. The daily energy of each type of module is shown in Table 6.4, which is the sum of the energy produced during uniform conditions and during partial shading for that day. During uniform conditions, it can be seen that both reconfigurable topologies have losses compared to the conventional topology (the percentage of gain w.r.t. the conventional module are shown in parenthesis in Table 6.4). The energy recovered from reconfigurable topologies during the part of the day where the module is partially shaded is more than enough to compensate for the losses under uniform conditions and both types of snake topologies show significant daily energy gains (11-12%).

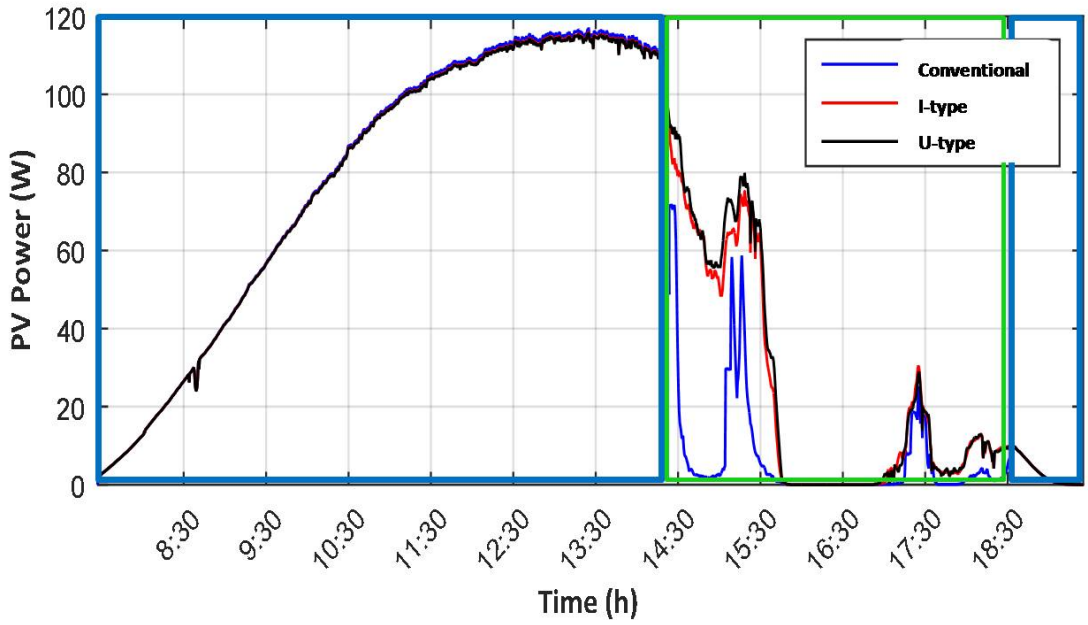

Fig. 6.11 Power curves of the three types of modules for Scenario 1 on 17th September 2014 (x=1)

Table 6.4 Daily energy of the three types of modules for Scenario 1 on 17th September 2014 (x=1)

Type of Module	Daily Energy (KWh)	Energy during uniform conditions (kWh)	Energy during partial shading (KWh)
Conventional	0.5777	0.5028	0.0749
I-type	0.6413 (+11.01%)	0.5018 (-0.21%)	0.1395 (+86.27%)
U-type	0.6466 (+11.92%)	0.5008 (-0.39%)	0.1457 (+94.52%)

In Table 6.5, the daily energy production of the modules for Scenario 1 is shown when half of the diffuse irradiation is affected by shade (x=0.5). When shaded cells receive part of the diffuse irradiation, they can contribute to the generated energy. There is an increase in the energy in all configurations, which is more prominent in the conventional topology. This leads to the decrease in the gain percentage and it can be concluded that the majority of the recovered power comes from cells which otherwise have a reduced current. However we still gain more than 10% daily.

Table 6.5 Daily energy of the three types of modules for Scenario 1 on 17th September 2014 (x=0.5)

Type of Module	Daily Energy (KWh)	Energy during uniform conditions (kWh)	Energy during partial shading (KWh)
Conventional	0.6033	0.5037	0.0996
I-type	0.6651 (+10.24%)	0.5022 (-0.29%)	0.1692 (+63.52%)
U-type	0.6695 (+10.97%)	0.5013 (-0.47%)	0.1682 (+68.88%)

In Table 6.6, the daily energy production of the modules for Scenario 1 is shown when the diffuse irradiation is not affected by shade (x=0). As shaded cells receive all the diffuse irradiation, their contribution in the overall energy is more prominent. The gains further drop, but still remain significant (8%). This further supports the conclusion that the majority of the recovered power is due to fully illuminated cells which in the conventional topology operate with a reduced current.

It is interesting to notice here the change in the amount of energy generation during the part of the day where the modules operate under uniform operating conditions, as the value of x changes. The difference is negligible, but cannot be attributed to shade, as the irradiation files for that part of the day are the same for all values of x. As seen in Figure 6.11,

Table 6.6 Daily energy of the three types of modules for Scenario 1 on 17th September 2014 (x=0)

Type of Module	Daily Energy (KWh)	Energy during uniform conditions (kWh)	Energy during partial shading (KWh)
Conventional	0.6436	0.5048	0.1388
I-type	0.6929 (+7.66%)	0.5026 (-0.44%)	0.1903 (+37.09%)
U-type	0.6962 (+8.17%)	0.5017 (-0.61%)	0.1945 (+40.09%)

uniform conditions are present for two different periods of the day (outlined in blue). The difference in energy under uniform conditions is because of temperature differences during the second part of the day where the module operates under uniform external operating conditions. It can be seen that the energy is lower when x=1. As the irradiation differences within the module are higher in this case when the module is partially shaded (outlined in green in Figure 6.11), larger internal temperature differences are observed among the cells. These differences are still present when the module operates again under uniform conditions. The static configuration of the conventional module causes larger temperature differences among the cells as can be seen by the low losses of reconfigurable topologies under uniform conditions when x=1 (0.29% and 0.47%). A difference of 50 degrees is observed in the conventional module, while the temperature difference in reconfigurable modules does not exceed 20 degrees. As the degree of non-uniformity within the module decreases (x=0.5 and x=0), the temperature of the cells does not increase so much in the conventional topology and the losses of the reconfigurable topologies under uniform conditions increase (0.44% and 0.61%).

In Figure 6.12, the irradiation files of shading scenario 2 are shown. In this location, the module is shaded for part of the morning and again in the evening. The casted shade is due to the roof and a nearby chimney, thus wind speed in this location is included in the simulation environment.

The daily energy generated by each module configuration is shown in Table 6.7 for all values of x and in Figure 6.13 the gains of reconfigurable topologies w.r.t. the conventional module are illustrated. Again it can be observed that the overall energy increases as the incident irradiation on shaded cells increases. What should be noted in this shading scenario is that the highest gains in percentage are when part of the diffuse irradiation is affected by the shade. It can be seen the increase of daily energy of the conventional module between the cases where all diffuse (x=1) and part of the diffuse is affected (x=0.5) is really small. This is

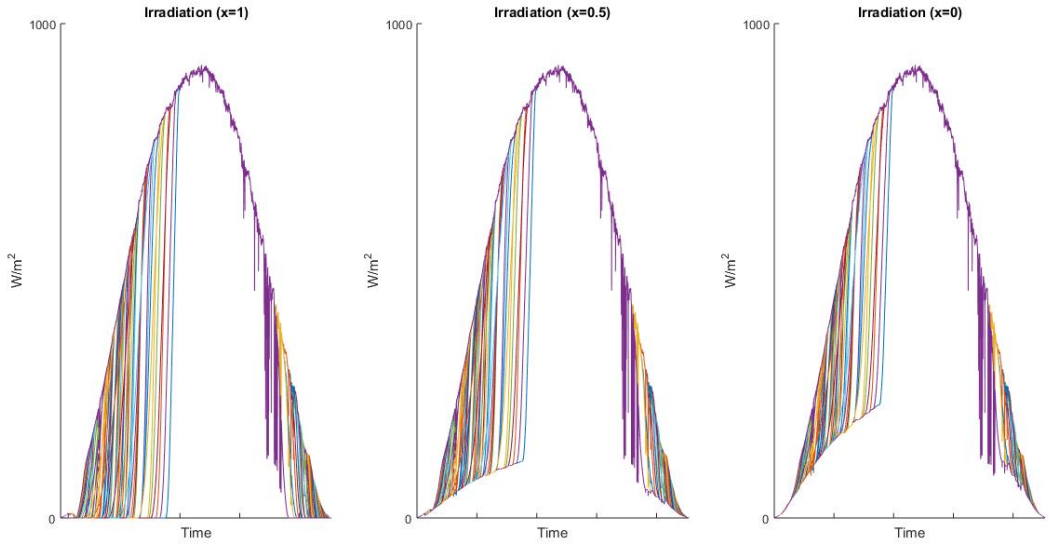

Fig. 6.12 Irradiation values for shading scenario 2 for 17/09/14 for all values of x

due to the shape of the casted shade for this scenario on this specific day (the sun path changes throughout the year) and the level of diffuse irradiation. As the shade moves along the long edge of the module, not all bypass sections of the module are affected simultaneously. This eventually creates local maxima in the instantaneous P-V curve of the conventional module. When the incident irradiation of the shaded cells increases, as part of the diffuse irradiation reaches the shaded cells, only one of the local maxima changes (the one which lies in the region where all cells are active). As the change of this is not as significant as in the case where all diffuse irradiation reaches the cells (x=0), the overall energy of the conventional module does not improve so much. Reconfigurable modules however can extract the extra power from the shaded cells and thus the gain is increased. When all diffuse reaches the shaded cells (x=0) and the degree of non-uniformity within the module drops, the energy of all configuration increases and the respective gains of reconfigurable modules are lower than in the other two cases.

The irradiation files for the third location are shown in Figure 6.14. The module is shaded only in the evening, by a chimney. As the object is static and wind does not affect it, wind speed is again included in the simulation environment.

The energy production and the gains w.r.t the conventional module of reconfigurable topologies for the third shading scenario are shown in Table 6.8 and Figure 6.15. The results between the different values of x, both in energy and in gains, are similar to the ones

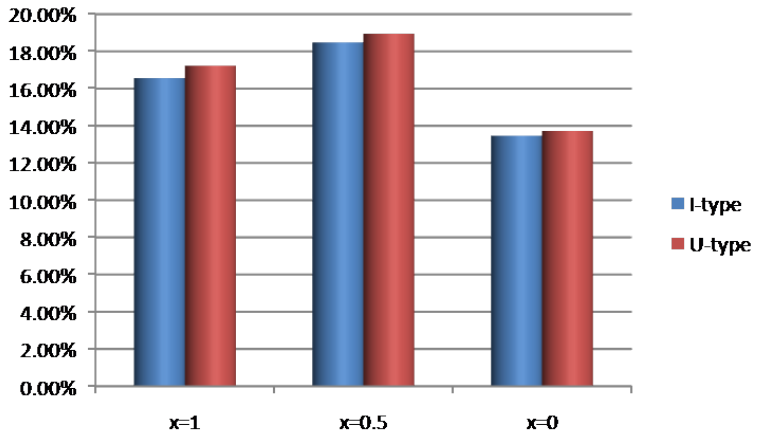

Fig. 6.13 Gains of reconfigurable module w.r.t conventional for shading scenario 2 (17/09/14)

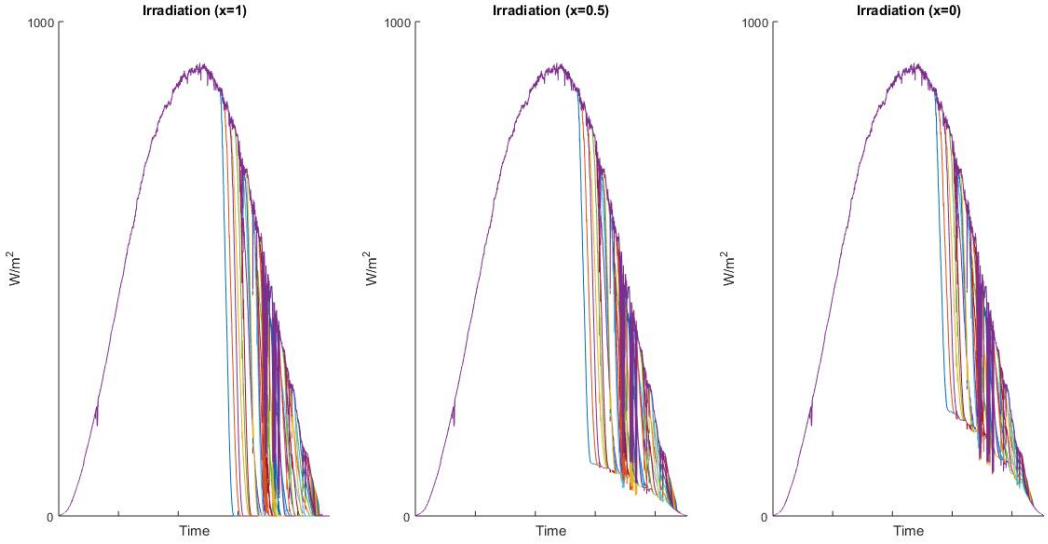

Fig. 6.14 Irradiation values for shading scenario 3 for 17/09/14 for all values of x

Table 6.7 Daily energy of the three module topologies for shading scenario 2 (17/09/14)

Topology	Energy (kWh)		
	x=1	x=0.5	x=0
Conventional	0.5810	0.5891	0.6374
I-type	0.6773	0.6979	0.7232
U-type	0.6812	0.7007	0.7248

Table 6.8 Shading Scenario 3

Topology	Energy (kWh)		
	x=1	x=0.5	x=0
Conventional	0.5777	0.6033	0.6436
I-type	0.6413	0.6651	0.6929
U-type	0.6466	0.6695	0.6962

of shading scenario 1, which is expected, as the shade affects all bypass sections of the conventional module simultaneously.

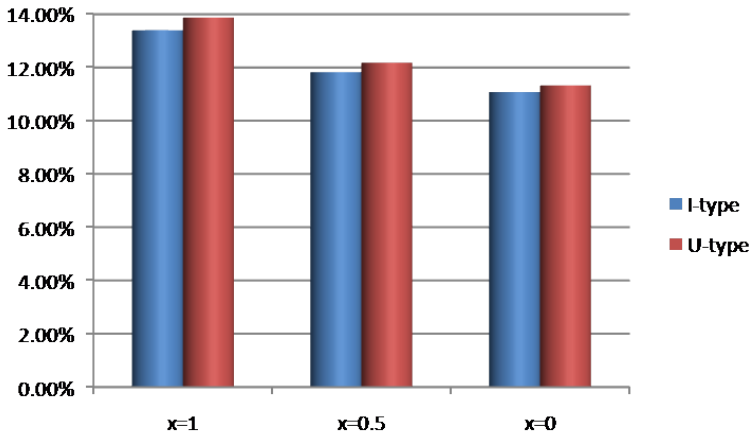

Fig. 6.15 Gains of reconfigurable module w.r.t conventional for shading scenario 3 (17/09/14)

It has to be noted here, that for all three locations of the module, the U-type template performs better than the I-type template. It has been shown in Table 6.3 that an all series connection of the cell-strings in uniform conditions for the I-type template has less losses than the U-type template. In order to be thorough, the operation of the other main class

(parallel connection of parallel groups of cell-strings) should be examined under uniform irradiation conditions. For the inputs of Figure 6.7, the output of the parallel connection of the groups is shown in Table 6.9 for the two templates. It can be seen, that even in this type of run-time instantiation of the modules, although the energy is significantly less than the series connection, the I-type template outperforms the U-type template. This proves that the better performance of the U-type template is because of the different cell-string layout of the module which has a finer granularity in both dimensions of the module and is better suited for of the shading patterns presented above.

Table 6.9 Energy for Uniform Conditions on 17th September 2014 (parallel connection of groups of cell-strings)

Type of Module	Energy with Wind (KWh)
I-type	0.7618
U-type	0.7603

In order to estimate the annual gain of reconfigurable modules, one day was simulated for each month (March-November). Shading tables and irradiation files were created for each of these days. Due to changes in the position of the sun, the shape of the casted shade on each day differs. The levels of diffuse and direct irradiance also change due to different periods of the year. The selected days are representative of the corresponding months average irradiation profiles. The winter months were excluded due to low irradiation levels. During these months, the diffuse irradiation is dominant and thus the level of non-uniformity within the module is extremely low.

The simulation results for each of these days are in the Appendix. Each Table contains the daily energy generated by the three module topologies, for the three shading scenarios for the three values of parameter x (Diffuse Horizontal Irradiance is completely blocked by shade ($x = 1$), Half of Diffuse Horizontal Irradiance is affected by shade ($x = 0.5$), Diffuse Horizontal Irradiance is not affected at all ($x = 0$)) and for uniform conditions.

For the two days of June and July, there is no incident shade for shading scenario 1 and thus the performance of the module coincides with operation under uniform conditions for these two days.

Table 6.10 shows the average gains for each location, type of irradiation, and for the two snake reconfigurable topologies compared to the conventional topology. The highest gains are observed when all irradiation is affected by the shade. It should be noted that reconfigurable modules perform poorly in some days when only direct irradiation is blocked by the shade. This is due to the fact that in those days the diffuse irradiation is dominant

Table 6.10 Average Gains

Topology	Gain (%)		
	x=1	x=0.5	x=0
Scenario 1			
I-type	2.04	1.84	1.03
U-type	2.27	1.91	1.02
Scenario 2			
I-type	18.32	15.17	8.31
U-type	18.76	15.36	8.32
Scenario 1			
I-type	9.67	8.261	4.68
U-type	10.29	8.61	4.81

and no significant irradiation difference is observed between the cells of the module. The gains are significantly higher for shading scenarios 2 and 3 where the casted shade is caused by objects with clear cut edges and partial shading occurs throughout the year. It should be noted, that for shading scenario 1 there is still some gain, although there is no shade during June and July which are months with high irradiation levels, thus high energy production. It can be seen that the U-type module outperforms the I-type for all shading scenarios. This means that the complete split achieved by the U-type is significant for the given simulated scenarios, as the U-type suffers more losses during uniform operating conditions. The only case where the U-type module outperforms the I-type is in the first scenario when $x = 0$ (diffuse irradiation is not affected by the shade). As the degree of non-uniformity is smaller and in this shading scenario uniform conditions are more frequent, the losses in uniform conditions become more significant.

In order to estimate the energy recovered throughout the year, an annual simulation was performed for uniform conditions for a conventional module (2014). Based on the output of this simulation and the average losses due to partial shading, the annual energy yield of the conventional module for each shading scenario can be estimated. By applying the average gains of Table 6.10, the annual energy yield of reconfigurable modules in each shading scenario can be estimated.

As the most realistic approach is considering that part of the diffuse irradiation is affected be casted shades, this analysis will be done for each shading scenario for the average annual gains when x=0.5.

The annual estimation of the energy yield of the conventional module used in this work is 162.70kWh. If no degradation effects are taken into account, and the cost of electricity is considered constant for the following years at 0.29 euros per kWh [67], the gain from not paying for the produced electricity in 20 years is as listed in Table 6.11.

Table 6.11 Ideal gain (in euros) for not paying for the generated electricity, in 20 years (x=0.5)

Module type	Scenario 1	Scenario 2	Scenario 3
I-type	15.22	106.23	68.85
U-type	15.80	107.56	66.05

In order to be more accurate, degradation effects and changes in the electricity price should be taken into account. Degradation is separated into two categories, degradation of the cells and degradation of the additional electronics. From the warranty of modules, a uniform degradation of the cells is considered which is a 1% yearly linear degradation ([68], [69]). This affects both conventional and reconfigurable topologies. Degradation of additional electronics concerns only the reconfigurable modules. A model of the degradation performance of additional electronics is not available, but based on the warranty of electronics ([70]), an additional linear degradation of 0.5% per year is considered for the recovered energy of reconfigurable topologies. The price of electricity is considered to increase with a rate of 2% per year [67]. The gains by including the above factors are shown in Table 6.12.

Table 6.12 Gain (in euros) for not paying for the generated electricity, in 20 years (x=0.5)

Module type	Scenario 1	Scenario 2	Scenario 3
I-type	15.32	106.93	66.49
U-type	15.90	108.27	69.30

It can be seen that the gains slightly increase. This is due to the fact that the expected rise of electricity prices counterbalance the extra degradation losses of reconfigurable topologies.

In order to have the actual gain, as described in Section 3.2, the investment cost which was computed in Section 6.2 has to be subtracted from the gains shown in Table 6.12. In the investment cost, the price of the local converters was omitted. Depending on the time period required for Return On Investment (ROI), the acceptable price of a local converter can be determined. If the target is to have an ROI in ten years, the price of each converter has to be maximally 12-7 euros for shading scenarios 2 and 3 respectively. The marginal gains of

shading scenario 1 do not allow an ROI of ten years. For a converter cost of 7 euros and 12 euros the expected net gains in 20 years are shown in Tables 6.13 and 6.14.

Table 6.13 Gain (in euros) for not paying for the generated electricity, in 20 years (x=0.5) for y=7 euros

Module type	Scenario 1	Scenario 2	Scenario 3
I-type	-17.18	74.44	33.99
U-type	-16.64	75.74	36.77

Table 6.14 Gain (in euros) for not paying for the generated electricity, in 20 years (x=0.5) for y=12 euros

Module type	Scenario 1	Scenario 2	Scenario 3
I-type	-37.18	54.44	13.99
U-type	-36.64	55.74	16.77

However, the cost of a power optimizer for this type of module is around 15 euros and it processes the power of the entire module. This leads to the reasonable conclusion that the cost of all local converters, which handle the same amount of power will be in the range of 15 euros. By using this value as the total cost of all local converters, the gains are as shown in Table 6.15.

Table 6.15 Gain (in euros) for not paying for the generated electricity, in 20 years (x=0.5) for 4*y=15 euros

Module type	Scenario 1	Scenario 2	Scenario 3
I-type	-4.18	87.44	46.99
U-type	-3.64	88.74	49.77

6.5 Conclusions

It is observed that reconfigurable snake topologies show promising gains when operating frequently under conditions of partial shading. The gain can be expressed in two ways, in terms of energy which in turn can be translated in financial terms.

In all three shading scenarios the total energy generated by reconfigurable topologies exceeds the energy of the conventional topology. This means that when the main objective is to increase the overall energy, reconfigurable topologies can be beneficial even in cases where partial shading is not present throughout the year (shading scenario 1).

The translation of the recovered/additional energy to financial gain is not straight-forward. It depends of the location of installation. Depending on the country, the price of electricity varies. Furthermore, in certain countries Feed-In Tariffs apply to PV installations. However, it is evident that the financial gain strongly depends on the amount of recovered energy. It is shown that for shading scenarios 2 and 3, financial gain is expected in the long-term. On the other hand, the marginal energy gains of shading scenario 1 are not enough to financially compensate for the additional cost of reconfigurable topologies. The lack of any partial shading in the summer months which have high insolation really limits the recovered energy. In terms of finance, installing a reconfigurable module which would operate under the conditions of shading scenario 1 is not beneficial. It should be noted though, that in order to recover enough energy it is not necessary to have non-uniform conditions throughout the year, but partial shading should be present in periods where there is a high energy production.

The simulation environment described in this Chapter is accurate, but requires a large computational time when it is applied with a cell granularity. Depending on the topology of the module, the complexity of the design, a daily simulation can be over 9 hours for a uniform day. When simulating days with non-uniform conditions the time can increase even more and a daily simulation can require up to 15 hours. In order to explore more design instantiations of the module and simulate longer periods a faster simulation process is required. For this reason, a different simulation framework is proposed in Chapter 7.

Chapter 7

Simulation Framework

Multiple options exist concerning the design of a reconfigurable module, as stated in chapters 4 and 5, which leads to a large number of potential topologies. In order to explore and determine the most promising configurations, a fast evaluation process is needed. Fabrication of all configurations is too cost demanding, while extensive simulations require a lot of time. In this chapter we propose an evaluation process which allows significantly faster estimation of the energy-yield of reconfigurable topologies by reusing and combining simulation results. At the same time, our approach allows to retain the desired accuracy of the produced metrics, like energy-yield, because of the special novel clustering techniques that are employed.

As stated in section 6.3 in our default exploration framework for slowly varying shading, the performance of this module is evaluated in a simulation environment. The core of the simulation is the cell. The model of the cell is derived based on the physical layer. The parameters of the cells and wires have been calibrated through extensive measurements. This has lead to a detailed model where all the operating conditions (irradiation, temperature, wind) are taken into account. In order to simulate reconfigurable topologies, extra elements (additional wires and switches) are added to this model. The final model involves both an electrical interconnection and a thermal interconnection of the cells.

Due to the complexity of the model -required for full accuracy - simulation time has increased considerably though. Considering all potential operating scenarios and all potential instantiations of a reconfigurable module, this is a too large overhead. Each simulation of a module for a shading pattern requires up to a minute to achieve the desired level of simulation accuracy. The number of shading patterns for a module with 60 cells is quite high. For any given irradiation level, even if a cell can only be completely shaded or not, restricting partial shading of cells, 2^{60} possible shading patterns are present. Of course not all of the shading patterns are realistic or relevant, but still thousands or even millions of simulations could be required to cover all possible operating conditions.

The goal here is to significantly speedup the simulation, while maintaining the accuracy level to a sufficiently high degree, i.e. close to the accuracy achieved by the model described above.

7.1 Thermal connections

Cells can be electrically connected in three different ways:

1. Straight cell-to-cell connection
2. Short stringing
3. Long stringing

The different electrical interconnections are shown in Figure 7.1.

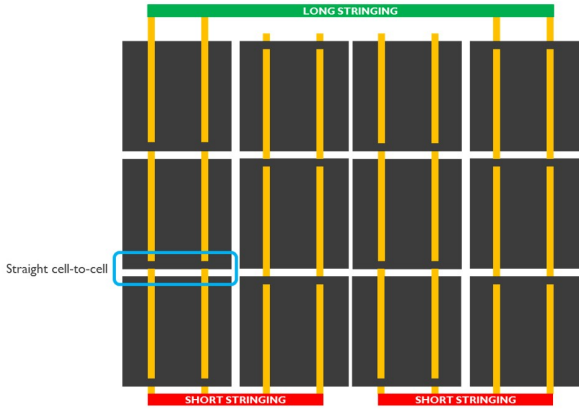

Fig. 7.1 Different electrical interconnections of cells

The way two cells are electrically connected affects the thermal dependency between the given cells [71]. Four different classes for thermal connection can be defined:

1. Strong (S). This is typical for straight cell-to-cell connection
2. Medium-Strong (MS). This is typical for short-stringing
3. Medium-Weak (MW). This is typical for long stringing
4. Weak (W). This is the typical class for electrically non-interconnected cells

The presence of a switch along an electrical connection reduces the thermal dependency between the given cells. Thus, whenever a switch is implemented within the electrical interconnection of two cells, the thermal class of such interconnection move one step down, e.g. from S to MS or from MW to W.

Using this methodology, it is possible to rank the thermal connections as following:

1. Straight cell-to-cell interconnection without a switch: Class S
2. Straight cell-to-cell interconnection with a switch: Class MS
3. Cells interconnected via short-stringing without a switch: Class MS
4. Cells interconnected via short-stringing with a switch: Class MW
5. Cells interconnected via long-stringing without a switch: Class MW
6. Cells interconnected via long-stringing with a switch: Class W
7. Cells that are not interconnected: Class W

The effect of ignoring thermal dependencies is lower accuracy. However, accuracy loss depends on the strength of any given thermal connection. In general, the weaker the thermal interconnection, the lower the reduction of accuracy that is obtained by ignoring it. Thus, a decision about which thermal connections can be safely ignored and which cannot may be taken depending on the "Class" of every thermal connection. However, there is no general rule to define which classes must be incorporated in the simulation. A previous analysis is needed for any given cell technology and module build-up, i.e. characteristics of the different layers of a PV module, in order to take this latter decision. Such analysis can be done via simulations. First, all thermal interconnections belonging to "Class W" are removed and the simulation results compared with the one of the reference. If accuracy loss is negligible, second step is done removing also thermal interconnections belonging to "Class MW". Again, simulation results are compared with the one of the reference. The procedure is repeated until a class is found for which accuracy loss is not negligible anymore. A threshold can be defined for ending the procedure, e.g. accuracy loss lower than 0.5%. Also, more classes or more ranking rules can be defined if needed, e.g. related to the position of the interconnection within the module (along the module's edges or at the center of the module for instance). For the PV modules that have been analyzed into the thesis, thermal interconnections belonging to the classes S and MS should not be neglected in order to keep high accuracy. On the other hand, thermal interconnections belonging to the classes MW and W may be ignored. This significantly improves simulation time while leading to negligible reduction of accuracy.

The same methodology can be used for any interconnection technology (e.g. busbar-less, smart-wires, ...).

7.2 Re-usability of the cell-strings IV curves

The main parameters and design choices of instantiating a reconfigurable module with the methodology described in Chapter 3 are:

- The size and shape of the cell-strings
- The complexity of the supporting network
  - Number of local converters
  - Number of potential series and parallel connections
  - Connection of local converters and connection to the module converter

It can be seen here, that for the same selection of cell-strings, multiple design instantiations of the module are possible and furthermore, for every design time instantiation even more run-time instances of the module can present themselves. All these run-time instances (active current paths) have to be simulated separately for the same external operating conditions.

The cell-string layout which will be used as an example for this chapter is the one used for the snake-type topologies, however this is merely for illustrative purposes as the simulation framework is not confined to the analysis of these topologies.

As all the above run-time instances of the module share the same cell-strings, the cell-strings can be seen as the main common component of all these simulations. The thermal and electrical connections of the cells (for two cell-strings) are shown in Figure 7.2. In [71] it has been demonstrated that the strongest thermal dependencies are situated between cells which are electrically interconnected within the module, thus within a cell-string. The interconnections of the cell-strings, which are outside of the module, do not result in strongly coupled cells.

The main idea is to break-down the simulation process of simulating the entire module, by combining appropriately selected IV curves (sections 7.3.1 and 7.3.3) and obtaining the IV curves at the inputs of the conversion units. Breaking down the simulation environment into simulations of individual cell-strings, means that thermal dependencies between cell-strings are completely removed and ignored. As these thermal connections are weak, this is an

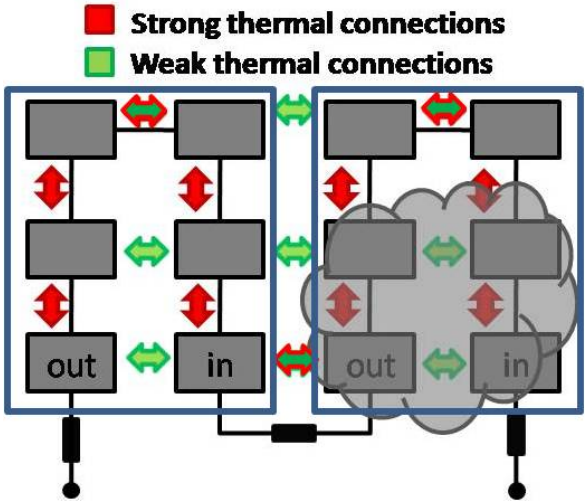

Fig. 7.2 Thermal and electrical connections of cells

acceptable simplification of the model. This by itself significantly improves simulation time, as the smaller, simpler models of the cell-strings run faster and can be executed in parallel.

In Chapter 3, it was stated that the majority of the cell-strings should have the same number of cells to allow a potential parallel connection of the cell-strings. This leads to cell-string layouts where the majority of the cell-strings are similar. In the case of the snake-type layouts, all cell-strings of the U-type template and most of the cell-strings of the I-type template are the same. This means that most cell-strings do not have to be re-simulated for the same operating conditions. These IV curves can then be connected in multiple ways, allowing re-usability of the IV curves for different run-time instances of the module (Figure 7.3). Re-usability can be seen in two ways; for different interconnections of the cell-strings and for same size and shaped cell-strings within the same run-time instance of the module. This allows additional large execution time savings.

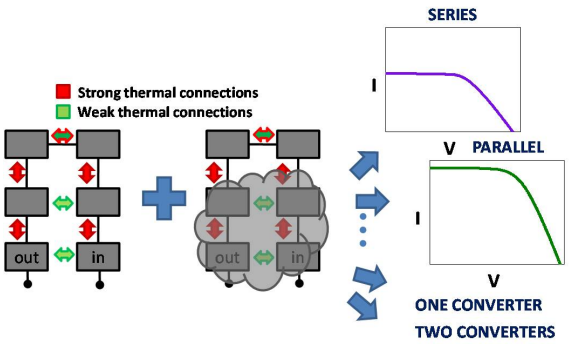

Fig. 7.3 Possible interconnections of cell-strings

7.3 Proposed Simulation Framework

The main flow of the proposed simulation framework is illustrated in Figure 7.4. The steps illustrated in this Figure are the ones that replace the simulation environment in spectre described in chapter 6. The inputs of the simulation framework are irradiation, ambient temperature and wind velocity. The output of the framework is the operating point for each conversion unit for each time step. When the local converters are active the output is the operating points at the input of each local converter; when only the module converter is active the output is the operating point at the input of the module converter. The basic steps of this simulation framework are temperature prediction, addition of resistances and combination of curves and selection of operating point. Each of these steps will be analyzed in the following sections.

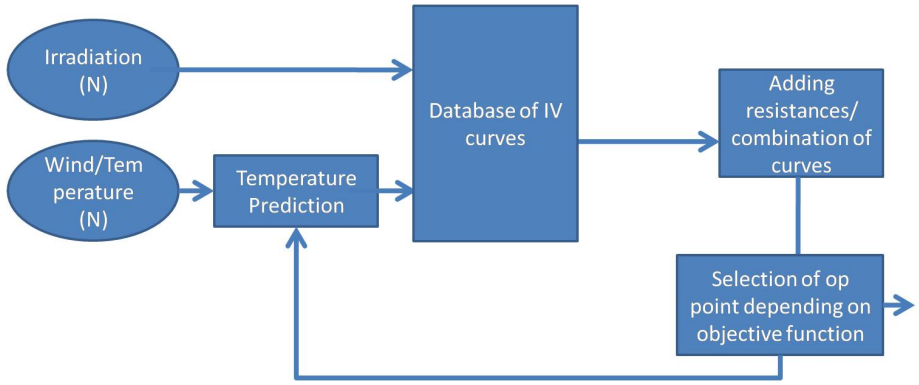

Fig. 7.4 Flow Chart of proposed simulation framework

It should be noted here, that the flow chart of Figure 7.4 describes the process which replaces the simulation environment in spectre and provides a single operating point for each local converter or for the module converter. However, the proposed simulation framework can be extended to provide the entire IV curve at the input of the module converter. This can be done by calculating the IV curves at the output of the local converters and combining them appropriately (depending on their type of connection and the resistances of their interconnection) to have the entire IV curve at the module converter.

7.3.1 Addition of resistances/Combination of the IV curves

When IV curves of two cell-strings are available, there are two options of how to connect them in our proposed topologies; in series or in parallel. However, depending on the type of the connection, the design-time and the specific run-time instantiation of the module, the interconnecting resistances between the two cell-strings can be different. The simulated

curves include the resistance up to the negative and positive terminal where the cell-string is connected to other elements of the module. These resistances are common for all cell-strings of the same size and shape and for all types of run-time instances of the module.

Independently of the type of interconnection of the two curves, before their combination, the appropriate resistances Rsconf and Rpconf need to be added to each curve (Figure 7.5. The extra resistance is added by evaluating the additional voltage drop according to the corresponding current. This leads to IV curves where the voltage step can differ depending on the additional resistance. This is illustrated in Figure 7.6. The outer loop indicates that this process has to be repeated for all conversion elements in the configuration.

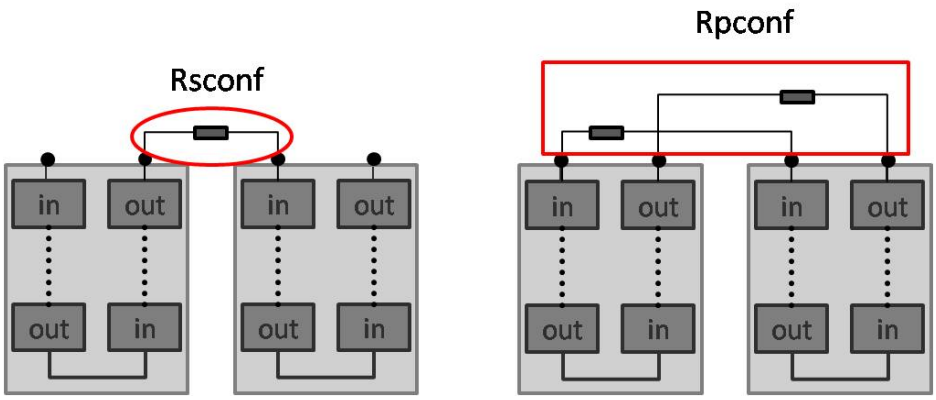

Fig. 7.5 Additional resistances of series and parallel connections

Series connection of two IV curves When the two cell-strings are connected in series, the cell-strings share the same current. In order to combine the two individual curves in a series connection, points of the two curves with the same current need to be located. For these points, where the current is the same, the two voltages are added. Missing points in each curve are computed by linear interpolation. In the proximity of the MPP, parabolic interpolation can be used instead of linear interpolation. However, linear interpolation was chosen for the entire curve due to its simplicity and the preservation of accuracy. Performing this process for all points of the two curves where the current is the same produces the IV curve of the series combination of the two cell-strings.

Parallel connection of two IV curves Two cell-strings which are connected in parallel, always share the same voltage across their terminals. In a similar way as in the series connection, the common voltage points are located in the two individual IV curves. Missing points are once again computed with linear interpolation. For these points, the two currents are added and the IV curve of the parallel connection of the two cell-strings is produced.

These procedures can be performed repetitively in order to produce any type of connections of cell-strings for any number of individual interconnected IV curves, including hybrid connections. Hybrid connections in this case, means that the group of cell-strings connected to a single local converter are not necessarily connected all in series or in parallel. To give an example, four cell-strings connected to the same local converter can be connected in pairs in series and then in parallel ([1+1]//[1+1]). In the end, the IV curves corresponding to the local converters or to the module converter of any run-time instance of the module can be produced.

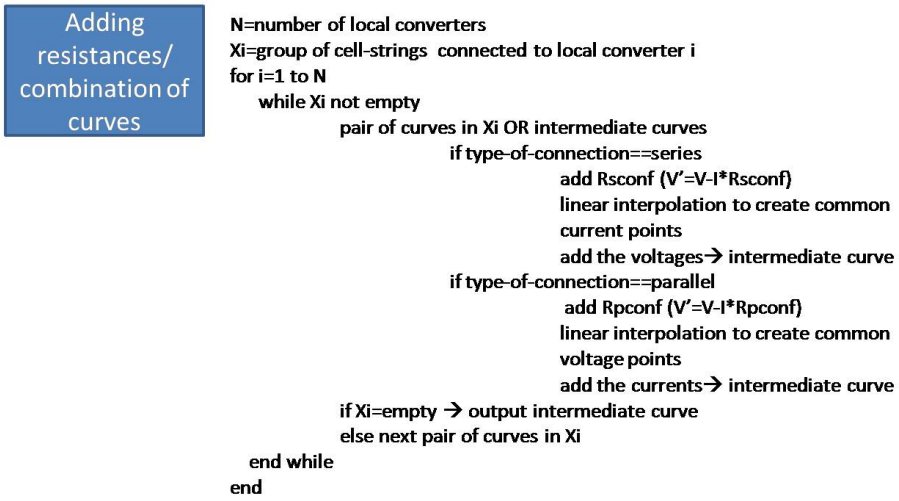

Fig. 7.6 Addition of resistances and Combination of IV curves

7.3.2 Selection of operating point

The combination of IV curves results to information for the entire IV curve at the input of each conversion element. These curves allow to select the best operating point for each local converter or for the module converter for the specific run-time conditions of the module for different objectives and allows the power calculation for each simulation step(Figure 7.7). The above approach enables additional execution time savings.

It should be stated here, that the best operating point (for the IV curves corresponding to the local converters) does not necessarily mean the maximum power point. In reconfigurable modules, mainly in run-time instances where local converters are active, the goal is to maximize the power of the entire module, thus the power reaching the module converter. Selecting the MPP as the best operating point for each local converter does not necessarily lead to the best overall power production. Converter efficiency as a function of operating voltage and conversion ratio and resistive losses after the local conversion stage can affect

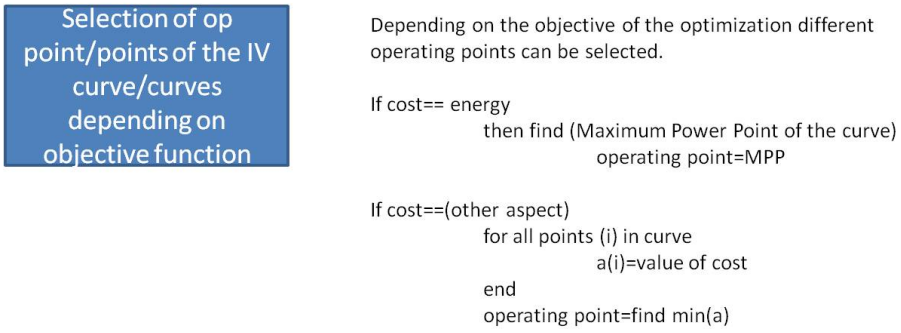

Fig. 7.7 Selection of operating point

the total power reaching the module converter. It was stated earlier, that the output of the simulation framework are operating points at the input of the local converters. Since the entire IV curve is available at the input of the converters, different operating points can be chosen for a ast multi-objective analysis with good accuracy. Potential objectives for optimization, other than energy, can be reliability or low temperature differences.

An extension of this framework can be made by combining the curves of the outputs of the local converters. This can be done by repeating the process of adding resistances and combining curves depending on the connection of the local converters. In example, when the converters are connected in parallel, the appropriate resistances are added in the curves and the currents of the IV curves are added.

7.3.3 Selection of IV curves from the IV curve Database

In section 7.3.1, the process of combining the IV curves of the cell-strings is discussed. The issue that is discussed here is how to select which curves need to be combined. For static shading patterns, this is not a complicated issue, as only the external conditions are needed. However for transient simulations it is more complicated.

In section 6.3.2, the inputs of the simulation model were analyzed. The external conditions are the irradiation, the ambient temperature and the wind, which are all known beforehand. In order to produce in the simulation environment in spectre an IV curve of a cell-string by utilizing only external inputs, two options are available. A dc sweep of the voltage or a pseudo-transient analysis. When a dc sweep is performed, the IV curve we obtain is a sequence of static I-V pairs for the given irradiation, ambient temperature and wind. A pseudo-transient analysis on the other hand, has almost the same internal temperature for all operating points (depending on the step and the speed of the analysis), but it initiates the temperature according to given ambient temperature. A different approach is used in

the proposed simulation process. In the simulation framework proposed here, IV curves are selected as a function of only two parameters:

1. The incident irradiation of each cell
2. The internal temperature of each cell

The use of the internal temperature of the cells as an input to select IV curves from the database means that the entire thermal network is moved outside of the simulation environment and should be incorporated into a temperature prediction scheme. More about the database of IV curves will be discussed in section 7.4.

7.3.4 Temperature Prediction

The irradiation of the module is an external input file, so there is no difference in this simulation framework and in the simulation environment in spectre which was used in chapter 6. The internal temperature of a cell however is a function of the ambient temperature, the wind and the operating point of the cell, as the power which is not extracted electrically is converted to heat. This creates a dependency loop, where in order to know the internal temperature the operating point needs to be known and vice versa. To break that time-consuming loop while incurring only a small accuracy loss, it is considered that the operating point of the previous simulation step can be used to estimate the internal temperature of the cell.

The internal temperature of each cell also depends on the temperatures of the neighboring cells, as shown in Figure 7.2, which are connected in the aforementioned simulation environment through a coupled electrical and thermal network. As the IV curves to combine are defined as a function of internal temperatures, the thermal dependencies of the surrounding cells are not included in the simulation process of the cell-strings.

As stated above, the parameters needed to select the appropriate IV curve at run-time are the irradiation level and the internal temperature of each cell. The irradiation is known, thus the main issue arises in predicting at run-time accurately the appropriate set of internal temperatures of the cell-strings.

To summarize, the factors that affect the internal temperatures of the cell-string are:

1. Energy which was not extracted (Irradiation level, operating point)
2. Ambient temperature and wind
3. Module build-up and previous state

4. Thermal connections with neighboring cells

The internal temperature of each cell firstly depends on the external conditions and the operating point. The current irradiation level indicates the energy received by the cell and the operating point determines the amount of energy which is extracted from the cell in the form of electricity. The energy which is not extracted is converted to heat and increases the internal temperature of the cells (factor 1). The ambient temperature acts as bias ("ground" for the thermal network), while wind cools down the cells (factor 2). The previous state of and the module build-up (materials) represent the different layers and the thermal network they create (factor 3). Furthermore, the close proximity of the cells means that cells are affected by the temperatures of their surrounding cells (factor 4). As the first three factors are more dominant, these are examined first (Figure 7.8). Once the temperature is predicted, this is used as input to select the IV curve. Thus we have Operating point OP(k). A comparison between OP(k) and OP(k-1) may be also used to refine the temperature prediction if needed.

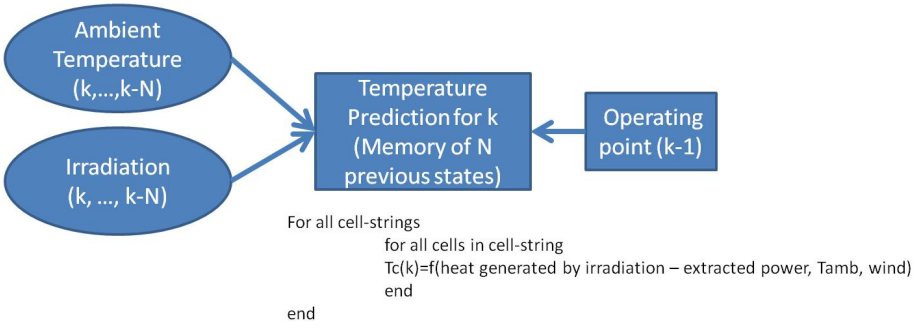

Fig. 7.8 Temperature Prediction

In [72], the effect of fast-varying weather conditions on simulated solar cells is discussed. The thermal network acts like a low pass filter with 2-3 different time constants for irradiation or wind changes. In the model used in chapter 6, these effects are modeled through the parameters of the thermal network (thermal capacitances and resistances of the different layers). The fact that all the poles of the system are real and single (no presence of multiple, real or complex, poles), the cell temperature does not oscillate and presents an exponential-like behavior.

Irradiation changes translate to variation of the heat generation within the thermal network. The thermal-electrical loop consists of a variation of heat generation (as the irradiation case) and the analysis done for irradiation variations is also valid for variations of the operating point. The wind effect which is currently modeled by the means of a variable resistance can be included into the temperature prediction process by means of a variation of system parameters. Another approach would be to investigate the potential decoupling of wind and

irradiation effects and the cell-temperature would be predicted as shown in the following state equation, where N is the order of the thermal model.

$$T_c(k) = f(T_{amb}(k,k-1,...,k-N), T_c(k-1,...,k-N), Irr(k,k-1,...,k-N)) + g(wind)$$

Depending on the time-period considered for simulation, which defines the fastest dynamics taken into account, the thermal network can be reasonably modeled by means of a first-, second- or third-order low-pass filter with two inputs: net heat (heat generated by the irradiation – extracted power) and ambient temperature. A digital implementation of such a Low Pass (LP) filter allows the prediction of the thermal behavior of a solar cell. A first approach was tried out by implementing a first-order LP filter with a bilinear transform. The operating point of the cells was known beforehand (through prior simulations) and the predicted temperature was reasonably accurate for a daily simulation with a 1 second resolution (Figure 7.9).

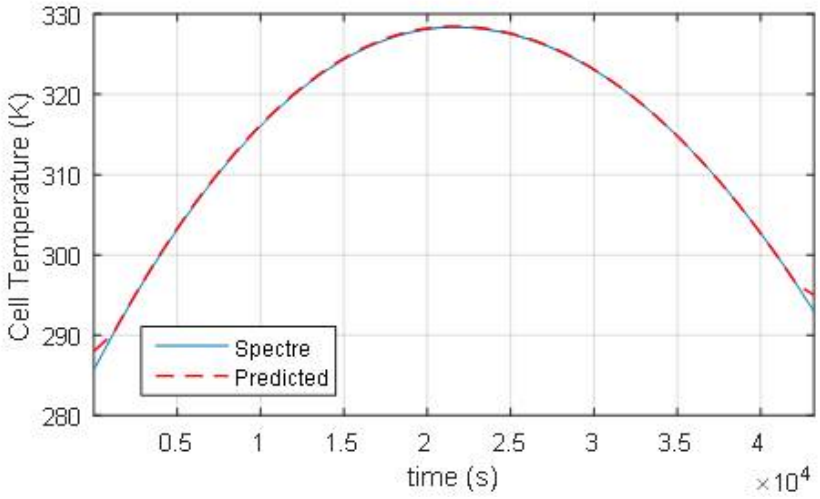

Fig. 7.9 Simulated (spectre) and Predicted temperature

The error for the entire day never exceeds 0.8% while for the majority of the day, excluding the early morning and late evening where the energy is really low, the error is under 0.15%.

The effect of the surrounding cells on the internal temperature of the cells is not strong and it is likely that they can be omitted without introducing significant errors. In order to be thorough however, these have to be examined. Including the thermal resistances and capacitances in a similar process as described above can be a solution but can be time demanding. It has to be noted here, that as the cell-strings are small, it is expected that for the

majority of the time each cell-string will have uniform conditions. The proposed approach is to simulate different external condition sequences for a single cell-string and observe the distribution of internal temperatures in the cells. By comparing the estimated temperature produced by the low-pass filter, we can decouple the influence of the surrounding cells and the heat due to internal power consumption. This will allow the formulation of parameterized equations to include the thermal connections of the neighboring cells. The latter can then be instantiated very fast, enabling a huge speed up during the parameter sweep explorations that we target.

7.4 Database of stored IV curves

Once the parameters of each individual cell-string for a simulation step are known, in principle, all the cell-strings can be simulated and the appropriate IV curves can be produced. This however requires multiple simulations for each step and increases the overall simulation time. It is proposed to create a database of IV curves and depending on the parameters, instead of simulating the IV curves to select the appropriate ones from a database. Although the number of distinct operating scenarios of a cell-string are less than that of the entire module, the possible parameter sets of a cell-string remain significantly large and it is not considered possible or optimal to save all possible IV curves. The flowchart which describes how the database can be created is depicted in Figure 7.10.

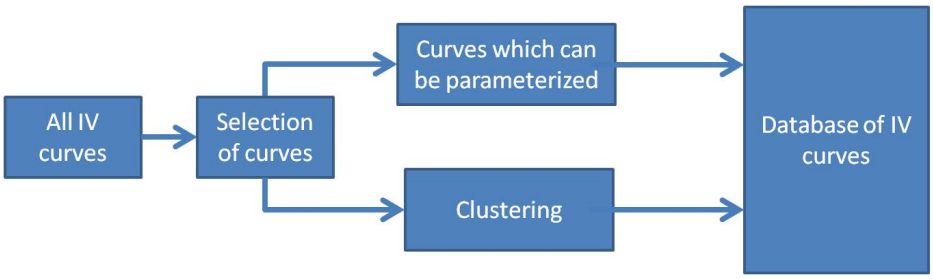

Fig. 7.10 Flowchart for creating the database of IV curves

7.4.1 Selection of IV curves

If the number of cell-strings is n, the number of irradiation levels is x and the number of temperature levels are y, then the number of unique operating conditions per cell is $k = x * y$. The unique operating conditions per cell-string are $((n\ k))$. Thus an actual need is present to reduce the number of actual curves. The first reduction can be made by excluding operating

conditions which are in principle either equivalent to others or unrealistic based on the design instantiation of the module (see Figure 7.11, which is explained next).

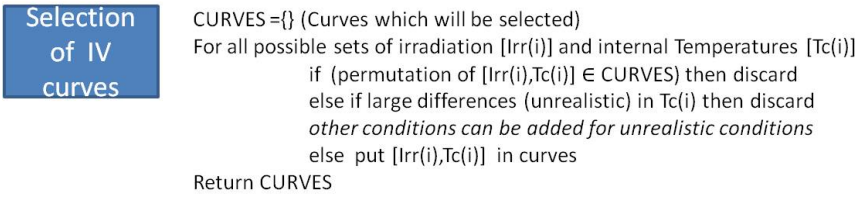

Fig. 7.11 Elimination of unrealistic and equivalent IV curves

Pruning of needed stored curves can be done by eliminating curves which are not realistic. The conditions of unrealistic curves can depend on the location of installation, thus this pruning must take into account if the desired goal is a single database applicable for all locations or multiple databases depending on the location. Through selected simulations however, universal unrealistic conditions may be identified.

Another condition which decreases the number of curves are permutations of the irradiation levels and internal temperatures. The IV curve corresponding to a certain set of $[Irr_i, T_i]$ is identical to any distribution of the specific parameter set. This is due to the assumption that all cells have the same electrical characteristics. In case of uneven degradation (depending on how is is modeled), this has to be reexamined.

After this pruning, the curves are reduced, however the number of remaining curves still remains large. Two basic concepts are introduced here in order to further reduce the number of curves which need to be stored it the database; parameterization of the IV curves and clustering. Each of these concepts introduces a source of potential errors and hence reduced accuracy of the simulation, so it should be considered carefully. But the exploitation of the scenario clustering know allows potentially huge additional savings in execution time, which are required for really large topology or shading exploration spaces.

7.4.2 Parameterization of the curves

Given an IV curve of a cell-string operating under conditions $(G1, T1)$, where $G1$ is the set of irradiation levels of the cells and $T1$ is the set of internal temperatures of the cells, the question is whether other curves with different conditions can be accurately estimated.

Firstly, the uniform operating conditions of a cell-string will be considered, so both $G1$ and $T1$ consist of a single value. The short-circuit current is proportional to the irradiation level. The IV curve of a cell-string with parameters $G2$ and $T1$ can be estimated based on the previous curve, given that once again $G2$ consists of a single value. The short-circuit

current is proportional to the irradiation level, however simply dividing the current of the IV curve with the proportionality of $G2$ to $G1$ is not sufficient. The knowledge however of the series and parallel resistance of the cell-string allows a more accurate parameterization of the new IV curve. In example, a uniform curve with G2 and T1 can be computed from a uniform curve with G1 and T1 by calculating the difference in short-circuit current (through the differences in irradiation level) and the voltage shift by computing the voltage drop in the series resistance of the cell-string from the difference in current. The simulated and parameterized curves are shown in Figure 7.12.

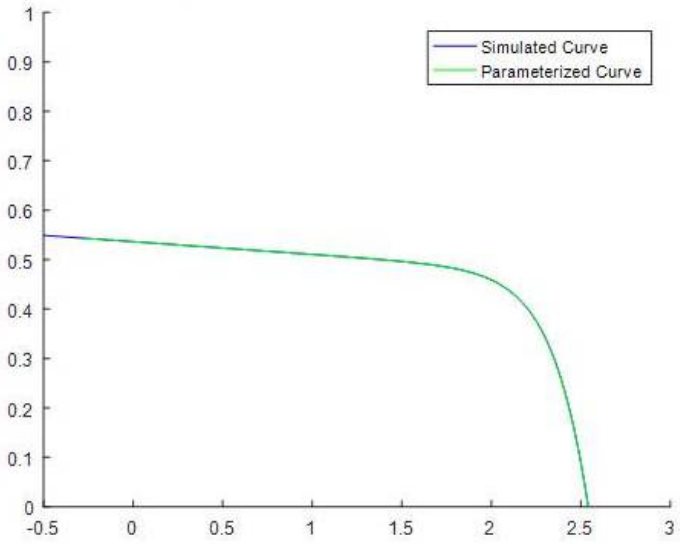

Fig. 7.12 Simulated and Parameterized curve of a cell-string with $100W/m^2$ from curve with $1000W/m^2$ in 300K

In order to parameterize the curve, uniformity of the cell-string is not necessary. When two irradiation levels are present, where the difference between the two levels are the same in both curves, the parameterized curve is proven to be accurate, with all error being lower that 0.3% (Figure 7.13).

Other pairs of curves should be examined to identify whether an accurate estimation is possible. Some of the proposed curves are uniform curves with different temperature levels (Irr(i)=Irr(k) & Tc(i)=a*Tc(k)) and curves with proportional differences in irradiation and temperature (Irr(i)=a*Irr(k) & Tc(i)=a*Tc(k)) (Figure 7.14). The variables i and k represent different operating conditions of cell-strings. For pairs of curves which have these characteristics, it should be investigated if a parameterized equation can be applied to derive one curve from another.

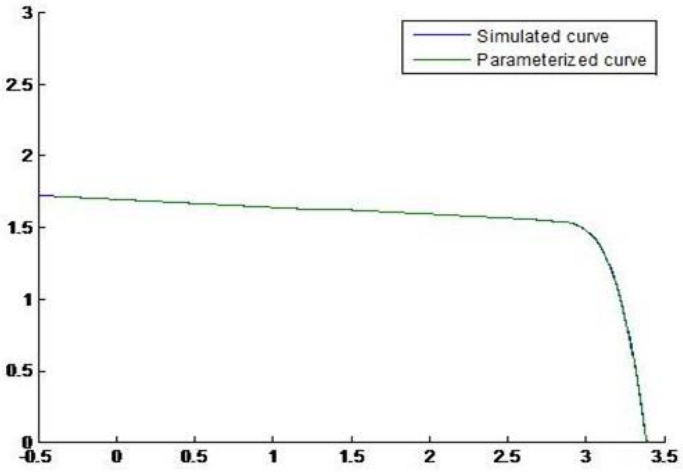

Fig. 7.13 Simulated and Parameterized curve of a cell-string with $500-300W/m^2$ from curve with $1000-800W/m^2$ in 300K

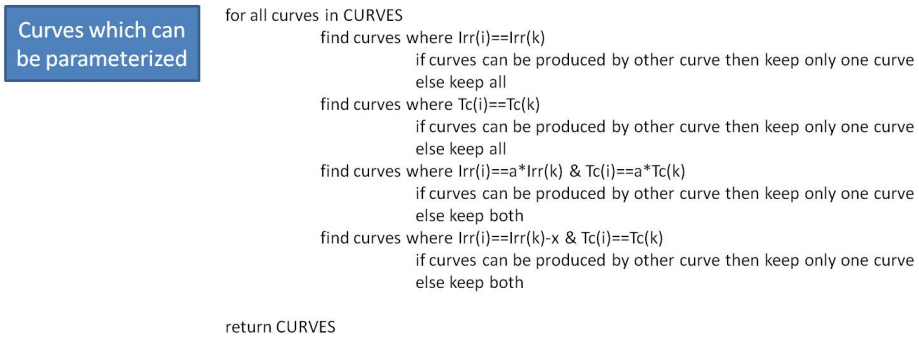

Fig. 7.14 Parameterization of IV curves

7.4.3 Clustering of the IV curves into system scenarios

In order to reduce the number of stored IV curves, a clustering of the IV curves is proposed. The main idea behind clustering is to group together a set of IV curves which are similar to each other and can be represented by a single IV curve (Figure 7.15). Similarity between two curves is assessed based on the shape and the relative position of the two curves. Each group is called a a "IV curve system scenario", in brief "scenario" in the remainder of this Chapter. It is combining a set of IV curves with different internal temperatures and irradiation levels that are close to each other in the I-V space.

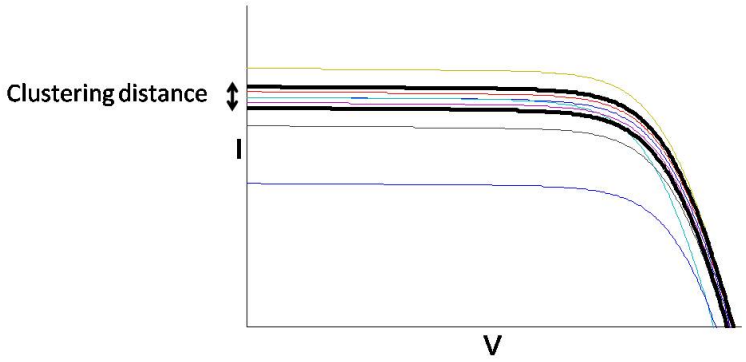

Fig. 7.15 Clustering of IV curves

The goal is to group together curves where the distance in possible operating points does not exceed a certain threshold. The choice of this threshold of course affects significantly the potential error introduced in the simulation and determines the required number of groups to be formed. It has to be noted here that each curve is stored as a set of points in a 2-dimensional space (pairs of voltage and current) and not as a function of either the voltage or the current. The computation of the distance between two curves requires a comparison between all the stored points of the two curves. This can be a quite complex and demanding process. To simplify this, the distance can be computed by accumulating the distance in well-chosen points of the curves. These points can be selected by taking into account the shape of the curves, e.g. strong linearity near the short circuit current, and the probability of selecting an operating point, i.e. close to the MPP of the curve. We do need to keep one point at least around the Isc and Voc positions. The selection of the points in the IV curve is also described in Figure 7.17.

Another important factor of clustering is the frequency of IV curves; how often does an IV curve present itself. Clusters of frequent IV curves should be treated with more caution and the distance in these scenarios should be as low as possible.

In order to be consistent, this distance function threshold should apply for all potential operating point of a cell-strings. In our case, where the goal is to group IV curves corresponding to different operating conditions of individual cell-strings, a major issue is that the distance between curves is not similar for the entire voltage range. In Figure 7.16, the IV curves corresponding to cell-strings operating in uniform conditions (with different irradiation levels and internal temperatures) are shown. It can be observed that similar irradiation levels result to small differences in low voltages while temperature differentiation affects the similarity near the "knee" of the curves. Hence, it can be difficult to cluster the IV curves for the entire range of voltages.

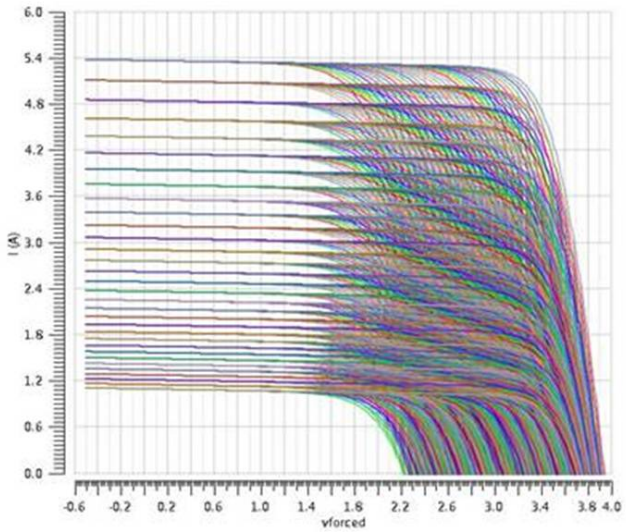

Fig. 7.16 IV curves of uniform cell-strings with different irradiation levels and internal temperatures, [Irradiation Levels: Max irradiation=1000W/m^2 and 5% difference from level to level (200-1000W/m^2), Temperature Levels: Max Temperature=370K and 1% difference from level to level (270-300K)]

Possible solution options to this issue are now summarized for different use cases of the model and simulation framework. As mentioned in Section 7.3.1, in our proposed topologies the IV curves are connected in two possible ways, series and parallel. It has to be stated here, that cell-strings are connected in series when their respective operating conditions are similar, while parallel connection is better suited when their respective operating conditions differ. This restricts the range of the potential operating points of each cell-string, allowing clustering to focus on a smaller voltage range of the IV curves. However, this simulation framework can be also used for other types of topologies where this restriction of potential operating voltage points is not possible, such as conventional topologies. In that case, clustering of

the curves can take place in divided regions (i.e. low and high voltages) and curves can be produced by a combining the representative curve of each individual region.

Depending on the desired level of accuracy, the process of clustering will not be able to further reduce the number of scenarios. In that case, resolving to a solution of sub-scenarios should be discussed. Sub-scenarios would go in a smaller granularity level of that of a cell-string where the number of sets of operating conditions are reduced. Sub-scenarios can be created for half cell-strings or even less, where the combination process of section 7.3.1 can be performed to produce the curve of the entire cell-string.

An important concept of clustering is the backup scenario. If during the selection of IV curves, a parameter set of irradiation and temperatures, which does not belong to any cluster, presents itself a backup scenario should be used. This should be extremely rare. If only one backup scenario is used, it is proposed to consider that the cell-string does not produce any power and remove it from the configuration. If needed, more than one backup scenario can be present to reduce the introduced error. The clustering process is shown in Figure 7.17.

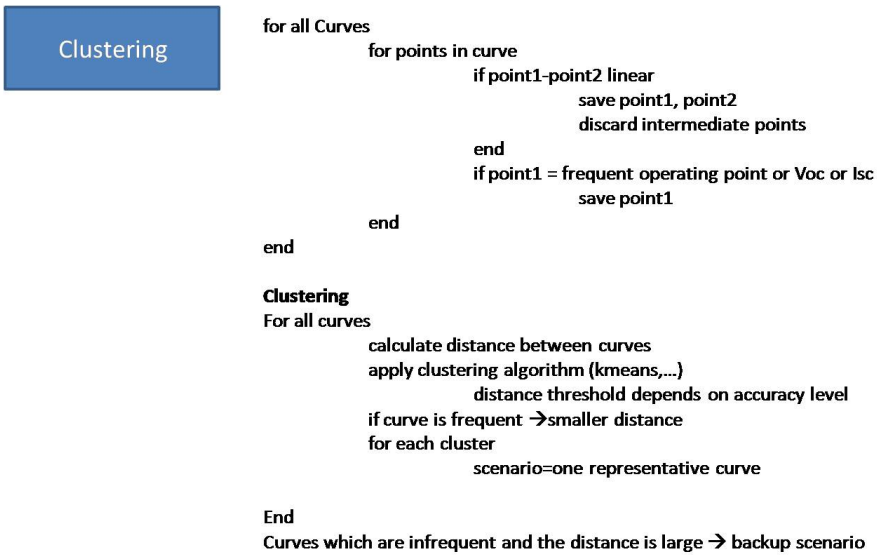

Fig. 7.17 Clustering Process

7.5 Potential Errors and Estimated Speedup

The proposed simulation framework has several steps which may introduce errors. The potential cause of errors are listed here:

- Removal of thermal connections between cell-strings

- Adding resistances
- Combination of curves
- Selection of curves (prediction of internal temperatures)
- System Scenarios

The first three steps where checked for uniform and non-uniform conditions and the combined error never exceeded 0.1% for all points in the IV curve. The final target error for this simulation framework is to have less than 0.5% error in power for a time resolution of 1 second, compared to the simulation environment in spectre discussed in Chapter 6. This will define the distance function for the clustering process and the required accuracy of the prediction scheme.

In the simulation environment that is described in Chapter 6, a uniform day with a series connection of the cell-strings required around 9 hours. A first application of the proposed simulation framework to simulate a uniform day is performed by combining IV curves of cell-strings. All cell-strings have uniform irradiation. All curves which were used have a constant internal temperature of the cells, which is the average internal temperature throughout that day. A single cell-string was simulated for 1000 levels of irradiation and one level of internal temperature resulting to 1000 curves. These curves are shown in Figure 7.19.

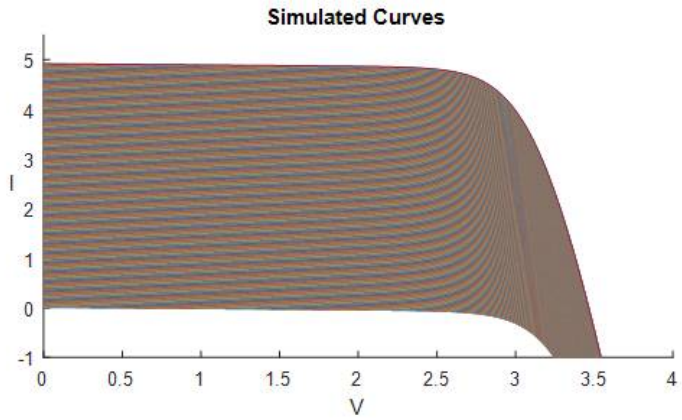

Fig. 7.18 Simulated IV curves of uniform cell-strings (1000 levels of irradiation and one internal temperature)

The simulation of a uniform day with a series connection of the cell-strings, required approximately 200 seconds in the simulation framework.This is a really significant improvement on simulation time of about a factor 165. The daily error in energy estimation is 1.5% and the average error in power per second around 5%. For the period of the day where the

power is over 20W, which corresponds to an irradiation level of over $150W/m^2$, the average error in power per second is 4%. These errors are calculated with respect to the simulation outcome of the model described in Chapter 6.

Instead of simulating and storing all IV curves, only one curve was simulated and strored in the database and the others were derived from that curve based on the approach described in section 7.4.2. This curve was stored in the database and other curves which were required were estimated from that curve (Figure 7.19).

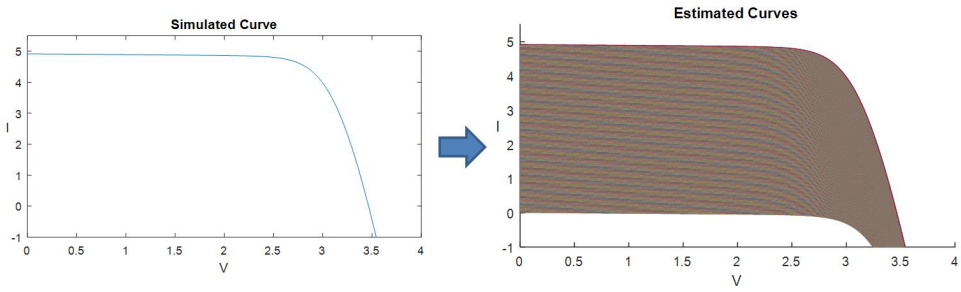

Fig. 7.19 Simulated IV curve and estimated curves (1000 levels of irradiation and one internal temperature)

The daily error remained at 1.5% while the average error in power per second raises to 6% (due to errors in low irradiation levels). For the period of the day where the power production is over 20W, the average error in power remains at around 4%. In Figure 7.20, the simulated power for the two approaches described here and the simulation model in spectre are illustrated. The simulated power for having all curves simulated and for having the curves estimated really coincide the two curves are indistinguishable.

It can be seen that by using only one internal temperature level for the entire day causes significant errors, which necessitates and motivates the use of a prediction scheme for changes in internal temperatures of the cells. However the estimation of IV curves from a single curve does not increase the error significantly and limits the number of simulations needed for the cell-strings, i.e. it limits the size of the database.

By simulating the curve of Figure 7.20 for five different temperature levels and having some temperature prediction, thus selecting between five available IV curves (Figure 7.21). The daily error drops to 0.4%. The average error per second is also improved (2.5%), while for the period of the day that the power is over 20W the average error is 1.1%. The two power curves from the simulation framework and the simulation environment in spectre are shown in Figure 7.22.

By increasing the temperature levels to 10, thus having 10 available curves (Figure 7.23), the accuracy level of the simulation framework really improves. The simulated power of the simulation framework and the simulation environment (spectre) are depicted in Figure 7.24.

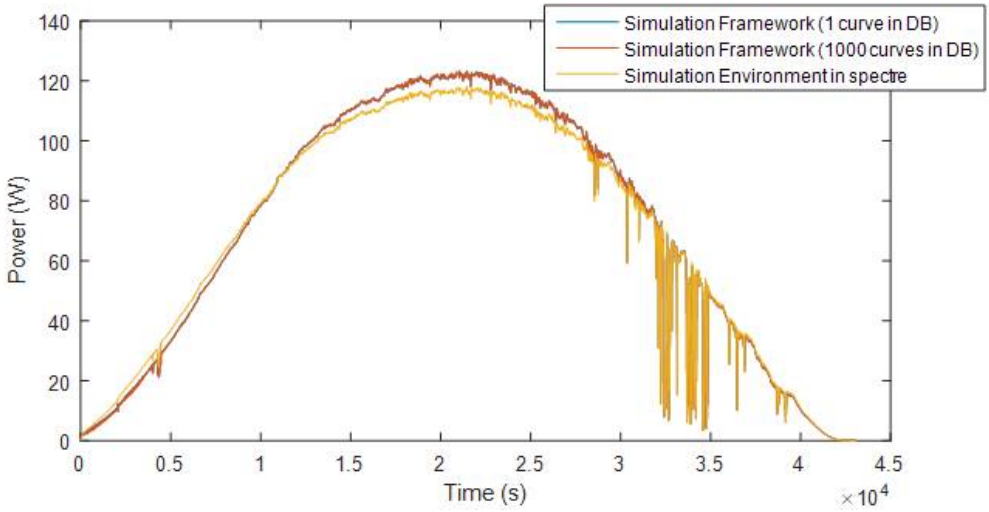

Fig. 7.20 Simulated power by the simulation model (spectre), the simulation framework with all simulated curves and the simulation framework with one curve

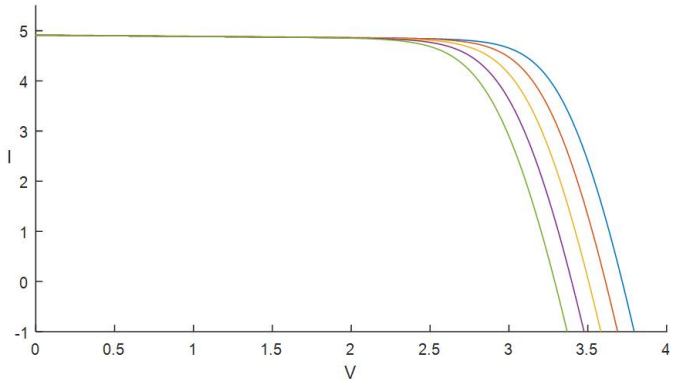

Fig. 7.21 Simulated IV curves for 5 temperature levels, which are stored in the database

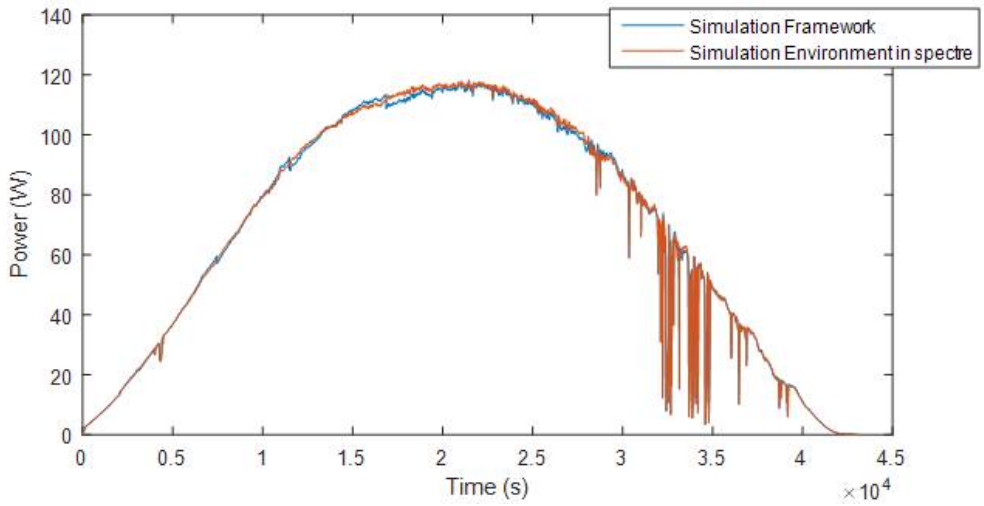

Fig. 7.22 Simulated power by the simulation model (spectre) and the simulation framework with 5 temperature levels

The daily error is negligible (0.02%), while the average error in power per second is 1.8%. For the period of the day where the power is over 20W, the average error in power is 0.6%.

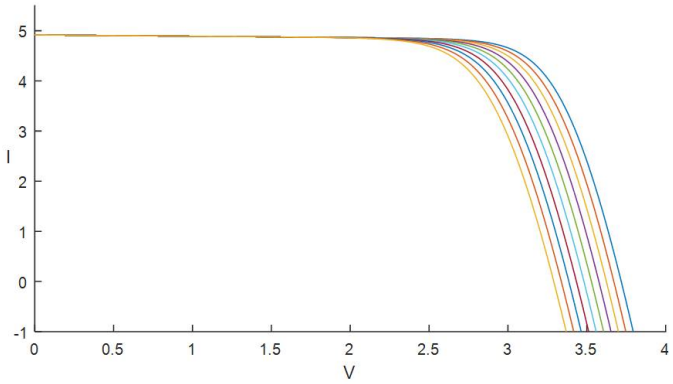

Fig. 7.23 Simulated IV curves for 10 temperature levels which are stored in the database

The accuracy level and the speed which is achieved by the simulation framework by using 10 stored IV curves, proves that this approach can significantly improve overall simulation time and allow investigation of more design topologies of the PV module.

An attention point should be the accuracy level at low irradiation level which is relevant when simulating partially shaded modules. The curves which were stored in the database were for high irradiation levels and when low irradiation levels were present, the curves were estimated from them. In order to improve the accuracy for low levels, while maintaining a

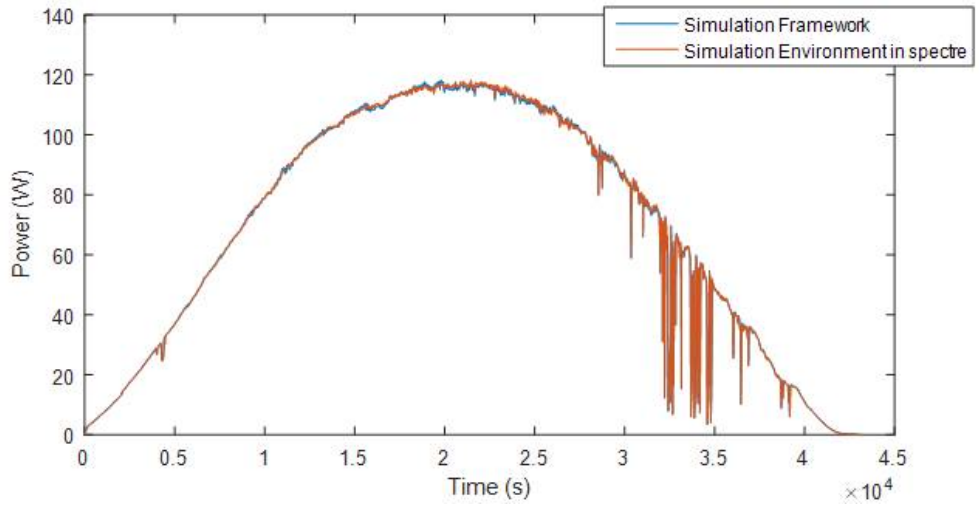

Fig. 7.24 Simulated power by the simulation model (spectre) and the simulation framework with 10 temperature levels

high accuracy for high ones, two sets of curves can be stored for high and low irradiation levels respectively.

7.6 Conclusions

As stated in chapter 6, the simulation model which is implemented in spectre and verilog provides accurate simulation results but requires large amounts of computational time. The proposed simulation framework aims to significantly improve the simulation time, thus enabling the evaluation of more module configurations, while maintaining a high accuracy level with respect to the simulation model implemented in spectre. Procedures and algorithmic techniques have been proposed and discussed for all the main steps in the flow.

This simulation framework has the extra advantage of providing the entire IV curve at each conversion unit, thus enabling the investigation of more than one potential operating point. The basic structure of the simulation framework has been implemented and tested in matlab. A first assessment of the accuracy shows that the errors are very reasonable (within 0.6% for power higher than 20W and 0.02% for daily energy estimation). The simulation speed up is significant (factor 165). Further work is required to build the IV curve database, but the main methods to complete it have been described in this chapter.

Chapter 8

Conclusions and Future Work

8.1 Summary & Conclusions

It is observed that partial shading/non-uniform conditions cause conventional PV modules to perform poorly. Energy losses in industrial modules due to partial shading can be as high as 25%. Conventional methods to mitigate for the effects of partial shading are limited and result to loss of energy which can potentially be recovered. The most promising solutions are dynamic configurations of the PV array which adapt to the operating conditions, especially in installations where non-uniform conditions are frequent. As analyzed and discussed in chapter 2, state-of-the-art either focuses on a granularity levels of the PV module or even higher, thus non-uniform conditions within the module itself can still cause significant power losses. Studies which go within the module itself are limited by either a low flexibility or a high cost overhead, i.e complex control schemes, high resistive losses, large investment cost.

In Chapter 3 a broadly applicable exploration methodology to design a reconfigurable PV module is introduced and analyzed. It is shown how reducing the granularity level can increase the energy produced by a PV module when it is operating under partial shading conditions. The basic components of the proposed approach (cell-string architecture) are introduced and the advantages and disadvantages of their potential types of interconnections are examined. The application of this method allows the design of reconfigurable modules which permits multiple run-time instantiations of the module, thus adaptation to the dynamic external conditions. A cost function is also presented which can be used to evaluate the performance of reconfigurable modules: the amount of expected recovered energy should compensate for all the additional cost (additional resistive losses and investment cost).

The methodology described in Chapter 3 is applied to rectangular modules of N by M cells in Chapter 4. In order to remain close to the fabrication process of industrial PV module, the rows/columns of the PV module form the cell-strings. The supporting network for

multiple potential interconnections of the cell-strings and independent operation of groups of cell-strings is explored. Potential benefits of this template are shown by simulation of the two configurations under static shading patterns, where for certain shading conditions the results are very promising compared to the performance of the conventional module. Selection of either the rows or columns of the module as cell-strings however limits the flexibility of the module to shading patterns from specific angles. On one dimension the module has a cell-level granularity while in the other there is no granularity at all. A vertical split of the original cell-strings (columns/rows) is proposed. This increases the initial cost of the PV module and introduces more energy losses under uniform conditions but the flexibility of the module is significanlty increased and this topology can recover power in more shading patterns [73], [74].

In Chapter 5, different types of templates of reconfigurable modules are explored. The main objective is to have a flexibility level similar to a PV module where the vertical split is applied, but which exhibits limited resistive losses under uniform conditions. Two design types of reconfigurable modules are proposed, a U-type module and an I-type module. In both types, dynamic elements (switches) are avoided in the main cell matrix and all additional elements are placed either around the module or potentially on the back side of the module. The potential run-time instantiations of the module analyzed in this work are limited to two main classes. An all series connection of the cell-strings which is best suited for uniform/near-uniform operating conditions and parallel connected groups of cell-strings which is optimal when non-uniformity within the module is present. The performance of these templates under uniform conditions and static shading patterns is presented [75], [76], [77],[78]. These two templates show promising gains under conditions of partial shading and the power losses of both templates are lower than 1% in uniform conditions.

The simplicity of having two main classes of run-time instantiations of the I-type and U-type modules allows the simulation of the snake topologies for dynamic shading scenarios. As the control scheme to decide at run-time the position of the knob-controlled elements is not designed, a comparison between the performance of the two run-time instantiations is made. This also provides insight on when it is beneficial to switch between the run-time instantiations and should be used as input for the design of the control scheme.

Three shading scenarios were explored throughout the year. Simulations were made for selected days which are representative of each months (March-November) average irradiation profile and are mostly clear sky days. The shading scenarios/patterns were created by using available meteorological data from a weathering station in Oldenburg and the SketchUp software. Two of the shading scenarios have incident shade due to nearby objects throughout the year. The casted shade moves along the long edge of the module in one scenario and

along the short edge in the other. From these two scenarios, the gains of shading scenarios where the shade is moving in other directions can be estimated. One more shading scenario was explored, where the shade is caused by a tree, thus the shading patterns are irregular. In this scenario, the tree also often shades the entire module, which leads again to uniform conditions of the module. Furthermore, no shade is cast in June and July, which are months of high energy generation. This makes this shading scenario more of an "outlier" for potential installation sites for reconfigurable modules.

In all three shading scenarios, the energy generation was increased in comparison with a conventional module equipped with a power optimizer. In the two main shading scenarios, the amount of recovered energy is significant leading to long-term financial gains. The "outlier" shading scenario has some energy gains, but when translated into financial terms, the recovered energy is not sufficient to compensate for the additional cost. It is worth to note that the financial gain does not depend only on the recovered energy, i.e. shading scenario and location-specific environmental conditions (yearly irradiation, diffuse portion, wind velocity, ambient temperature), but it also depends on the location of installation from a strictly financial point of view. Indeed, different countries may have or not have Feed-In Tariffs and they also have different electricity prices. Thus, the profitability of reconfigurable modules is extremely location dependent. However, the results of the analysis presented in Chapter 6 allow to conclude that, in general, installation of reconfigurable module is suitable in areas, where the expected amount of recovered energy is significant, i.e. locations where partial shading is frequent and the energy generation is still high.

The simulation environment (spectre) used in this work has been validated and is really accurate for uniform days. The days that have been simulates are mainly clear sky days where partial shading is introduced due to objects located nearby. The accuracy level may be reduced but no topology is favored since trends are maintained. However the computation time is large. When the number of shading and topology instances grows above a reasonable size, a less complex simulation approach is needed. So for that latter class of problems, another faster simulation approach is proposed [79]. The main core is to have a faster comparison process of different topologies, by allowing some loss of accuracy while maintaining relative errors. The expected speed up factor is higher than 100x, while simulation results show a daily energy error of 0.02% and an average power error per second of 0.6% when the power is over 20W. Furthermore, the proposed simulation process enables a multi-objective analysis and can easily include additional components in the same simulation environment. Having a faster simulation process will enable evaluation of more design-time instantiations of the module, in different shading scenarios in a reasonable time window.

8.2 Future Work

The simulation framework described in Chapter 7 needs to be finalized. The basic methodology has been described, but further work is needed on the creation of the IV curve database and on the process of selecting the appropriate curves at run-time. In more detail, which IV curves can be parameterized and predicted by other curves has to be explored. This will limit the number of curves which need to be stored in the database. Once these curves have been identified, clustering techniques can be applied to further reduce the number of stored IV curves. The finalization of the simulation framework will allow a faster evaluation of more module topologies under different shading scenarios and for different objective functions.

This works focuses on the exploration of design of reconfigurable modules and the performance of the modules under different operating conditions. A design approach is analyzed and two basic templates are proposed for installations on locations where non-uniform conditions are frequent. Future work is needed on exploration of more topologies to optimize the design-time instantiation under specific classes of operating conditions, eg. mostly soiling by sand/dust, mostly nearby objects (like BIPV), mostly very variable clouding, strong dynamic objects (like solar car) and others.

Furthermore, the goal of this study is to determine which module topologies can produce more energy depending on the location of the installation and the dominant operating conditions. This is done by comparing the performance of different run-time instantiations of the module. Once the conditions where each topology should trigger a switch of run-time configuration are known, a more elaborate control scheme can be designed and implemented.

The reconfigurable topologies described in this work require additional electronics. The outputs of the simulation are needed to know the specifications required for these additional elements. Future works should focus on the design of efficient, low-cost, reliable electrical components for the smart PV topologies.

References

[1] Luis Castañer and Tom Markvart. Practical handbook of photovoltaics (second edition), 2012.

[2] S. Saravanan and N. Ramesh Babu. Maximum power point tracking algorithms for photovoltaic system – a review. *Renewable and Sustainable Energy Reviews*, 57:192 – 204, 2016.

[3] Nicu Bizon. Global maximum power point tracking (gmppt) of photovoltaic array using the extremum seeking control (esc): A review and a new gmppt esc scheme. *Renewable and Sustainable Energy Reviews*, 57:524 – 539, 2016.

[4] F. Pulvirenti, A. La Scala, and S. Pennisi. Low voltage-drop bypass switch for photovoltaic applications. In *2012 IEEE International Symposium on Circuits and Systems*, pages 2283–2286, May 2012.

[5] V. S., G. R. Bindu, and S. R. Iyer. Estimation of power losses in photovoltaic array configurations under moving cloud conditions. In *2014 Fourth International Conference on Advances in Computing and Communications*, pages 366–369, Aug 2014.

[6] E. Díaz-Dorado, A. Suárez-García, C. Carrillo, and J. Cidrás. Influence of the shadows in photovoltaic systems with different configurations of bypass diodes. In *SPEEDAM 2010*, pages 134–139, June 2010.

[7] C. Olalla, C. Deline, and D. Maksimovic. Performance of mismatched pv systems with submodule integrated converters. *IEEE Journal of Photovoltaics*, 4(1):396–404, Jan 2014.

[8] N. Pragallapati and V. Agarwal. Flyback configuration based micro-inverter with distributed mppt of partially shaded pv module and energy recovery scheme. In *2013 IEEE 39th Photovoltaic Specialists Conference (PVSC)*, pages 2927–2931, June 2013.

[9] T. Wardle, B. Bram Sadlik, and L. Rubin. Global maximum power point tracking and the available gains in conjunction with high degree diode bypassed modules. In *26th European Photovoltaic Solar Energy Conference and Exhibition*, 2011.

[10] G. Spagnuolo, G. Petrone, B. Lehman, C. A. Ramos Paja, Y. Zhao, and M. L. Orozco Gutierrez. Control of photovoltaic arrays: Dynamical reconfiguration for fighting mismatched conditions and meeting load requests. *IEEE Industrial Electronics Magazine*, 9(1):62–76, March 2015.

[11] B. Subudhi and R. Pradhan. A comparative study on maximum power point tracking techniques for photovoltaic power systems. *IEEE Transactions on Sustainable Energy*, 4(1):89–98, Jan 2013.

[12] A. Bidram, A. Davoudi, and R. S. Balog. Control and circuit techniques to mitigate partial shading effects in photovoltaic arrays. *IEEE Journal of Photovoltaics*, 2(4):532–546, Oct 2012.

[13] Ramaprabha Ramabadran and Dr B. L. Mathur. A comprehensive review and analysis of solar photovoltaic array configurations under partial shaded conditions. 12, 02 2012.

[14] Y. J. Wang and S. S. Lin. Analysis of a partially shaded pv array considering different module connection schemes and effects of bypass diodes. In *2011 International Conference Utility Exhibition on Power and Energy Systems: Issues and Prospects for Asia (ICUE)*, pages 1–7, Sept 2011.

[15] L. F. L. Villa, D. Picault, B. Raison, S. Bacha, and A. Labonne. Maximizing the power output of partially shaded photovoltaic plants through optimization of the interconnections among its modules. *IEEE Journal of Photovoltaics*, 2(2):154–163, April 2012.

[16] D. Picault, B. Raison, S. Bacha, J. Aguilera, and J. De La Casa. Changing photovoltaic array interconnections to reduce mismatch losses: a case study. In *2010 9th International Conference on Environment and Electrical Engineering*, pages 37–40, May 2010.

[17] S. Guo, T. M. Walsh, A. G. Aberle, and M. Peters. Analysing partial shading of pv modules by circuit modelling. In *2012 38th IEEE Photovoltaic Specialists Conference*, pages 002957–002960, June 2012.

[18] C. Barreiro, P. M. Jansson, A. Thompson, and J. L. Schmalzel. Pv by-pass diode performance in landscape and portrait modalities. In *2011 37th IEEE Photovoltaic Specialists Conference*, pages 003097–003102, June 2011.

[19] Fei Lu, Siyu Guo, Timothy M. Walsh, and Armin G. Aberle. Improved pv module performance under partial shading conditions. *Energy Procedia*, 33:248 – 255, 2013. PV Asia Pacific Conference 2012.

[20] B. Braisaz, G. Kwiatkowski, A. Plotton, and D. Tessier. Impacts of decentralised mppt systems on the performances of photovoltaic installations. In *26th European Photovoltaic Solar Energy Conference and Exhibition*, 2011.

[21] Miguel García, Jose Miguel Maruri, Luis Marroyo, Eduardo Lorenzo, and Miguel Pérez. Partial shadowing, mppt performance and inverter configurations: observations at tracking pv plants. *Progress in Photovoltaics: Research and Applications*, 16(6):529–536, 2008.

[22] R. Alonso, P. Ibáñez, V. Martínez, E. Román, and A. Sanz. Analysis of performance of new distributed mppt architectures. In *2010 IEEE International Symposium on Industrial Electronics*, pages 3450–3455, July 2010.

[23] A. I. Bratcu, I. Munteanu, S. Bacha, D. Picault, and B. Raison. Cascaded dc-dc converter photovoltaic systems: Power optimization issues. *IEEE Transactions on Industrial Electronics*, 58(2):403–411, Feb 2011.

[24] E. Roman, R. Alonso, P. Ibanez, S. Elorduizapatarietxe, and D. Goitia. Intelligent pv module for grid-connected pv systems. *IEEE Transactions on Industrial Electronics*, 53(4):1066–1073, June 2006.

[25] A. Sanz, I. Vidaurrazaga, A. Pereda, R. Alonso, E. Román, and V. Martinez. Centralized vs distributed (power optimizer) pv system architecture field test results under mismatched operating conditions. In *2011 37th IEEE Photovoltaic Specialists Conference*, pages 002435–002440, June 2011.

[26] Chris Deline, B Marion, J Granata, and S Gonzalez. Performance and economic analysis of distributed power electronics in photovoltaic systems. 01 2011.

[27] S. MacAlpine, M. Brandemuehl, and R. Erickson. Potential for recoverable power: Simulated use of distributed power converters at various levels in partially shaded photovoltaic arrays. In *26th European Photovoltaic Solar Energy Conference and Exhibition*, 2011.

[28] S. M. MacAlpine, R. W. Erickson, and M. J. Brandemuehl. Characterization of power optimizer potential to increase energy capture in photovoltaic systems operating under nonuniform conditions. *IEEE Transactions on Power Electronics*, 28(6):2936–2945, June 2013.

[29] P. Mazumdar, P. N. Enjeti, and R. S. Balog. Analysis and design of smart pv modules. In *2013 Twenty-Eighth Annual IEEE Applied Power Electronics Conference and Exposition (APEC)*, pages 84–91, March 2013.

[30] G. Adinolfi, N. Femia, G. Petrone, G. Spagnuolo, and M. Vitelli. Energy efficiency effective design of dc/dc converters for dmppt pv applications. In *2009 35th Annual Conference of IEEE Industrial Electronics*, pages 4566–4570, Nov 2009.

[31] L. Kerachev, K. Vladimirova, V. Gaude, J. Widiez, J. C. Crebier, N. Rouger, and Y. Lembeye. Implementation of monolithic multiple vertical power diodes in a multiphase converter. In *2012 Twenty-Seventh Annual IEEE Applied Power Electronics Conference and Exposition (APEC)*, pages 169–175, Feb 2012.

[32] P. S. Shenoy, K. A. Kim, B. B. Johnson, and P. T. Krein. Differential power processing for increased energy production and reliability of photovoltaic systems. *IEEE Transactions on Power Electronics*, 28(6):2968–2979, June 2013.

[33] Patrizio Manganiello, Pietro Carotenuto, Salvatore Curcio, Giovanni Petrone, Giovanni Spagnuolo, and Massimo Vitelli. Algorithms and devices for the dynamical reconfiguration of pv arrays, 05 2013.

[34] M. Z. Shams El-Dein, M. Kazerani, and M. M. A. Salama. Optimal photovoltaic array reconfiguration to reduce partial shading losses. *IEEE Transactions on Sustainable Energy*, 4(1):145–153, Jan 2013.

[35] J. P. Storey, P. R. Wilson, and D. Bagnall. Improved optimization strategy for irradiance equalization in dynamic photovoltaic arrays. *IEEE Transactions on Power Electronics*, 28(6):2946–2956, June 2013.

[36] G. Velasco-Quesada, F. Guinjoan-Gispert, R. Pique-Lopez, M. Roman-Lumbreras, and A. Conesa-Roca. Electrical pv array reconfiguration strategy for energy extraction improvement in grid-connected pv systems. *IEEE Transactions on Industrial Electronics*, 56(11):4319–4331, Nov 2009.

[37] Mahmoud Alahmad, Mohamed Amer Chaaban, Su kit Lau, Jonathan Shi, and Jill Neal. An adaptive utility interactive photovoltaic system based on a flexible switch matrix to optimize performance in real-time. *Solar Energy*, 86(3):951 – 963, 2012.

[38] M. A. Chaaban, M. Alahmad, J. Neal, J. Shi, C. Berryman, Y. Cho, S. Lau, H. Li, A. Schwer, Z. Shen, J. Stansbury, and T. Zhang. Adaptive photovoltaic system. In *IECON 2010 - 36th Annual Conference on IEEE Industrial Electronics Society*, pages 3192–3197, Nov 2010.

[39] S. Vemuru, P. Singh, and M. Niamat. Analysis of photovoltaic array with reconfigurable modules under partial shading. In *2012 38th IEEE Photovoltaic Specialists Conference*, pages 001437–001441, June 2012.

[40] Juan David Bastidas-Rodriguez, Carlos Andres Ramos-Paja, and Andres Julian Saavedra-Montes. Reconfiguration analysis of photovoltaic arrays based on parameters estimation. *Simulation Modelling Practice and Theory*, 35:50 – 68, 2013.

[41] J. H. Huang, Y. Zhao, B. Lehman, and D. Nguyen. Fast switching reconfigurable photovoltaic modules integrated within dc-dc converters. In *2013 IEEE 14th Workshop on Control and Modeling for Power Electronics (COMPEL)*, pages 1–7, June 2013.

[42] Ze Cheng, Zhichao Pang, Yanli Liu, and Peng Xue. An adaptive solar photovoltaic array reconfiguration method based on fuzzy control. In *2010 8th World Congress on Intelligent Control and Automation*, pages 176–181, July 2010.

[43] Y. Wang, X. Lin, Y. Kim, N. Chang, and M. Pedram. Architecture and control algorithms for combating partial shading in photovoltaic systems. *IEEE Transactions on Computer-Aided Design of Integrated Circuits and Systems*, 33(6):917–930, June 2014.

[44] X. Lin, Y. Wang, S. Yue, D. Shin, N. Chang, and M. Pedram. Near-optimal, dynamic module reconfiguration in a photovoltaic system to combat partial shading effects. In *DAC Design Automation Conference 2012*, pages 516–521, June 2012.

[45] A. A. Elserougi, M. S. Diab, A. M. Massoud, A. S. Abdel-Khalik, and S. Ahmed. A switched pv approach for extracted maximum power enhancement of pv arrays during partial shading. *IEEE Transactions on Sustainable Energy*, 6(3):767–772, July 2015.

[46] J. Storey, P. R. Wilson, and D. Bagnall. The optimized-string dynamic photovoltaic array. *IEEE Transactions on Power Electronics*, 29(4):1768–1776, April 2014.

[47] Vaibhav Vaidya and Denise Wilson. Maximum power tracking in solar cell arrays using time-based reconfiguration. *Renewable Energy*, 50:74 – 81, 2013.

[48] B. Patnaik, P. Sharma, E. Trimurthulu, S. P. Duttagupta, and V. Agarwal. Reconfiguration strategy for optimization of solar photovoltaic array under non-uniform illumination conditions. In *2011 37th IEEE Photovoltaic Specialists Conference*, pages 001859–001864, June 2011.

[49] C.L. Craig. Solar array switching unit, May 9 2000. US Patent 6,060,790.

[50] R. Dorn, B. Hachtmann, D. Harris, I. Gur, D. Pearce, W. Sanders, and B. Tarbell. Photovoltaic module utilizing a flex circuit for reconfiguration, June 26 2008. WO Patent App. PCT/US2007/025,483.

[51] T. Takehara and S. Takada. System for controlling power from a photovoltaic array by selectively configurating connections between photovoltaic panels, February 14 2012. US Patent 8,115,340.

[52] H. HAUF and S. VAN. Method of operation and device for controlling an energy installation with photovoltaic modules, September 30 2010. US Patent App. 12/773,447.

[53] Y.H. Kuo. Apparatus and method for controlling the output of a photovoltaic array, March 26 2009. US Patent App. 11/903,983.

[54] M. Vermeersch, B. Estibals, and C. Alonso. Electronic management system for photovoltaic cells, March 22 2012. US Patent App. 13/140,628.

[55] R.A. Sherif and K.S. Boutros. Solar module array with reconfigurable tile, February 26 2002. US Patent 6,350,944.

[56] Luigi Piegari, R Rizzo, Ivan Spina, and Pietro Tricoli. Optimized adaptive perturb and observe maximum power point tracking control for photovoltaic generation. 8:3418–3436, 05 2015.

[57] Sukhvinder Singh, Barry O'Sullivan, Maria Recaman Payo, Angel Uruena, Maarten Debucquoy, Jozef Szlufcik, and J Poortmans. Process development on photolithography free ibc solar cells. In *29th European Photovoltaic Solar Energy Conference and Exhibition*, 09 2014.

[58] Pieter Bauwens and Jan Doutreloigne. Integrated switch for substring reconfiguration to optimize module power under partial shading. In *31st EUPVSEC, At Hamburg, Germany*, 09 2015.

[59] ECTC. Electronic components and technology conference, -.

[60] QRTC. Quality and reliability technical symposium (qrts), -.

[61] http://www.solarplanet.de/pdfs/bp7185.pdf.

[62] REC Solar Pte. Ltd. Potential for recoverable power: Simulated use of distributed power converters at various levels in partially shaded photovoltaic arrays.

[63] H. Goverde, B. Herteleer, D. Anagnostos, G. Köse, D. Goossens, B. Aldalali, J. Govaerts, K. Baert, F. Catthoor, J. Driesen, and J. Poortmans. Configurable module topology to recover power lost due to current mismatch. page 29th European Photovoltaic Solar Energy Conference and Exhibition, 09 2014.

[64] http://www.uni-oldenburg.de/en/physics/research/ehf/energiemeteorology/measurements/.

[65] http://www.sketchup.com.

[66] Richard Perez, Robert Seals, Pierre Ineichen, Ronald Stewart, and David Menicucci. A new simplified version of the perez diffuse irradiance model for tilted surfaces. 39:221–231, 12 1987.

[67] http://ec.europa.eu/eurostat/statistics-explained/index.php/electricity_price_statistics.

[68] https://www.jinkosolar.com/ftp/final-jinko%20solar%20-%20global%20limited%20warranty%20linear%20(20140501).pdf.

[69] http://www.solarworld-usa.com/ /media/www/files/warranties-certifications/archived/solarworld-usa-limited-warranty.pdf.

[70] https://www.solaredge.com/sites/default/files/solaredge-warranty-june-2016.pdf.

[71] H. Goverde, J. Govaerts, J. Baert, F. Catthoor, J. Driesen, and J. Poortmans. Optical-thermal-electrical model for a single cell pv module in non-steady-state and non-uniform conditions build in spice. In *28th European Photovoltaic Solar Energy Conference and Exhibition*, 2013.

[72] H. Goverde, D. Anagnostos, B. Herteleer, J. Govaerts, K. Baert, B. Aldalali, F. Catthoor, J. Driesen, and J. Poortmans. Model requirements for accurate short term energy yield predictions during fast-varying weather conditions. In *31st European Photovoltaic Solar Energy Conference and Exhibition*, 2016.

[73] Maria Iro Baka, Antonis Papanikolaou, Francky Catthoor, and Dimitrios Soudris. Configurable module topology to recover power lost due to current mismatch. page 29th European Photovoltaic Solar Energy Conference and Exhibition, 09 2014.

[74] F. Catthoor and M.I. Baka. Reconfigurable pv configuration, May 1 2013. EP Patent App. EP20,110,186,415.

[75] M. Baka, F. Catthoor, and D. Soudris. Smart pv module topology with a snake-like configuration. In *31st European Photovoltaic Solar Energy Conference and Exhibition*, 2015.

[76] P. Bauwens, J. Govaerts, M. Baka, F. Catthoor, K. Baert, G. Van den Broeck, H. Goverde, D. Anagnostos, J. Doutreloigne, and J. Poortmans. Reconfigurable topologies for smarter pv modules: Simulation, evaluation and implementation. In *32nd European Photovoltaic Solar Energy Conference and Exhibition*, 2016.

[77] Maria-Iro Baka, Francky Catthoor, and Dimitrios Soudris. Near-static shading exploration for smart photovoltaic module topologies based on snake-like configurations. *ACM Trans. Embed. Comput. Syst.*, 15(2):27:1–27:21, March 2016.

[78] M.I. Baka and F. Catthoor. Reconfigurable photovoltaic module, March 15 2017. EP Patent App. EP20,150,184,967.

[79] M. Baka, F. Catthoor, and D. Soudris. Proposed evaluation framework for exploration of smart pv module topologies. In *32nd European Photovoltaic Solar Energy Conference and Exhibition*, 2016.

Simulation Results

Table 1 Energy of the three module configurations x values of (0,0.5,1) for 06/03/2014 for the three shading scenarios

Type of Irradiation	Topology	Energy (KWh)		
		Scenario1	Scenario 2	Scenario 3
All Irradiation (x=0)	Conventional	0.5027	0.5126	0.6062
	I-type	0.5015	0.6031	0.6600
	U-type	0.5032	0.6068	0.6633
Half Diffuse (x=0.5)	Conventional	0.5409	0.5222	0.6076
	I-type	0.5425	0.6197	0.6689
	U-type	0.5436	0.6222	0.6713
Only Direct (x=0)	Conventional	0.5889	0.5670	0.6335
	I-type	0.5916	0.6392	0.6795
	U-type	0.5920	0.6407	0.6810
Uniform	Conventional	0.7208		
	I-type	0.7172		
	U-type	0.7160		

It should be noted here, that for the day 06/03/2104, Table 1, the I-type module performs poorly compared to the conventional module when all irradiation is affected equally. The difference in performance is negligible, but it is observed that the shape of the shade and the irradiation conditions of this day do not allow the I-type to optimize the configuration of the module.

Table 2 Energy of the three module configurations x values of (0,0.5,1) for 07/04/2104 for the three shading scenarios

Type of Irradiation	Topology	Energy (KWh)		
		Scenario1	Scenario 2	Scenario 3
All Irradiation (x=0)	Conventional	0.3998	0.3430	0.3645
	I-type	0.4068	0.4024	0.4222
	U-type	0.4108	0.3588	0.4248
Half Diffuse (x=0.5)	Conventional	0.4310	0.3846	0.4023
	I-type	0.4389	0.4349	0.4445
	U-type	0.4390	0.4369	0.4458
Only Direct (x=0)	Conventional	0.4697	0.4559	0.4671
	I-type	0.4719	0.4750	0.4731
	U-type	0.4715	0.4759	0.4729
Uniform	Conventional	0.4919		
	I-type	0.4901		
	U-type	0.4895		

Table 3 Energy of the three module configurations x values of (0,0.5,1) for 06/05/2014 for the three shading scenarios

Type of Irradiation	Topology	Energy (KWh)		
		Scenario1	Scenario 2	Scenario 3
All Irradiation (x=0)	Conventional	0.3141	0.1909	0.2892
	I-type	0.3195	0.2313	0.3013
	U-type	0.3194	0.2351	0.3022
Half Diffuse (x=0.5)	Conventional	0.3196	0.2531	0.3045
	I-type	0.3224	0.2804	0.3122
	U-type	0.3223	0.2805	0.3124
Only Direct (x=0)	Conventional	0.3263	0.3318	0.3283
	I-type	0.3262	0.3311	0.3277
	U-type	0.3260	0.3310	0.3275
Uniform	Conventional	0.3357		
	I-type	0.3354		
	U-type	0.3347		

Table 4 Energy of the three module configurations x values of (0,0.5,1) for 18/06/2014 for two shading scenarios

Type of Irradiation	Topology	Energy (KWh)	
		Scenario 2	Scenario 3
All Irradiation (x=0)	Conventional	0.2433	0.2849
	I-type	0.2824	0.3058
	U-type	0.2743	0.3085
Half Diffuse (x=0.5)	Conventional	0.3012	0.3103
	I-type	0.3192	0.3282
	U-type	0.3192	0.3293
Only Direct (x=0)	Conventional	0.3656	0.3584
	I-type	0.3657	0.3576
	U-type	0.3654	0.3573
Uniform	Conventional	0.3703	
	I-type	0.3694	
	U-type	0.3692	

Table 5 Energy of the three module configurations x values of (0,0.5,1) for 04/07/2014 for two shading scenarios

Type of Irradiation	Topology	Energy (KWh)	
		Scenario 2	Scenario 3
All Irradiation (x=0)	Conventional	0.6443	0.7641
	I-type	0.7558	0.8390
	U-type	0.7668	0.8439
Half Diffuse (x=0.5)	Conventional	0.6741	0.8007
	I-type	0.8112	0.8700
	U-type	0.8088	0.8740
Only Direct (x=0)	Conventional	0.7165	0.8323
	I-type	0.8402	0.9049
	U-type	0.8375	0.9081
Uniform	Conventional	1.0051	
	I-type	0.9984	
	U-type	0.9964	

Table 6 Energy of the three module configurations x values of (0,0.5,1) for 16/08/14 for the three shading scenarios

Type of Irradiation	Topology	Energy (KWh)		
		Scenario1	Scenario 2	Scenario 3
All Irradiation (x=0)	Conventional	0.4152	0.2744	0.3869
	I-type	0.4256	0.3390	0.4114
	U-type	0.4250	0.3384	0.4140
Half Diffuse (x=0.5)	Conventional	0.4276	0.3239	0.4076
	I-type	0.4334	0.3727	0.4256
	U-type	0.4329	0.3718	0.4264
Only Direct (x=0)	Conventional	0.4427	0.3948	0.4448
	I-type	0.4437	0.4148	0.4459
	U-type	0.4431	0.4139	0.4453
Uniform	Conventional	0.4488		
	I-type	0.4472		
	U-type	0.4470		

Table 7 Energy of the three module configurations x values of (0,0.5,1) for 05/10/2014 for the three shading scenarios

Type of Irradiation	Topology	Energy (KWh)		
		Scenario1	Scenario 2	Scenario 3
All Irradiation (x=0)	Conventional	0.3685	0.3454	0.4114
	I-type	0.3692	0.4047	0.4399
	U-type	0.3697	0.4063	0.4420
Half Diffuse (x=0.5)	Conventional	0.4003	0.3633	0.4227
	I-type	0.4033	0.4232	0.4493
	U-type	0.4033	0.4242	0.4505
Only Direct (x=0)	Conventional	0.4445	0.4164	0.4570
	I-type	0.4440	0.4463	0.4614
	U-type	0.4436	0.4463	0.4616
Uniform	Conventional	0.4730		
	I-type	0.4711		
	U-type	0.4705		

Table 8 Energy of the three module configurations x values of (0,0.5,1) for 18/10/2014 for the three shading scenarios

Type of Irradiation	Topology	Energy (KWh)		
		Scenario1	Scenario 2	Scenario 3
All Irradiation (x=0)	Conventional	0.1231	0.1672	0.1546
	I-type	0.1237	0.1872	0.1834
	U-type	0.1239	0.1897	0.1853
Half Diffuse (x=0.5)	Conventional	0.1503	0.1794	0.1654
	I-type	0.1509	0.1953	0.1914
	U-type	0.1510	0.1967	0.1925
Only Direct (x=0)	Conventional	0.1851	0.2035	0.1922
	I-type	0.1848	0.2063	0.2013
	U-type	0.1848	0.2067	0.2016
Uniform	Conventional	0.2126		
	I-type	0.2122		
	U-type	0.2121		

Table 9 Energy of the three module configurations x values of (0,0.5,1) for 04/11/2014 for the three shading scenarios

Type of Irradiation	Topology	Energy (KWh)		
		Scenario1	Scenario 2	Scenario 3
All Irradiation (x=0)	Conventional	0.0937	0.1083	0.1131
	I-type	0.0990	0.1135	0.1162
	U-type	0.0996	0.1145	0.1170
Half Diffuse (x=0.5)	Conventional	0.1047	0.1147	0.1174
	I-type	0.1083	0.1177	0.1190
	U-type	0.1086	0.1179	0.1192
Only Direct (x=0)	Conventional	0.1208	0.1231	0.1229
	I-type	0.1217	0.1230	0.1228
	U-type	0.1217	0.1230	0.1228
Uniform	Conventional	0.1231		
	I-type	0.1230		
	U-type	0.1229		

Table 10 Energy of the three module configurations x values of (0,0.5,1) for 12/11/2014 for the three shading scenarios

Type of Irradiation	Topology	Energy (KWh)		
		Scenario1	Scenario 2	Scenario 3
All Irradiation (x=0)	Conventional	0.0208	0.0289	0.0286
	I-type	0.0220	0.0293	0.0295
	U-type	0.0221	0.0296	0.0298
Half Diffuse (x=0.5)	Conventional	0.0250	0.0302	0.0301
	I-type	0.0257	0.0305	0.0305
	U-type	0.0257	0.0306	0.0307
Only Direct (x=0)	Conventional	0.0318	0.0319	0.0319
	I-type	0.0319	0.0319	0.0319
	U-type	0.0319	0.0319	0.0319
Uniform	Conventional	0.0319		
	I-type	0.0319		
	U-type	0.0319		